

# Simulating and Characterizing HNLs at Forward Physics Experiments

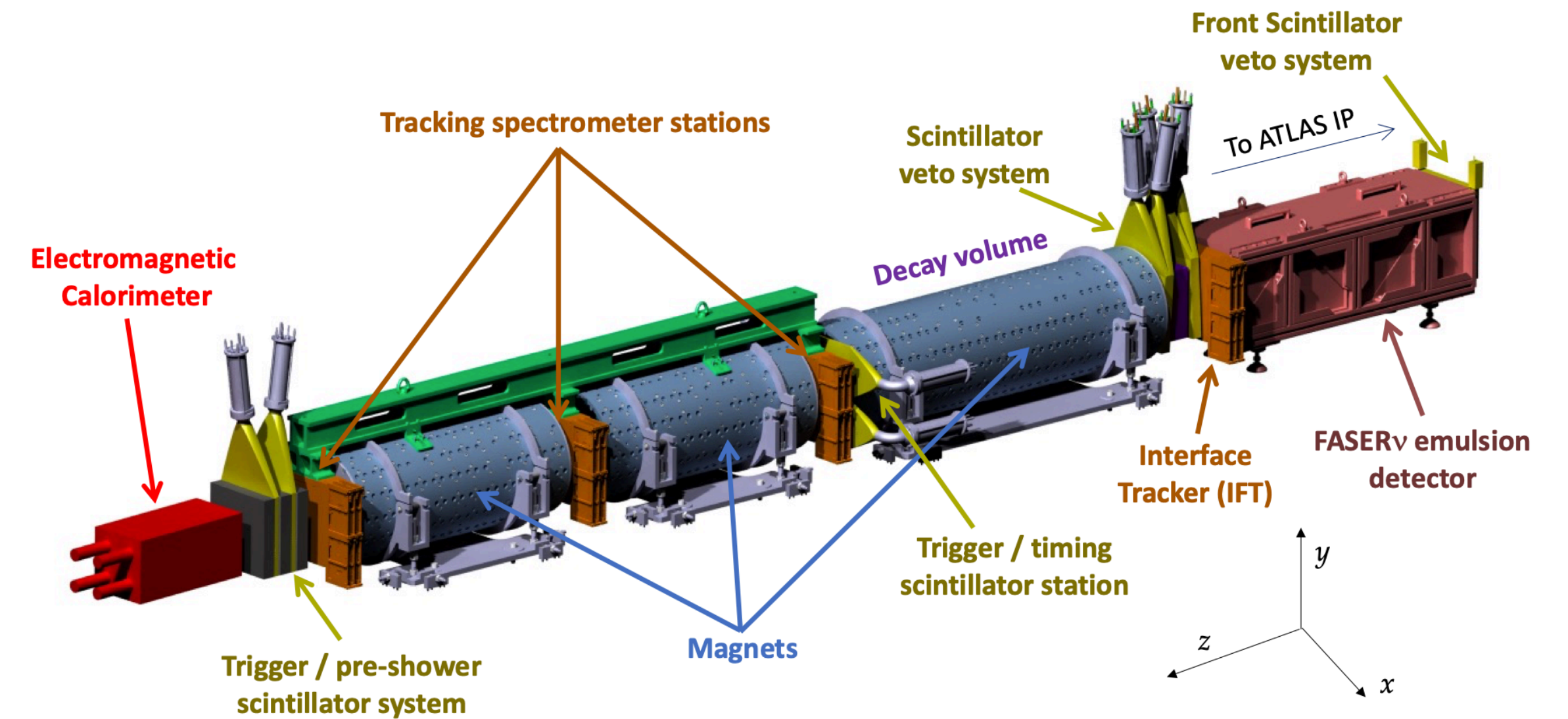
Daniel La Rocco

[2405.07330](#), [2510.16107](#)

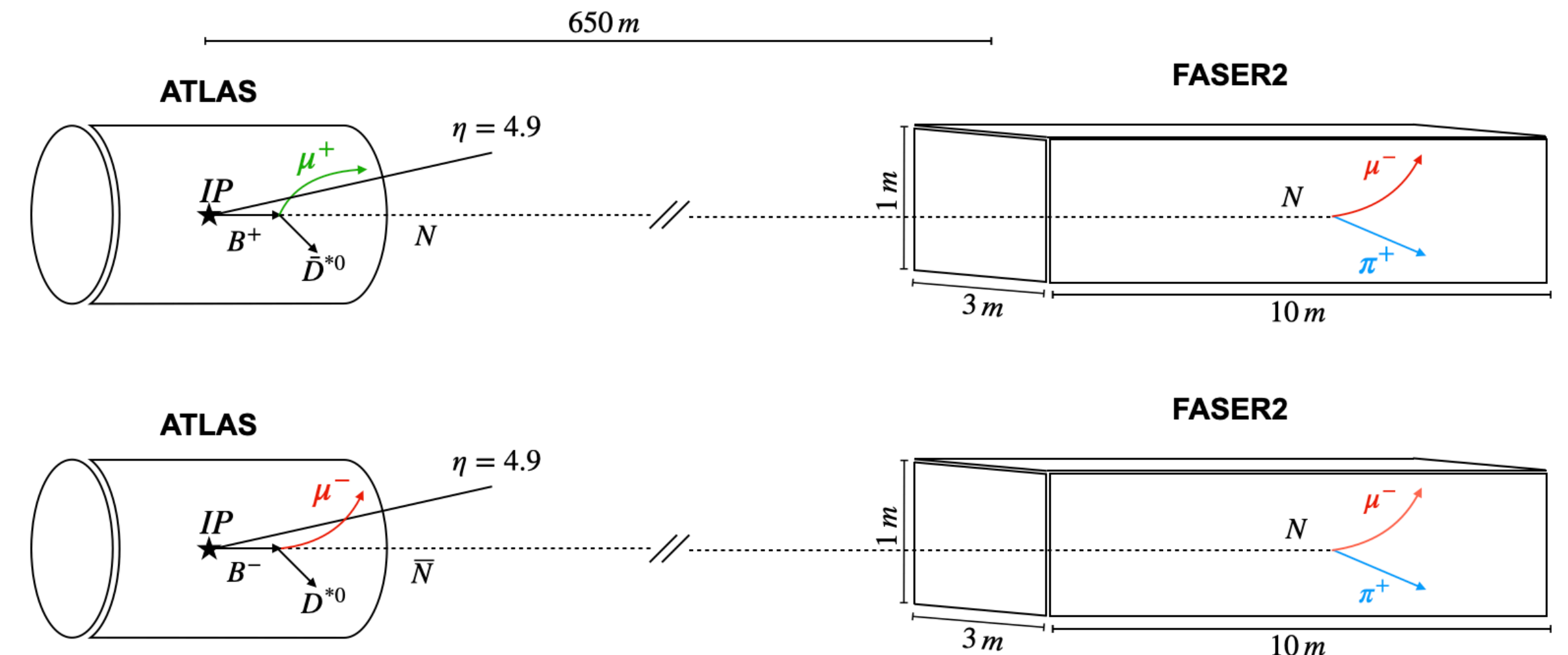
*Collaboration: Jonathan L. Feng, **Alec Hewitt**, Felix Kling, **Daniel La Rocco**, and Daniel Whiteson*

# Outline

1. Introduction to Heavy Neutral Leptons
2. **HNLCalc** - comprehensive python package for HNL phenomenology
3. Simulating **HNLs** in **FORESEE**
4. **Discovery prospects** for FASER/FASER2
5. **Characterizing HNLs**
  - A. Parameter Estimation
  - B. **Dirac vs. Majorana** Discrimination
    - Kinematics
    - **FASER2 as a trigger for ATLAS**

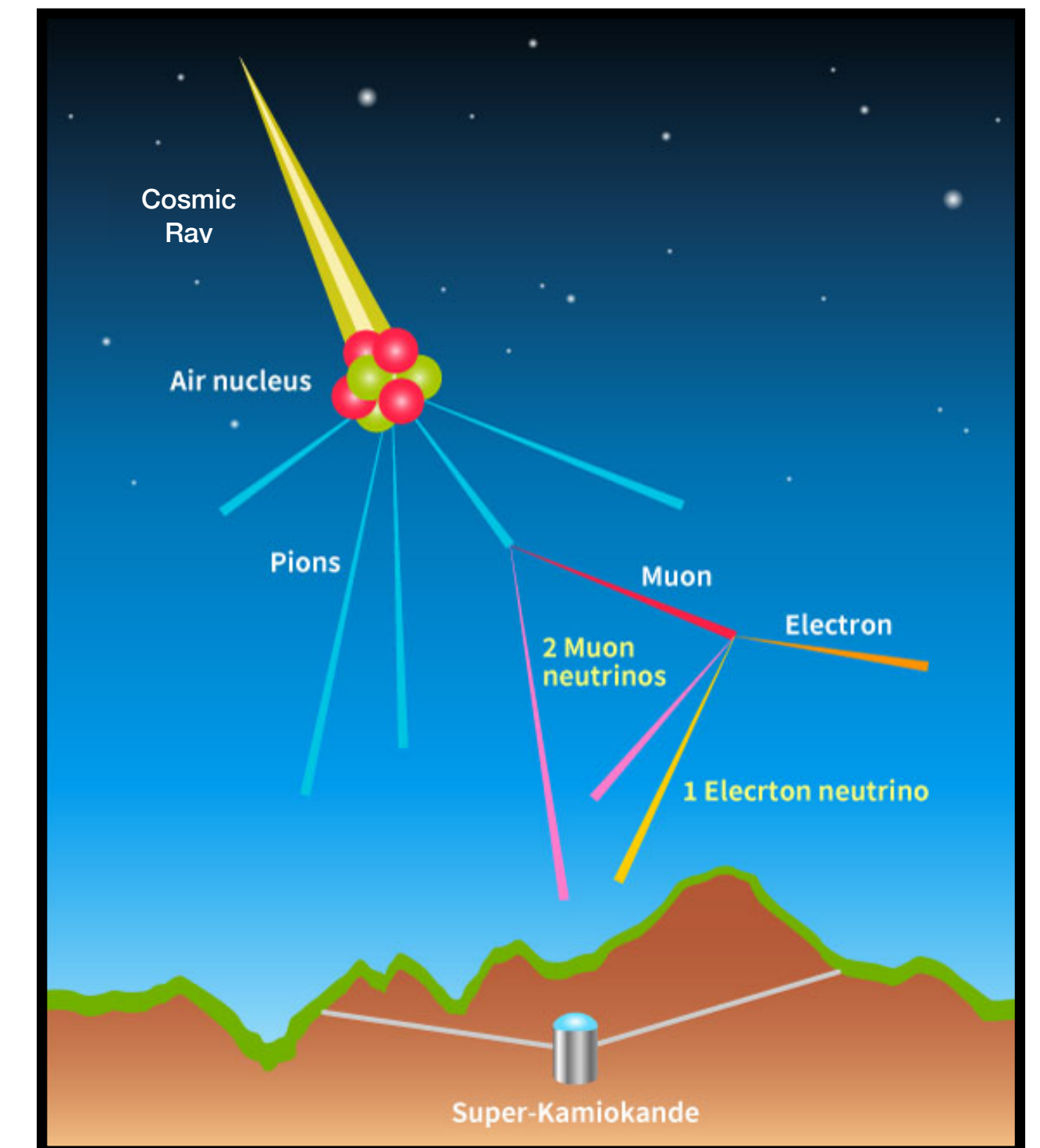


[FASER Collaboration 2207.11427]



# Evidence for physics beyond the SM

- **Neutrino oscillations** are a phenomenon in which a neutrino's lepton flavor ( $e$ ,  $\mu$ , or  $\tau$ ) oscillates as it propagates through space
- First conclusive evidence was discovered at the Super-Kamiokande (Super-K) neutrino observatory
- A deficit in the flux of  $\nu_\mu$ 's produced in cosmic ray collisions in the upper atmosphere (aka atmospheric neutrinos) was observed, implying that they had oscillated into an non-observable flux of  $\nu_\tau$ 's
- This indicates that  $\nu_e$ ,  $\nu_\mu$ , and  $\nu_\tau$  are not eigenstates of the Hamiltonian (i.e. mass eigenstates) and that the mass eigenstates must oscillate with varying phase (i.e. at least one  $\Delta m \neq 0$ )



[<https://www-sk.icrr.u-tokyo.ac.jp/en/sk/about/research/>]

$$|\nu_e(L)\rangle = V_{e1} \exp\left(-i\frac{m_1^2 L}{2E}\right) |\nu_1\rangle + V_{e2} \exp\left(-i\frac{m_2^2 L}{2E}\right) |\nu_2\rangle + V_{e3} \exp\left(-i\frac{m_3^2 L}{2E}\right) |\nu_3\rangle$$

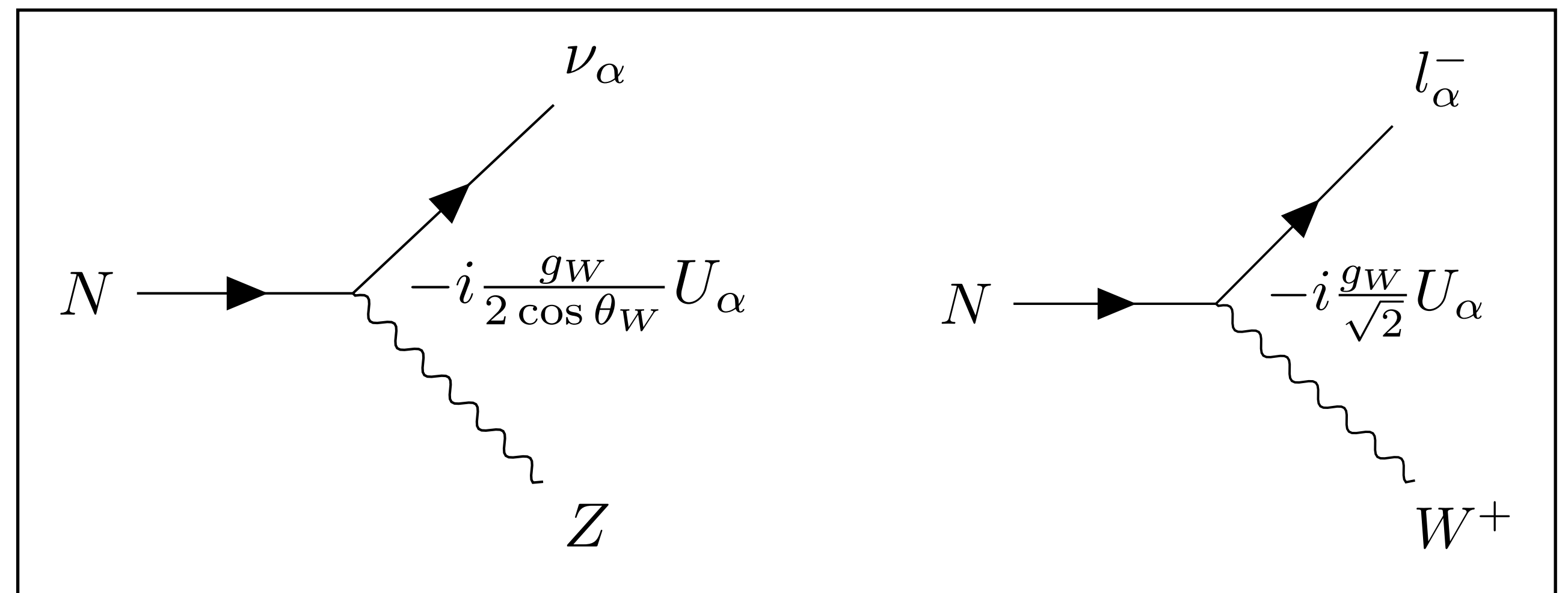


# Heavy Neutral Leptons (HNLs)

- A simple solution to the neutrino mass problem is the introduction of a **right-handed sterile neutrino** (HNL if referring to the mass eigenstate)
- This allows for the inclusion of a **Dirac mass** through a Yukawa interaction after electroweak symmetry breaking (EWSB)
- Additionally, one can incorporate **Majorana mass** terms which violate lepton number
- After diagonalization, the mass eigenstates pick up suppressed neutral current (NC) and charged-current (CC) interactions with the  $Z$  and  $W$  bosons, respectively

$$\mathcal{L} \supset - \underbrace{\sum_{\alpha} Y_{\alpha} \bar{L}_{\alpha} \tilde{\phi} N'}_{\text{Dirac}} - \underbrace{M_R \overline{N'^c} N'}_{\text{Majorana}} - \sum_{\alpha\beta} \frac{C_5^{\alpha\beta}}{\Lambda} \bar{L}_{\alpha} \tilde{\phi} \tilde{\phi}^T L_{\beta}^c + \text{h.c.}$$

$$M_{\nu} = \begin{pmatrix} M_L & M_D \\ M_D^T & M_R \end{pmatrix} \rightarrow \nu_{\alpha} = \sum_{i=1}^3 V_{\alpha i} \nu_i + U_{\alpha} N^c$$





# GeV-scale HNLs

- HNLs in the MeV to GeV range (this work) have been studied as early as the 1970's:
  - [Bjorken & Llewellyn Smith](#) (1973)
  - [Shrock](#) (1974)
- In this range, HNLs can generate neutrino masses through the **Type-I Seesaw** mechanism, in which  $M_L, M_D \ll M_R$  and
 
$$m_l \propto \frac{1}{m_N}$$
- GeV mass HNLs can also provide an explanation for dark matter (DM) and the observed baryon asymmetry of the universe (BAU):
  - [Ghiglieri & Laine](#) (2019)

## Type-1 Seesaw mechanism

$$M_\nu = \begin{pmatrix} M_L & M_D \\ M_D^T & M_R \end{pmatrix}$$

$$M_D = \frac{v}{2} Y \approx i V_{PMNS} \sqrt{\hat{m}_l} O \sqrt{\hat{m}_N} \quad \hat{m}_l = \text{diag}(m_1, m_2, m_3)$$

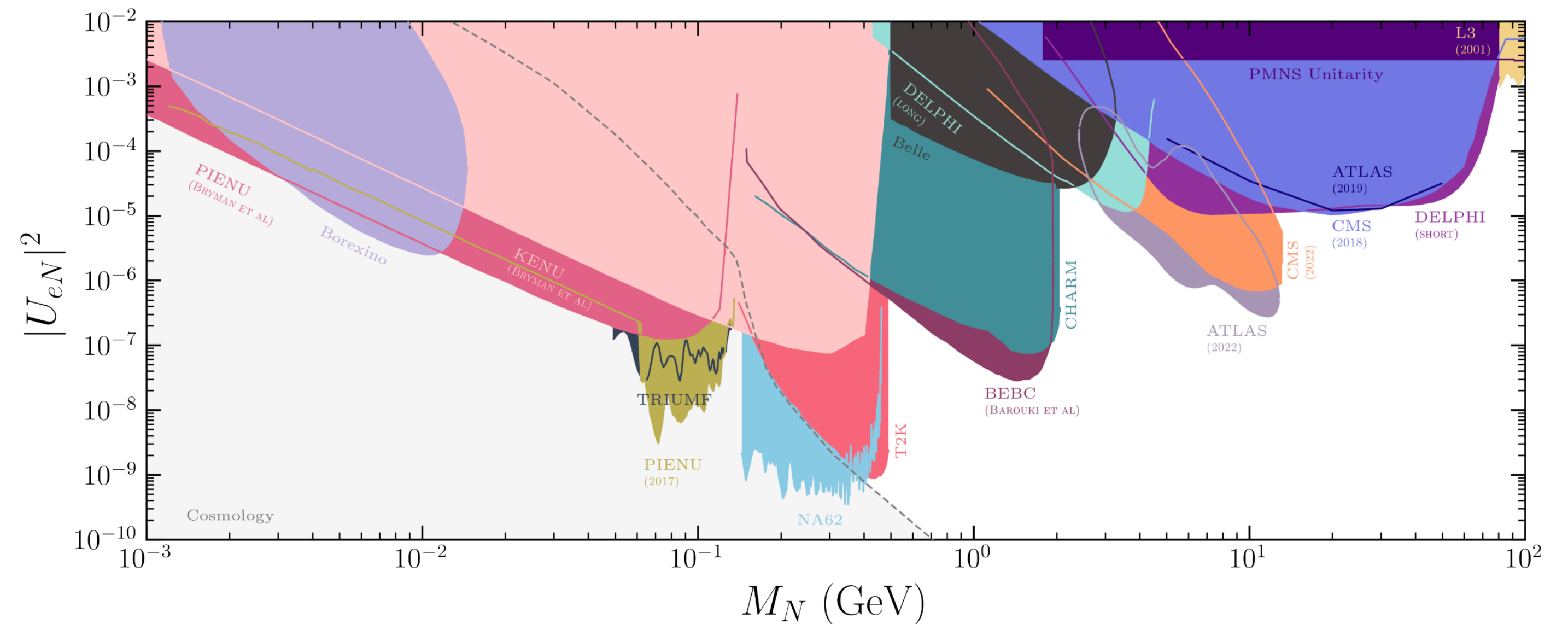
$$U = M_D \hat{m}_N^{-1} \propto \hat{m}_l^{1/2} O \hat{m}_N^{-1/2} \quad \hat{m}_N = \text{diag}(m_4, \dots, m_{3+n})$$

$$M_D \sim \mathcal{O}(keV), m_l \sim \mathcal{O}(0.1 eV) \rightarrow m_N \sim \mathcal{O}(MeV - GeV)$$

# General coupling scenarios

- There is a wide landscape of experiments searching for HNLs in the MeV - GeV range!
- Singly-coupled HNL models have served as well-defined simple benchmarks for these searches to draw exclusion contours (Physics Beyond Colliders Working Group [1901.09966](#))
- However, models with more general mixed couplings are well motivated and appear naturally in many SM extensions! (e.g. models with flavor symmetries)
- Recently, more realistic benchmarks have been proposed (Drewes, Klarić, & López-Pavón [2207.02742](#)):

- $U_\mu = U_\tau \neq 0, \quad U_e = 0$
- $U_e = U_\mu = U_\tau \neq 0$  (Presented in this talk)

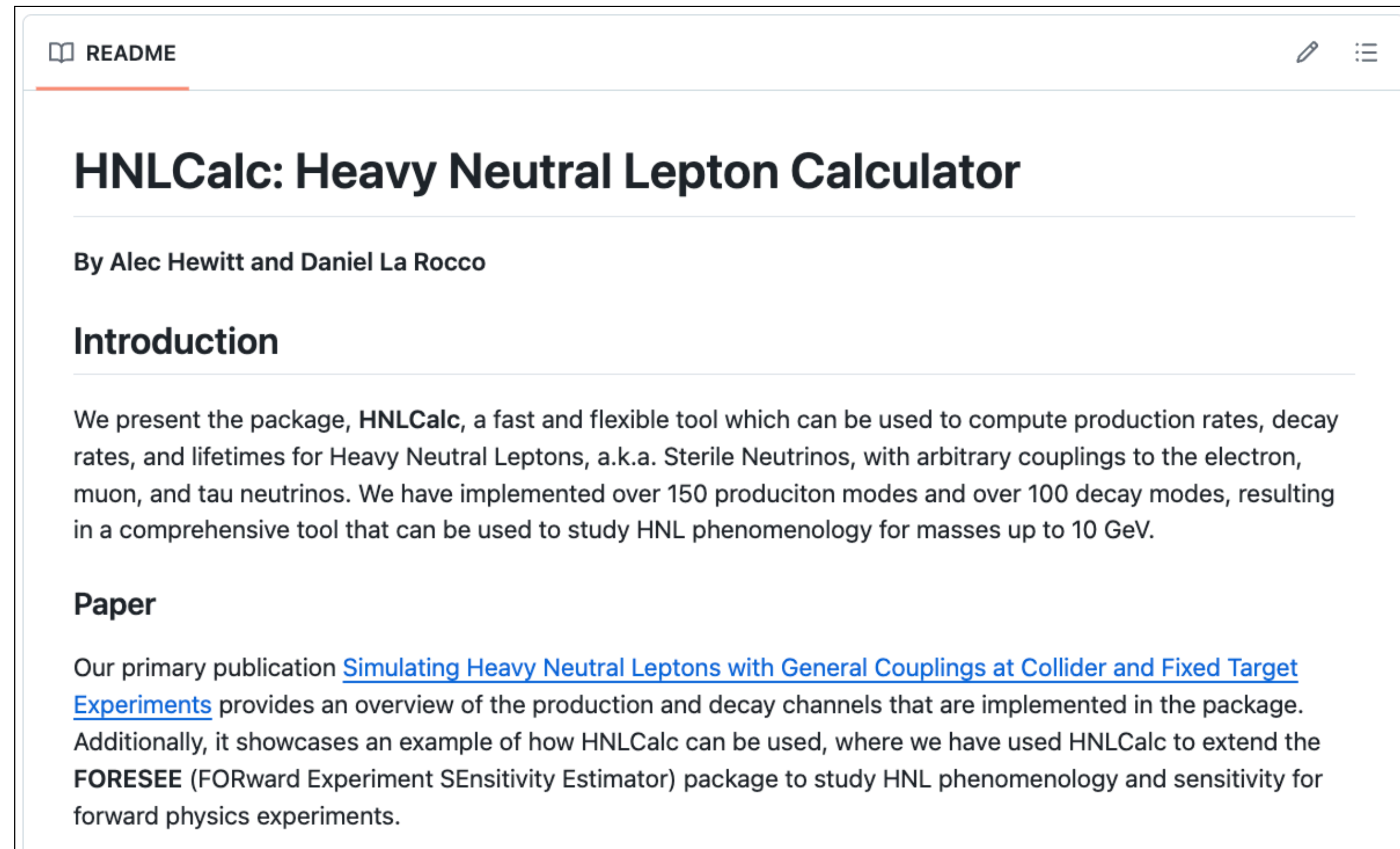


[Fernández-Martínez et al. 2304.06772]

# HNLCalc

*A fast, flexible, and comprehensive python package for calculating HNL production and decay rates with arbitrary couplings*

- Allows user to specify an arbitrary coupling ratio,  $U_e : U_\mu : U_\tau$  and normalization  $\epsilon^2 = |U_e|^2 + |U_\mu|^2 + |U_\tau|^2$ .
- Features:
  - Calculates HNL production branching fractions,  $B(A \rightarrow N\dots)$  and provides differential branching fractions for use in MC event generators
  - Calculates HNL decay branching fractions,  $B(N \rightarrow A\dots)$  and decay lengths,  $c\tau$
  - Includes plotting tools for visualization



Available on [GitHub](#)



# Production/Decay Inputs

## Hadron Decay Constants

$$\langle 0 | \bar{q}_1 \gamma^\mu \gamma_5 q_2 | P(k) \rangle = i f_P k^\mu$$

$$\langle 0 | \bar{q}_1 \gamma^\mu q_2 | V(k, \epsilon) \rangle = i f_V M_V \epsilon^\mu$$

| $P$          | $f_P$ (MeV) | $V$           | $f_V$ (MeV) |
|--------------|-------------|---------------|-------------|
| $\pi^0$ [55] | 130.3       | $\rho^0$ [56] | 220         |
| $\pi^+$ [55] | 130.3       | $\rho^+$ [56] | 220         |
| $K^+$ [55]   | 156.4       | $\omega$ [56] | 195         |
| $\eta$ [57]  | 78.4        | $K^{*+}$ [55] | 204         |
| $\eta'$ [57] | -95.7       | $\phi$ [55]   | 229         |
| $D^+$ [58]   | 222.6       |               |             |
| $D_s^+$ [59] | 280.1       |               |             |
| $B^+$ [21]   | 190         |               |             |
| $B_c^+$ [21] | 480         |               |             |

## Hadron Transition Form Factors

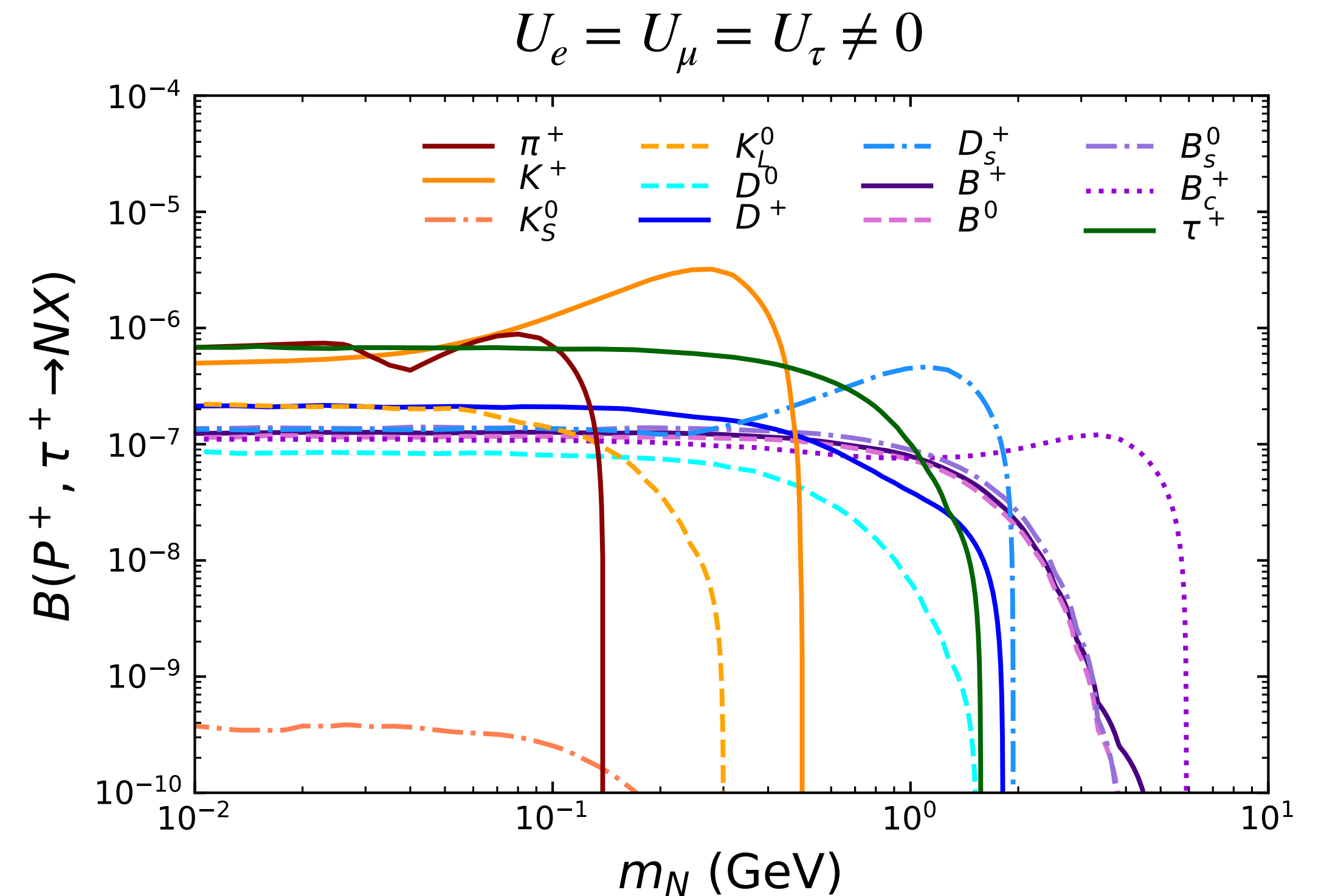
$$\langle P_2 | \bar{q}_1 \gamma^\mu q_2 | P_1 \rangle = f_+(q^2)(p_1^\mu + p_2^\mu) + f_-(q^2)q^\mu$$

$$\langle V | \bar{q}_1 \gamma_\mu \gamma^5 q_2 | P \rangle = i \epsilon^{*\nu} \left[ f(q^2) g_{\mu\nu} + a_+(q^2) p_{1\nu} (p_{1\mu} + p_{2\mu}) + a_-(q^2) p_{1\nu} q_\mu \right]$$

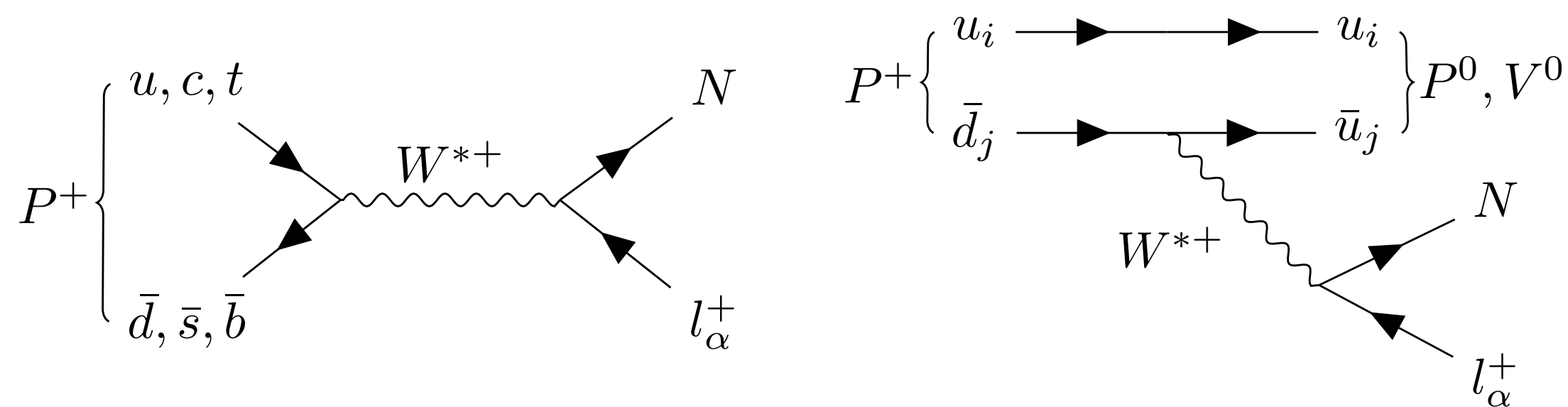
|                                     | $A_0$    |            |            | $A_1$    |            |            | $A_2$    |            |            | $V$    |            |            |       |
|-------------------------------------|----------|------------|------------|----------|------------|------------|----------|------------|------------|--------|------------|------------|-------|
| Decay Channel                       | $f_0(0)$ | $\sigma_1$ | $\sigma_2$ | $f_0(0)$ | $\sigma_1$ | $\sigma_2$ | $f_0(0)$ | $\sigma_1$ | $\sigma_2$ | $f(0)$ | $\sigma_1$ | $\sigma_2$ | $c_V$ |
| $D^0 \rightarrow \rho^-$ [64]       | 0.66     | 0.36       | 0          | 0.59     | 0.50       | 0          | 0.49     | 0.89       | 0          | 0.90   | 0.46       | 0          | 1     |
| $D^0 \rightarrow K^{*-}$ [64]       | 0.76     | 0.17       | 0          | 0.66     | 0.3        | 0          | 0.49     | 0.67       | 0          | 1.03   | 0.27       | 0          | 1     |
| $D^+ \rightarrow \rho^0$ [64]       | 0.66     | 0.36       | 0          | 0.59     | 0.50       | 0          | 0.49     | 0.89       | 0          | 0.90   | 0.46       | 0          | 1/2   |
| $D^+ \rightarrow \omega$ [64]       | 0.66     | 0.36       | 0          | 0.59     | 0.50       | 0          | 0.49     | 0.89       | 0          | 0.90   | 0.46       | 0          | 1/2   |
| $D^+ \rightarrow \bar{K}^{*0}$ [64] | 0.76     | 0.17       | 0          | 0.66     | 0.3        | 0          | 0.49     | 0.67       | 0          | 1.03   | 0.27       | 0          | 1     |
| $D_s^+ \rightarrow K^{*0}$ [64]     | 0.67     | 0.2        | 0          | 0.57     | 0.29       | 0.42       | 0.42     | 0.58       | 0          | 1.04   | 0.24       | 0          | 1     |
| $D_s^+ \rightarrow \phi$ [64]       | 0.73     | 0.10       | 0          | 0.64     | 0.29       | 0          | 0.47     | 0.63       | 0          | 1.10   | 0.26       | 0          | 1     |
| $B^+ \rightarrow \rho^0$ [64]       | 0.30     | 0.54       | 0          | 0.26     | 0.73       | 0.1        | 0.29     | 1.4        | 0.5        | 0.31   | 0.59       | 0          | 1/2   |
| $B^+ \rightarrow \omega$ [64]       | 0.30     | 0.54       | 0          | 0.26     | 0.54       | 0.1        | 0.24     | 1.40       | 0.50       | 0.31   | 0.59       | 0          | 1/2   |
| $B^+ \rightarrow \bar{D}^{*0}$ [64] | 0.69     | 0.58       | 0          | 0.66     | 0.78       | 0          | 0.62     | 1.04       | 0          | 0.76   | 0.57       | 0          | 1     |
| $B^0 \rightarrow \rho^-$ [64]       | 0.30     | 0.54       | 0          | 0.26     | 0.54       | 0.1        | 0.24     | 1.40       | 0.50       | 0.31   | 0.59       | 0          | 1     |
| $B^0 \rightarrow D^{*-}$ [64]       | 0.69     | 0.58       | 0          | 0.66     | 0.78       | 0          | 0.62     | 1.04       | 0          | 0.76   | 0.57       | 0          | 1     |
| $B_s^0 \rightarrow K^{*-}$ [64]     | 0.37     | 0.60       | 0.16       | 0.29     | 0.86       | 0.6        | 0.26     | 1.32       | 0.54       | 0.38   | 0.66       | 0.30       | 1     |
| $B_s^0 \rightarrow D_s^{*-}$ [71]   | 0.67     | 0.35       | 0          | 0.70     | 0.463      | 0          | 0.75     | 1.04       | 0          | 0.95   | 0.372      | 0          | 1     |
| $B_c^+ \rightarrow D^{*0}$ [69]     | 0.56     | 0          | 0          | 0.64     | 0          | 0          | -1.17    | 0          | 0          | 0.98   | 0          | 0          | 1     |

# HNL Production

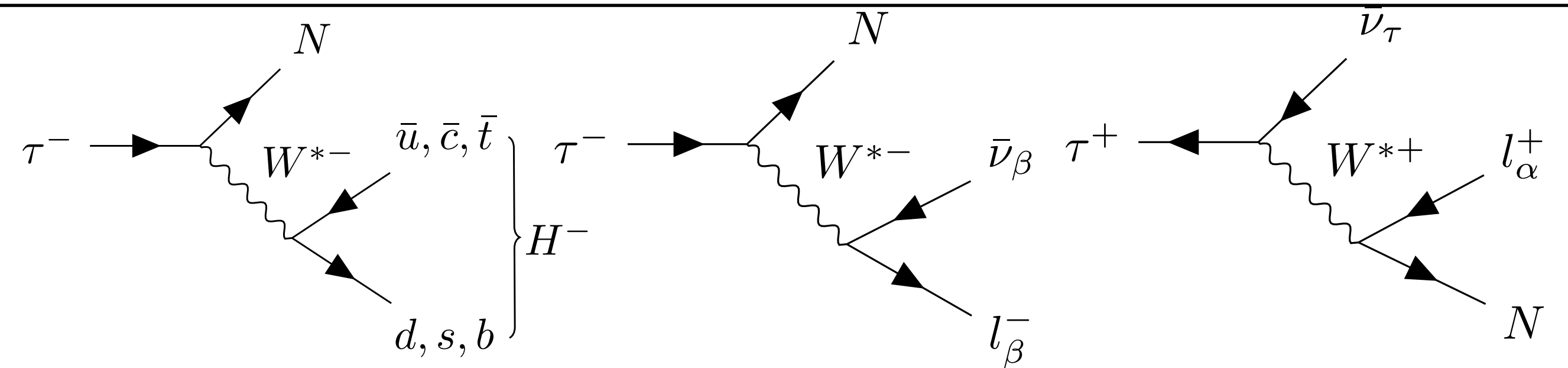
- HNLCalc includes HNL production from the decay of pseudoscalar mesons and tau leptons
- For HNLs in the mass range 100 MeV to 10 GeV, these are the dominant production mechanisms



## Pseudoscalar



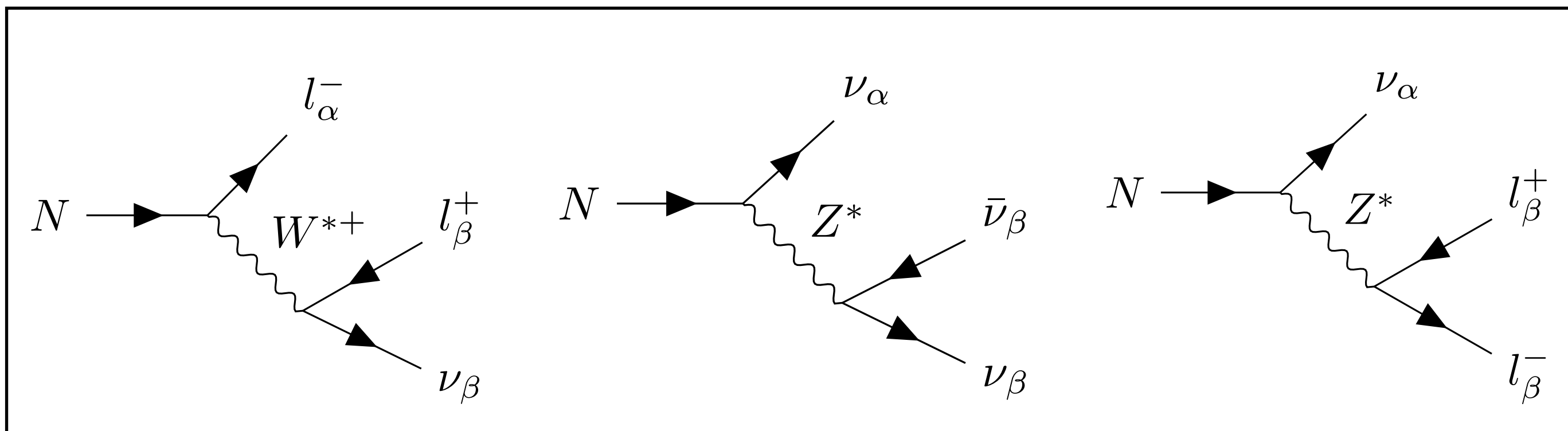
## Tau



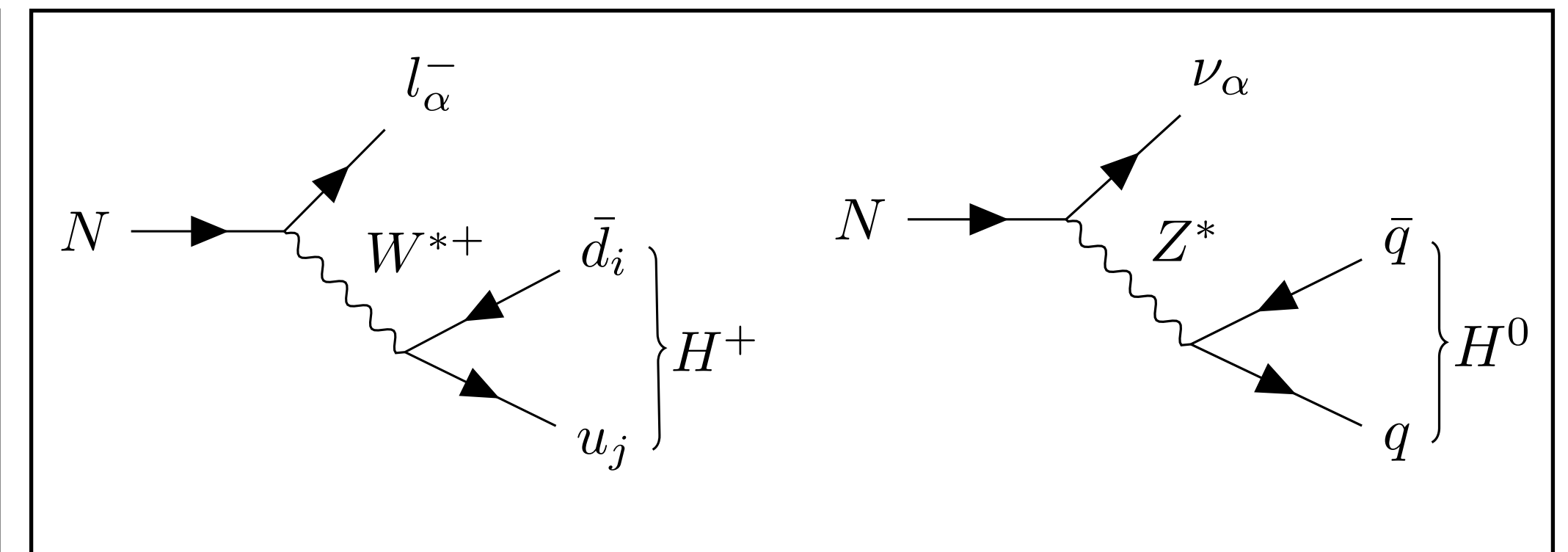
# HNL Decay

- HNLs can decay at tree-level into leptonic or hadronic final states through virtual W and Z exchange
- In order to properly simulate detector response, one must accurately represent the final states
  - i.e.  $N \rightarrow \nu \rho \rightarrow \nu \pi^+ \pi^-$  vs  $N \rightarrow \nu \pi^0 \rightarrow \nu \gamma \gamma$
  - Quark-level final states are insufficient!

## Leptonic



## Hadronic

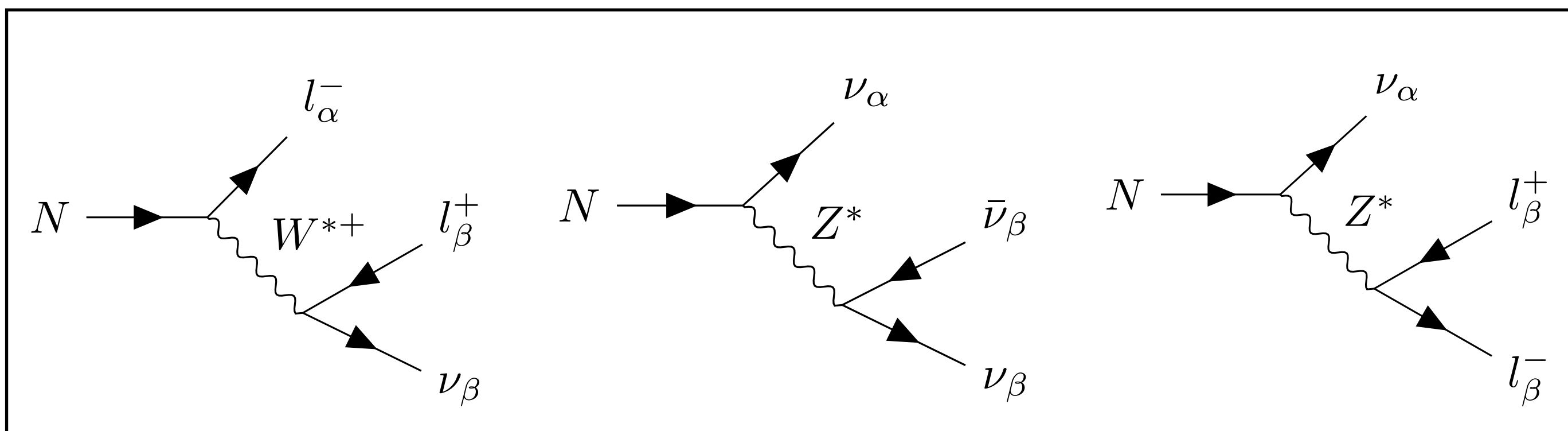




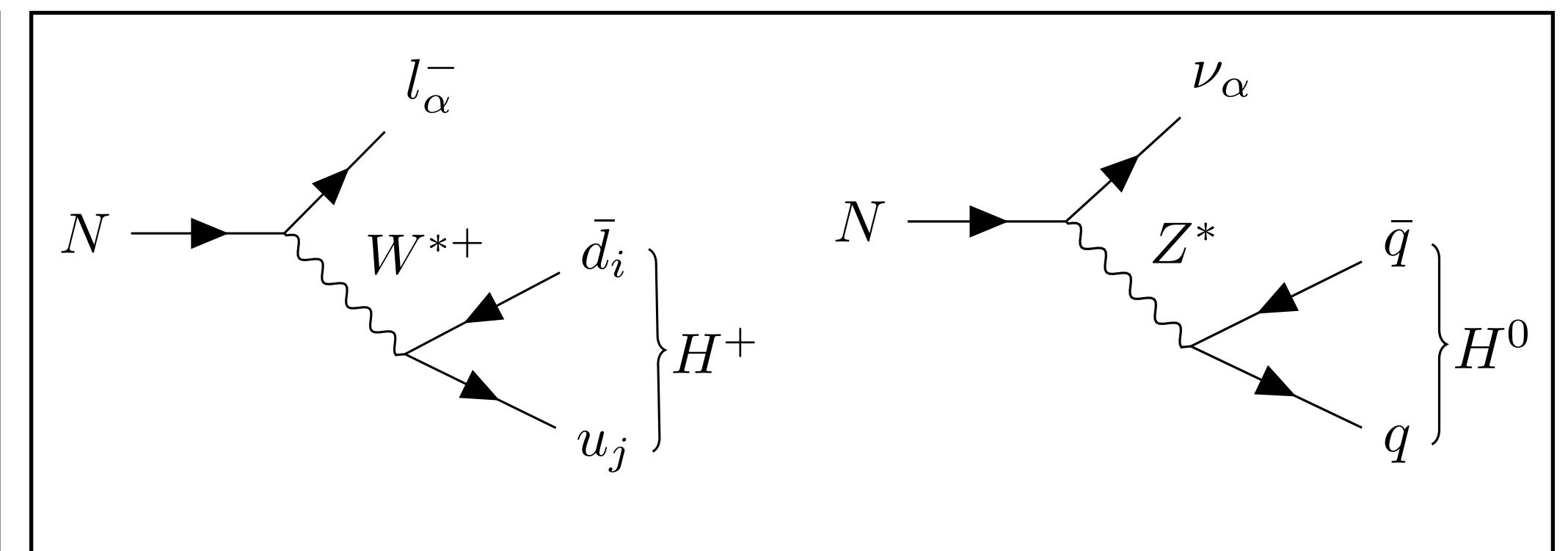
# HNL Decay

- However, for  $m_N > 1$  GeV, decays into single hadronic states are insufficient for modeling the total HNL decay width, since in this regime multi-meson final states become relevant
- We adopt the approach in Bondarenko et al. (1805.08567) for calculating the total hadronic width:
  - For  $m_N < 1$  GeV: Single meson decays
  - For  $m_N > 1$  GeV: Quark-level decays + QCD Correction

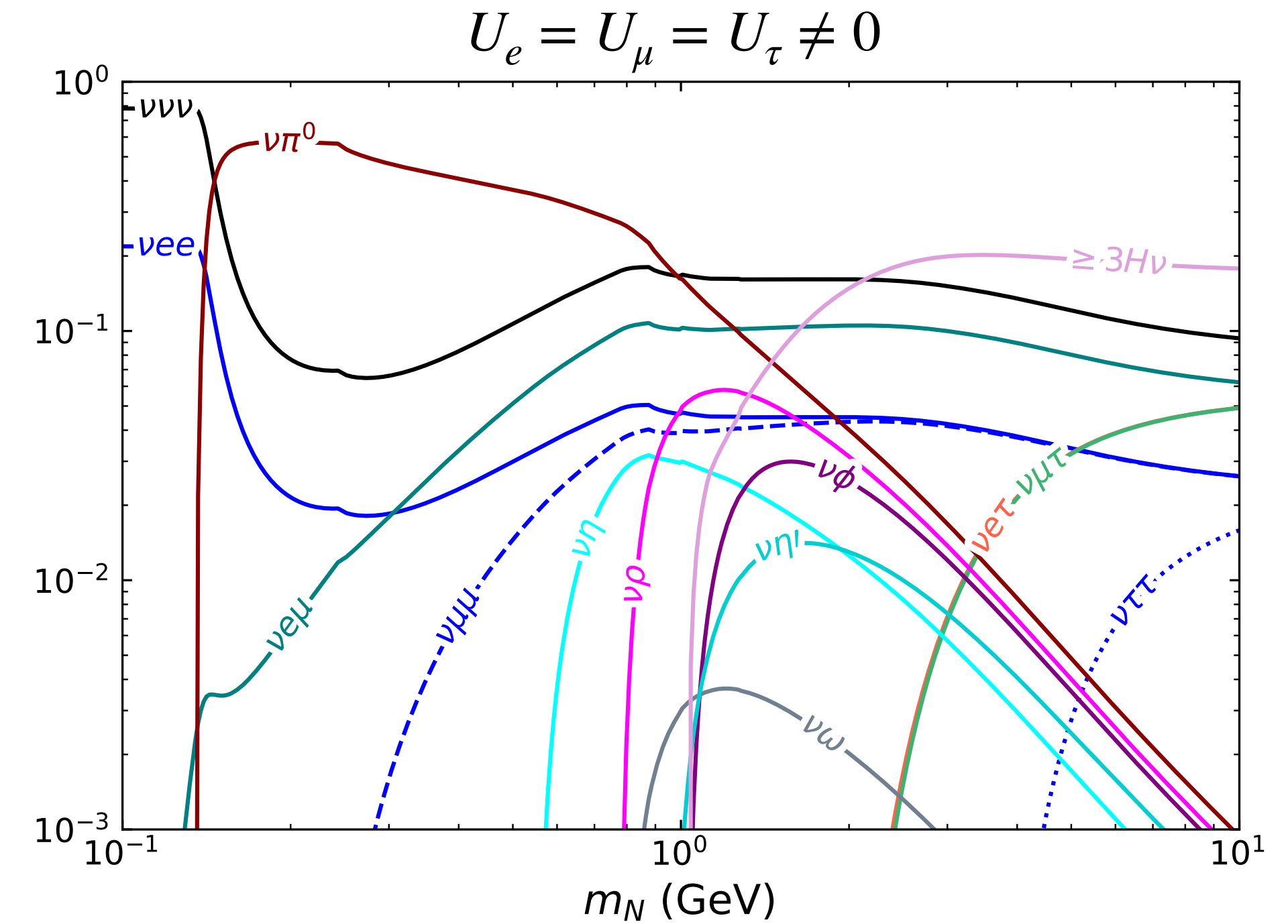
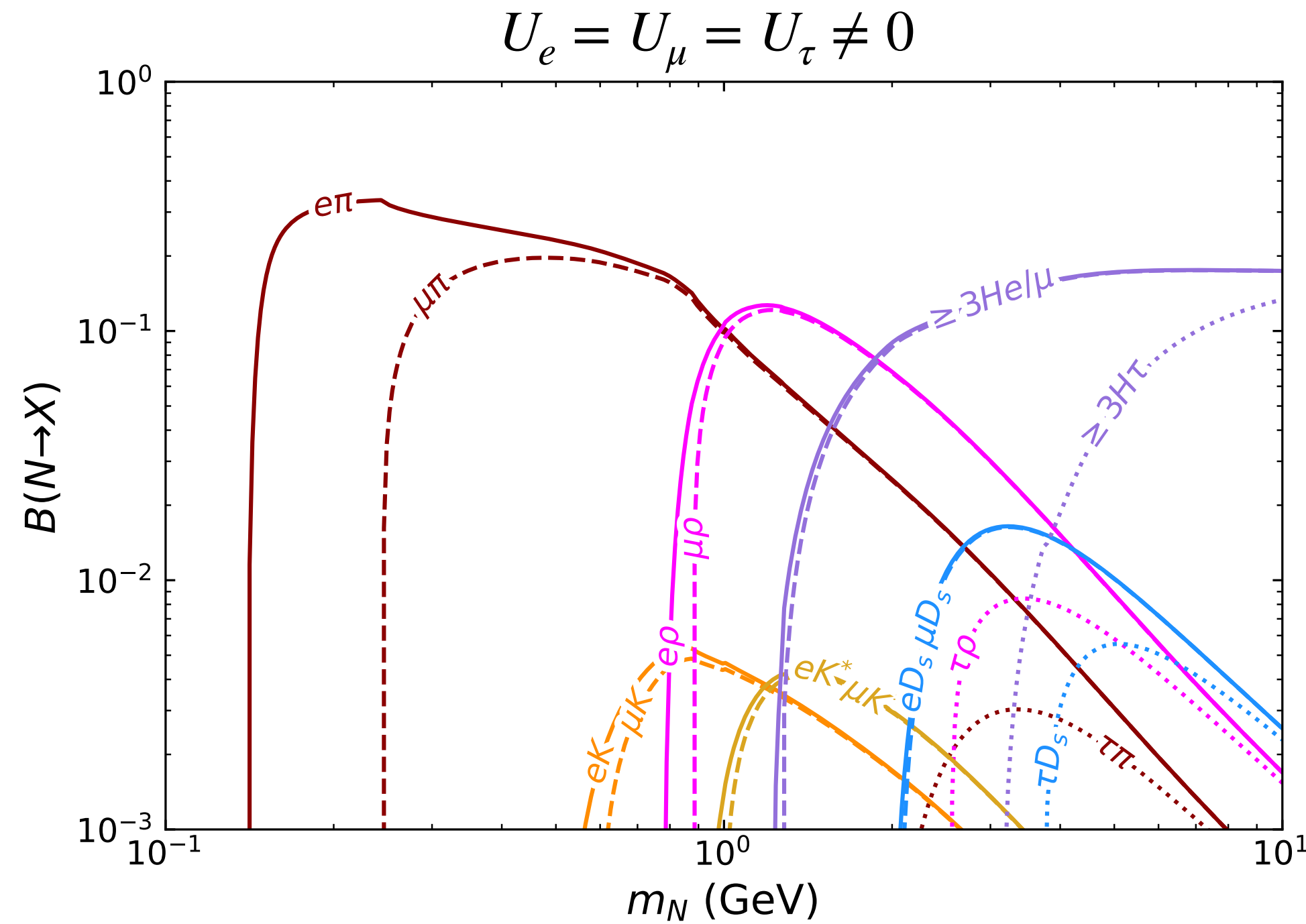
## Leptonic



## Hadronic



# HNL Decay



- HNLCalc includes HNL decays into leptonic and hadronic final states
- HNLs with masses  $\sim 130$  MeV - 1 GeV decay dominantly into  $\pi^\pm/\pi^0$
- Above 1 GeV, multi-hadron and leptonic decays become most relevant

# HNLCalc Summary

| HNL Decay Modes       |            |                           |                               |                                 |                   |                   |                  |
|-----------------------|------------|---------------------------|-------------------------------|---------------------------------|-------------------|-------------------|------------------|
| $\nu l^+ l^-$         | Fig. 3 (a) | $\nu_l e^+ e^-$           | $\nu_l \mu^+ \mu^-$           | $\nu_l \tau^+ \tau^-$           |                   |                   |                  |
| $l^\pm \nu_l l'^\mp$  | Fig. 3 (b) | $l^\pm \nu_e e^\mp$       | $l^\pm \nu_\mu \mu^\mp$       | $l^\pm \nu_\tau \tau^\mp$       |                   |                   |                  |
| $\nu_l \bar{\nu} \nu$ | Fig. 3 (c) | $\nu_l \bar{\nu}_e \nu_e$ | $\nu_l \bar{\nu}_\mu \nu_\mu$ | $\nu_l \bar{\nu}_\tau \nu_\tau$ |                   |                   |                  |
| $\nu_l H^0$           | Fig. 3 (d) | $\nu_l \pi^0$             | $\nu_l \eta$                  | $\nu_l \eta'$                   | $\nu_l \rho^0$    | $\nu_l \omega$    | $\nu_l \phi$     |
| $l^\pm H^\mp$         | Fig. 3 (e) | $l^\pm \pi^\mp$           | $l^\pm K^\mp$                 | $l^\pm D^\mp$                   | $l^\pm D_s^\mp$   | $l^\pm \rho^\mp$  | $l^\pm K^{*\mp}$ |
| $\nu_l q \bar{q}$     | Fig. 3 (d) | $\nu_l u \bar{u}$         | $\nu_l d \bar{d}$             | $\nu_l s \bar{s}$               | $\nu_l c \bar{c}$ | $\nu_l b \bar{b}$ |                  |
| $l^\pm u \bar{d}'$    | Fig. 3 (e) | $l^- \bar{u} \bar{d}$     | $l^- \bar{u} \bar{s}$         | $l^- \bar{u} \bar{b}$           | $l^+ \bar{u} d$   | $l^+ \bar{u} s$   | $l^+ \bar{u} b$  |
|                       |            | $l^- \bar{c} \bar{d}$     | $l^- \bar{c} \bar{s}$         | $l^- \bar{c} \bar{b}$           | $l^+ \bar{c} d$   | $l^+ \bar{c} s$   | $l^+ \bar{c} b$  |

| HNL Production Processes       |              |   |                                    |                                   |                                      |                                      |                                    |
|--------------------------------|--------------|---|------------------------------------|-----------------------------------|--------------------------------------|--------------------------------------|------------------------------------|
| $P \rightarrow l N$            | Fig. 1 (a)   | $\pi^+ \rightarrow l^+ N$                 | $K^+ \rightarrow l^+ N$            | $D^+ \rightarrow l^+ N$           | $D_s^+ \rightarrow l^+ N$            | $B^+ \rightarrow l^+ N$              | $B_c^+ \rightarrow l^+ N$          |
| $P \rightarrow P' l N$         | Fig. 1 (b)   | $K^+ \rightarrow \pi^0 l^+ N$             | $K_S \rightarrow \pi^+ l^- N$      | $K_L \rightarrow \pi^+ l^- N$     | $D^0 \rightarrow K^- l^+ N$          | $\bar{D}^0 \rightarrow \pi^+ l^- N$  | $D^+ \rightarrow \pi^0 l^+ N$      |
|                                |              | $D^+ \rightarrow \eta l^+ N$              | $D^+ \rightarrow \eta' l^+ N$      | $D^+ \rightarrow \bar{K}^0 l^+ N$ | $D_s^+ \rightarrow \bar{K}^0 l^+ N$  | $D_s^+ \rightarrow \eta l^+ N$       | $D_s^+ \rightarrow \eta' l^+ N$    |
|                                |              | $B^+ \rightarrow \pi^0 l^+ N$             | $B^+ \rightarrow \eta l^+ N$       | $B^+ \rightarrow \eta' l^+ N$     | $B^+ \rightarrow \bar{D}^0 l^+ N$    | $B^0 \rightarrow \pi^- l^+ N$        | $B^0 \rightarrow D^- l^+ N$        |
|                                |              | $B_s^0 \rightarrow K^- l^+ N$             | $B_s^0 \rightarrow D_s^- l^+ N$    | $B_c^+ \rightarrow D^0 l^+ N$     | $B_c^+ \rightarrow \eta_c l^+ N$     | $B_c^+ \rightarrow B^0 l^+ N$        | $B_c^+ \rightarrow B_s^0 l^+ N$    |
| $P \rightarrow V l N$          | Fig. 1 (b)   | $D^0 \rightarrow \rho^- l^+ N$            | $D^0 \rightarrow K^{*-} l^+ N$     | $D^+ \rightarrow \rho^0 l^+ N$    | $D^+ \rightarrow \omega l^+ N$       | $D^+ \rightarrow \bar{K}^{*0} l^+ N$ | $D_s^+ \rightarrow K^{*0} l^+ N$   |
|                                |              | $D_s^+ \rightarrow \phi l^+ N$            | $B^+ \rightarrow \rho^0 l^+ N$     | $B^+ \rightarrow \omega l^+ N$    | $B^+ \rightarrow \bar{D}^{*0} l^+ N$ | $B^0 \rightarrow \rho^- l^+ N$       | $B^0 \rightarrow D^{*-} l^+ N$     |
|                                |              | $B_s^0 \rightarrow K^{*-} l^+ N$          | $B_s^0 \rightarrow D_s^{*-} l^+ N$ | $B_c^+ \rightarrow D^{*0} l^+ N$  | $B_c^+ \rightarrow J/\psi l^+ N$     | $B_c^+ \rightarrow B^{*0} l^+ N$     | $B_c^+ \rightarrow B_s^{*0} l^+ N$ |
| $\tau \rightarrow H N$         | Fig. 1 (c)   | $\tau^+ \rightarrow \pi^+ N$              | $\tau^+ \rightarrow K^+ N$         | $\tau^+ \rightarrow \rho^+ N$     | $\tau^+ \rightarrow K^{*+} N$        |                                      |                                    |
| $\tau^+ \rightarrow l^+ \nu N$ | Fig. 1 (d,e) | $\tau^+ \rightarrow l^+ \bar{\nu}_\tau N$ | $\tau^+ \rightarrow l^+ \nu_l N$   |                                   |                                      |                                      |                                    |

**Over 150 production modes and 100 decay channels implemented!**

## Decay Formulae:

Coloma, Fernandez-Martinez, Gonzalez-Lopez, Hernandez-Garcia & Pavlovic  
[2007.03701](#)

Bondarenko, Boyarsky, Gorbunov, & Ruchayskiy [1805.08567](#)

## Production Formulae:

Gorbunov & Shaposhnikov [0705.1729](#)

## Form Factors:

Melikhov & Stech [0001113](#)

## Decay Constants:

Faustov & Galkin [1212.3167](#)

Ivanov, Korner, & Santorelli [0007169](#)

Chang, Li X.N., Li X.Q., Su [1805.00718](#)

Feldmann [9907491](#)

Artuso et al. [0508057](#)

Stone [0610026](#)



# Application: HNLs in FORESEE

*Collaboration: Jonathan L. Feng, **Alec Hewitt**, Felix Kling, and **Daniel La Rocco***

[2405.07330 \(2024\)](#)

# Application: HNLs in FORESEE

- The FORward Experiment SEnsitivity Estimator (FORESEE) is a MC event generator and reach estimator used to simulate forward physics LLP searches with customizable detector geometries
- Contains a model library with various BSM Models: ALPs, Dark Photons, Dark Higgs, etc...
- In our work, we have utilized HNLCalc to extend the FORESEE model library to include HNLs, which we will use this to compute sensitivity estimates for FASER and FASER2

[README](#) [MIT license](#)

## FORESEE: FORward Experiment SEnsitivity Estimator

By Felix Kling and Sebastian Trojanowski

arXiv 2105.07077 License MIT

### Introduction

We present the numerical package **FORward Experiment SEnsitivity Estimator**, or **FORESEE**, that can be used to simulate the expected sensitivity reach of experiments placed in the far-forward direction from the proton-proton interaction point. We also provide a comprehensive list of validated forward spectra of various SM species.

### Paper

Our main publication [FORESEE: FORward Experiment SEnsitivity Estimator for the LHC and future hadron colliders](#) provides an overview over this package. We recommend reading it first before jumping into the code.

Available on [GitHub](#)

## FORESEE Models: Heavy Neutral Leptons (HNLs)

### Load Libraries

```
[ ]: ...  
from HNLCalc import *
```

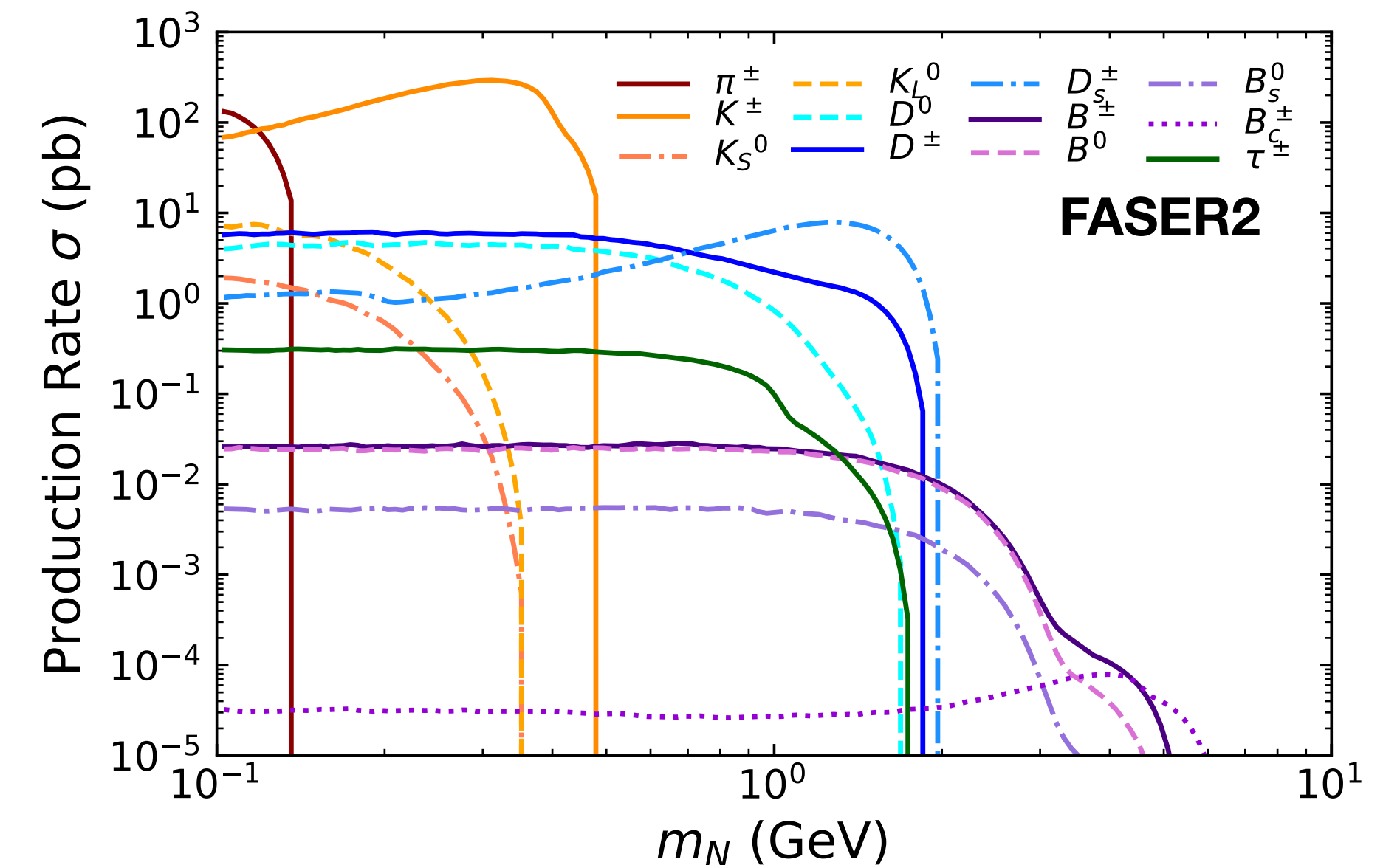
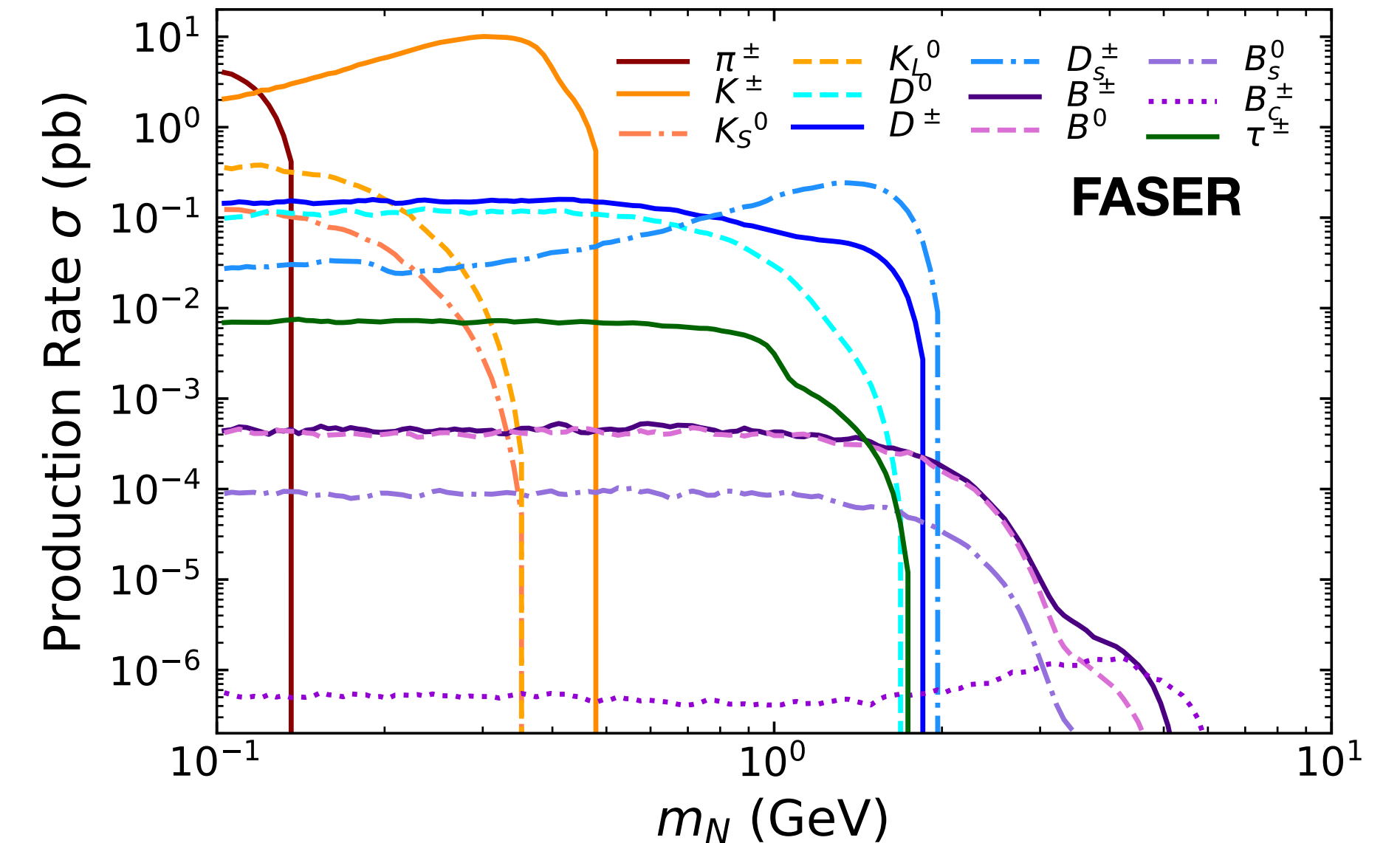
### 1. Specifying the Model

Heavy Neutral Leptons, denoted by  $N$ , are fermionic gauge singlets that can be added as an extension to the standard model. These HNLs mix with the SM active neutrinos, and thus pick up couplings to the SM which are suppressed by a small mixing angle,  $U_\alpha$  for  $\alpha = e, \mu, \tau$ . The phenomenology of these interactions can be described by the following Lagrangian:

$$\mathcal{L} \supset -m_N \bar{N}^c N - \frac{1}{\sqrt{2}} g \sum_{\alpha=e,\mu,\tau} U_\alpha^* W_\mu^+ \bar{N}^c \gamma^\mu l_\alpha - \frac{1}{2 \cos \theta_W} g \sum_{\alpha=e,\mu,\tau} U_\alpha^* Z_\mu \bar{N}^c \gamma^\mu \nu_\alpha + \text{h.c.}$$

# Hadron Production

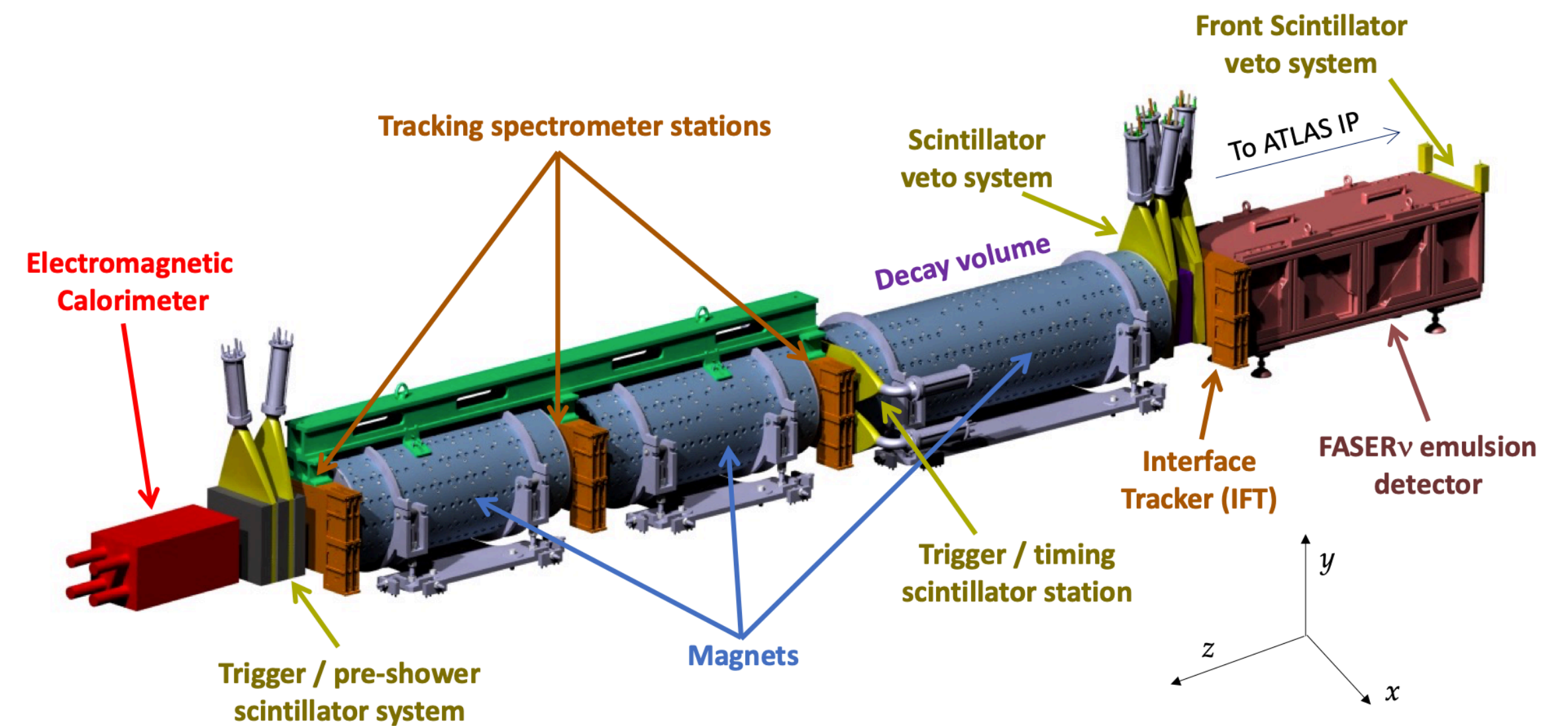
- FORESEE generates HNL production rates through sampling of decays of parent particles, whose spectra are generated via MC event generators
- The primary source of uncertainty in HNL production rates is the modeling of the hadron fluxes
- For light hadrons ( $\pi$ ,  $K$ ), we estimate this uncertainty by considering the predictions of EPOS-LHC, QGSJET 2.04, and Sibyll 2.3d
- For heavy hadrons and taus, the uncertainty is estimated by considering predictions from POWHEG+Pythia with different choices of factorization scale



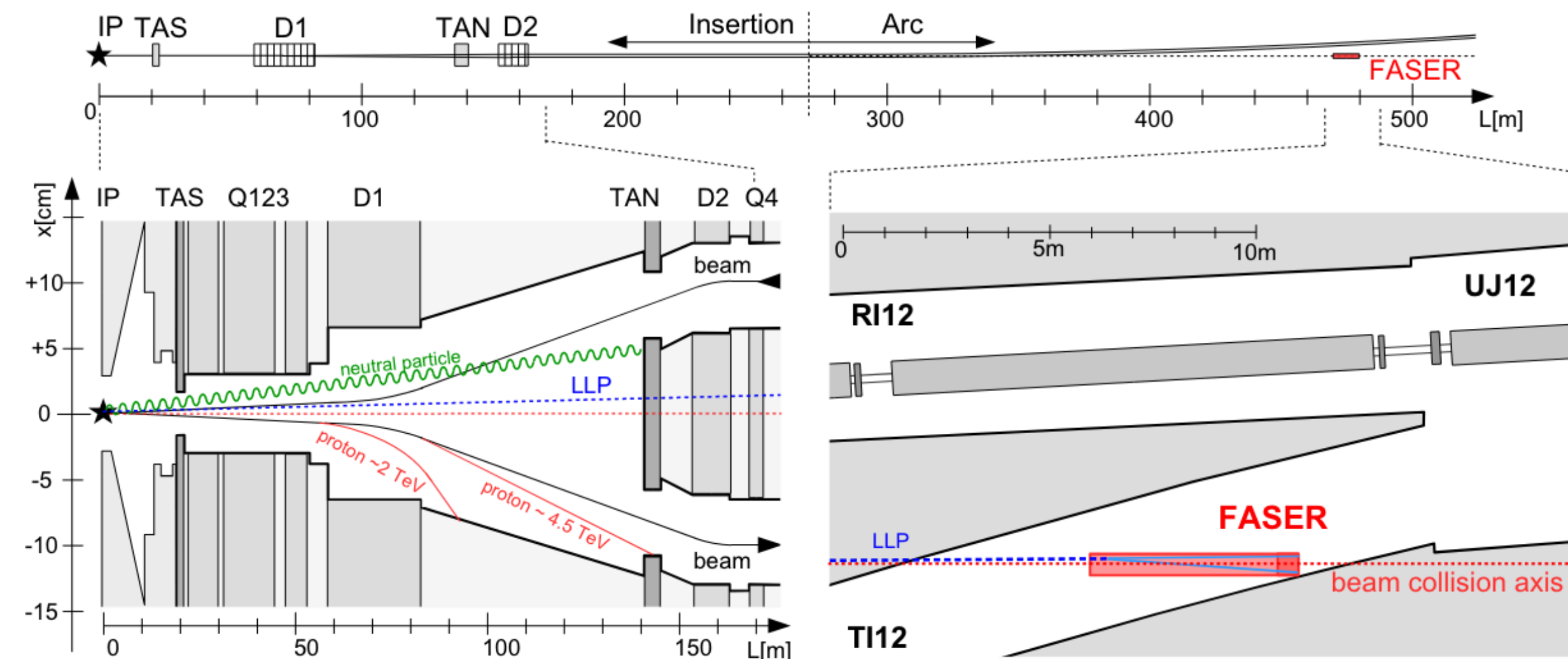


# FASER

- The ForwArd Search ExpeRiment (FASER) is an experiment at the LHC designed to detect forward boosted LLPs produced at the ATLAS interaction point
- Located 480 meters down the beam axis, through 100m of rock
- Features a cylindrical decay volume with radius  $R = 10$  cm and length  $\Delta = 1.5$  m
- Angular coverage of  $\theta \lesssim 0.2$  mrad ( $\eta \gtrsim 9.2$ )



[FASER Collaboration 2207.11427]



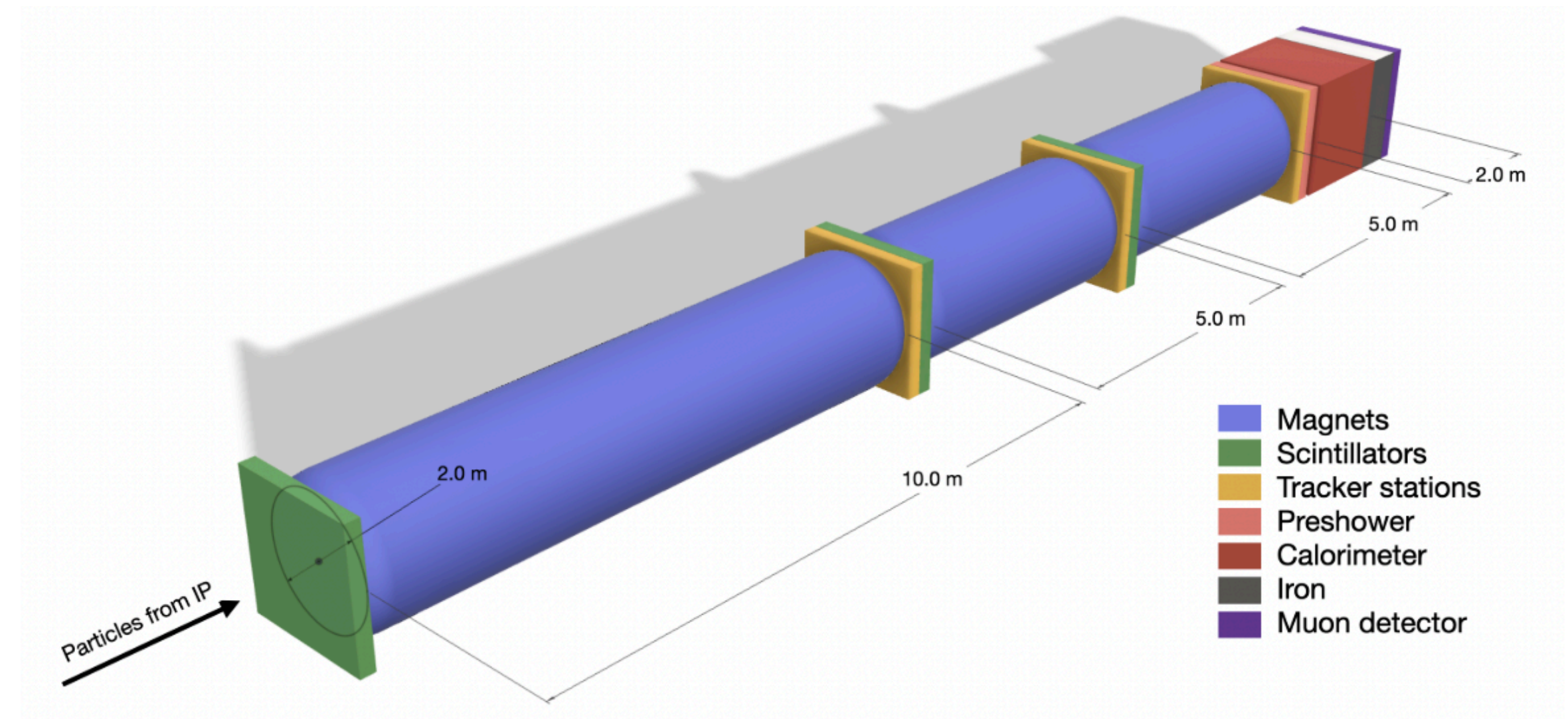
[FASER Collaboration 1811.12522]



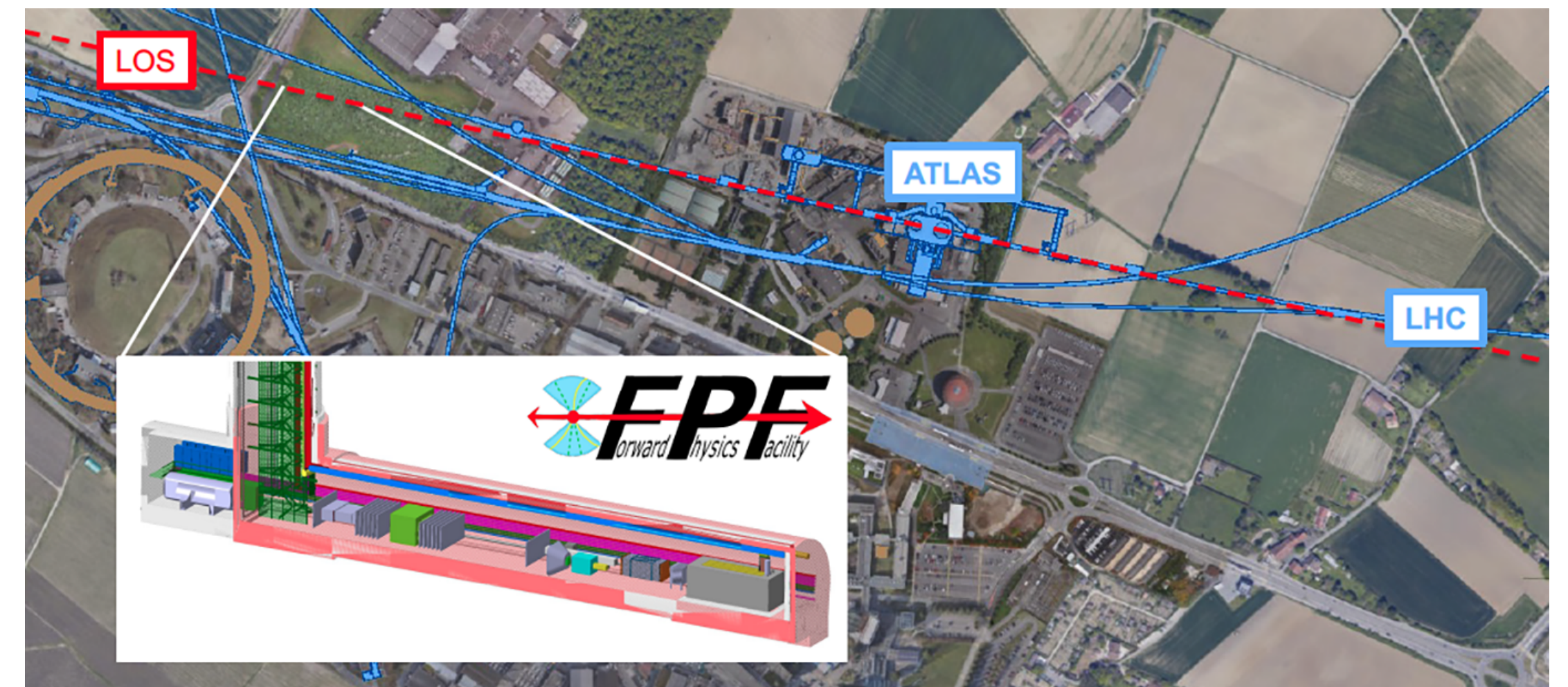


# FPF: FASER2

- The Forward Physics Facility (FPF) is a proposed underground facility to house a suite of forward physics experiments during the High-Luminosity LHC era (HL-LHC)
- FASER2 is a proposed FPF experiment with an enlarged decay volume compared to FASER, which could extend the physics reach of the FASER program significantly
- Located 650 meters down the beam axis, with a rectangular decay volume with cross-section  $3 \text{ m} \times 1 \text{ m}$  and length  $\Delta = 10 \text{ m}$ .
- Angular coverage of  $\theta \lesssim 2.4 \text{ mrad}$  ( $\eta \gtrsim 6.7$ )



[Feng et al. 2203.05090]



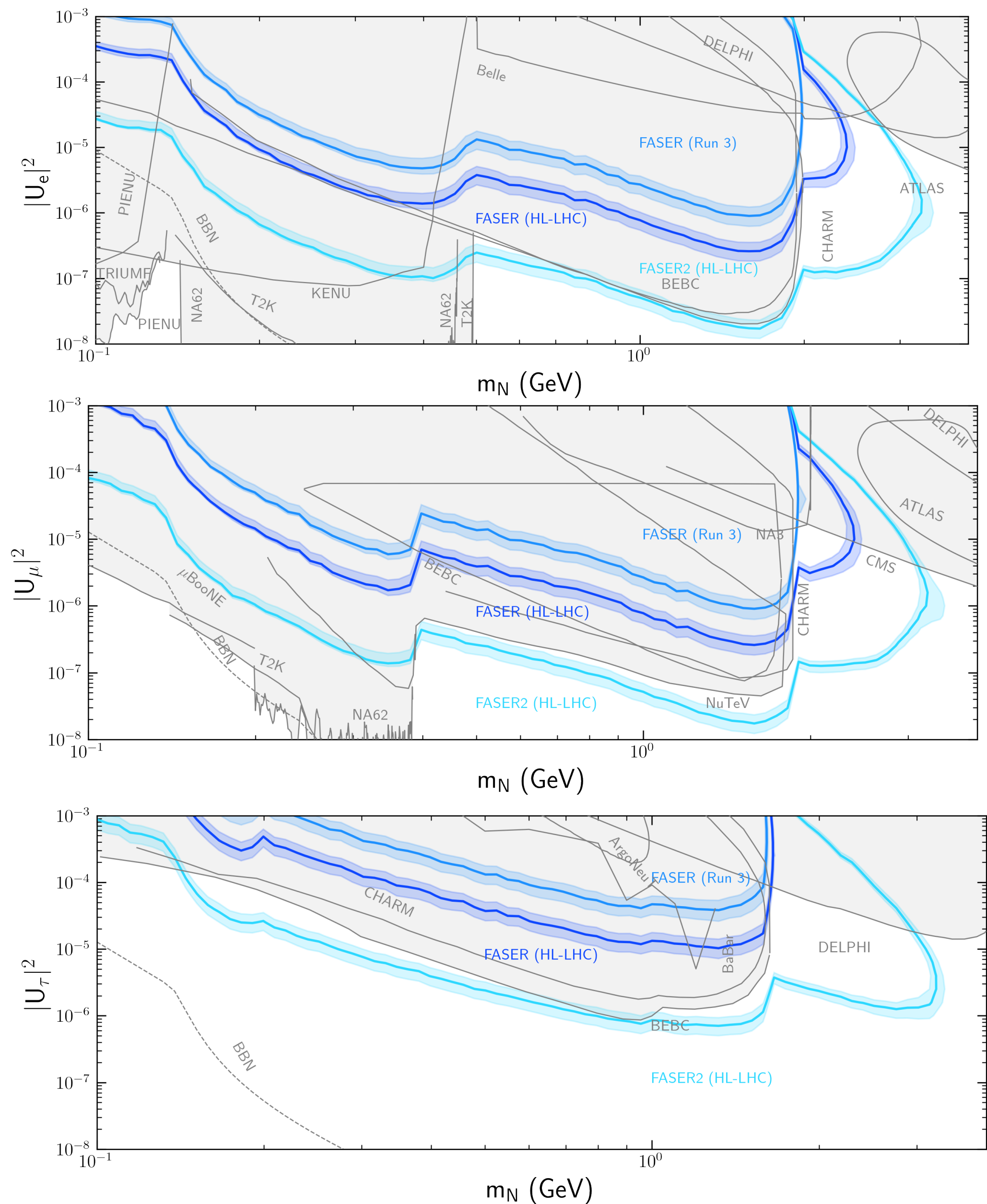
[<https://fpf.web.cern.ch/>]





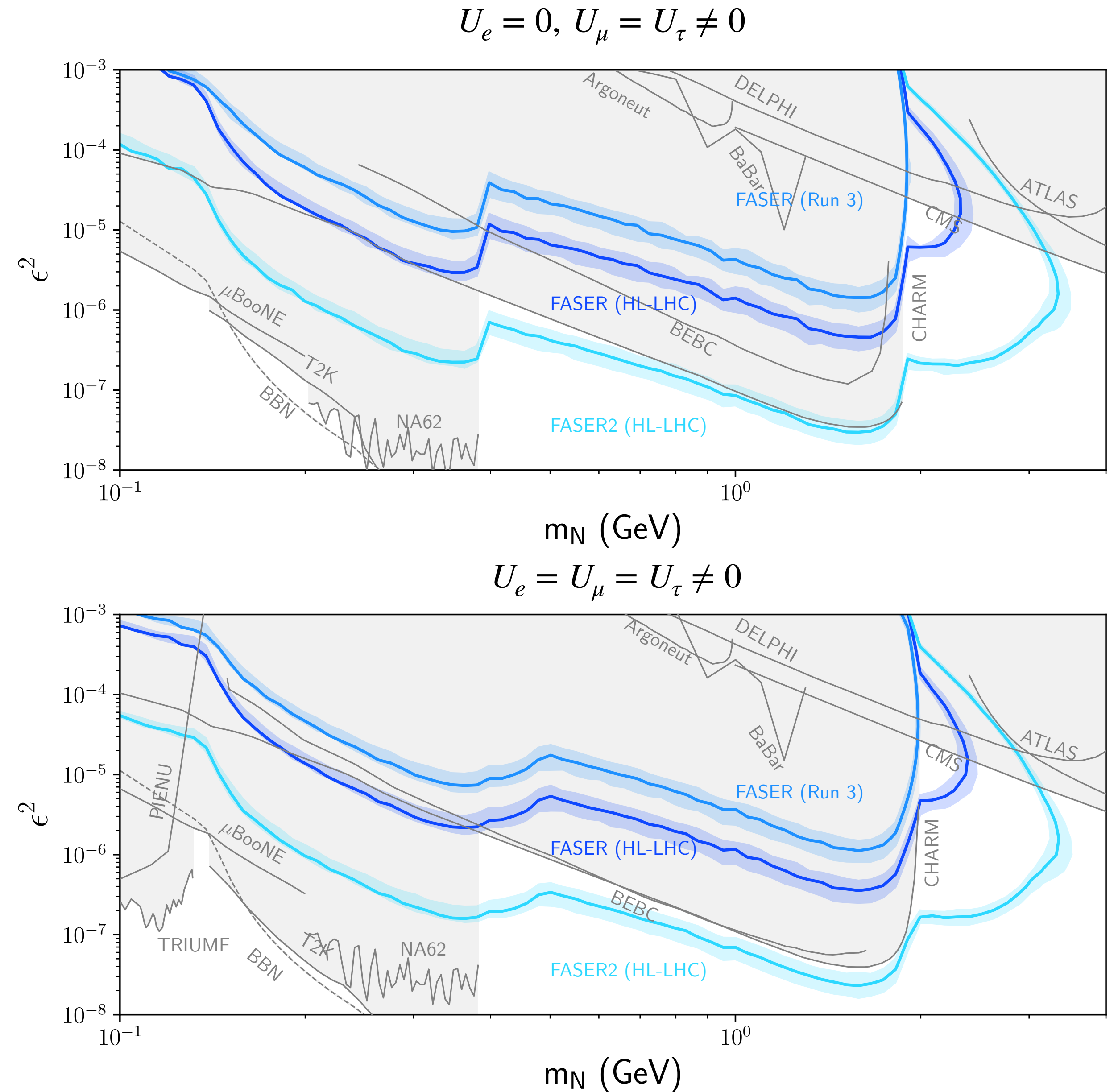
# Results: FASER Sensitivity

- We present results for FASER during Run 3 ( $\mathcal{L} = 250 \text{ fb}^{-1}$ ), and FASER/FASER2 during HL-LHC ( $\mathcal{L} = 3000 \text{ fb}^{-1}$ )
- We find that the HL-LHC upgrade will enhance the reach of FASER/FASER2 into unconstrained parameter space, with FASER2 seeing a significant increase in sensitivity due to its larger decay volume
- Results are easily obtained for different coupling ratios using the FORESEE Module!



# Results: FASER Sensitivity

- We present results for FASER during Run 3 ( $\mathcal{L} = 250 \text{ fb}^{-1}$ ), and FASER/FASER2 during HL-LHC ( $\mathcal{L} = 3000 \text{ fb}^{-1}$ )
- We find that the HL-LHC upgrade will enhance the reach of FASER/FASER2 into unconstrained parameter space, with FASER2 seeing a significant increase in sensitivity due to its larger decay volume
- Results are easily obtained for different coupling ratios using the FORESEE Module!
- Bounds from previous experiments are estimated from singly-coupled studies





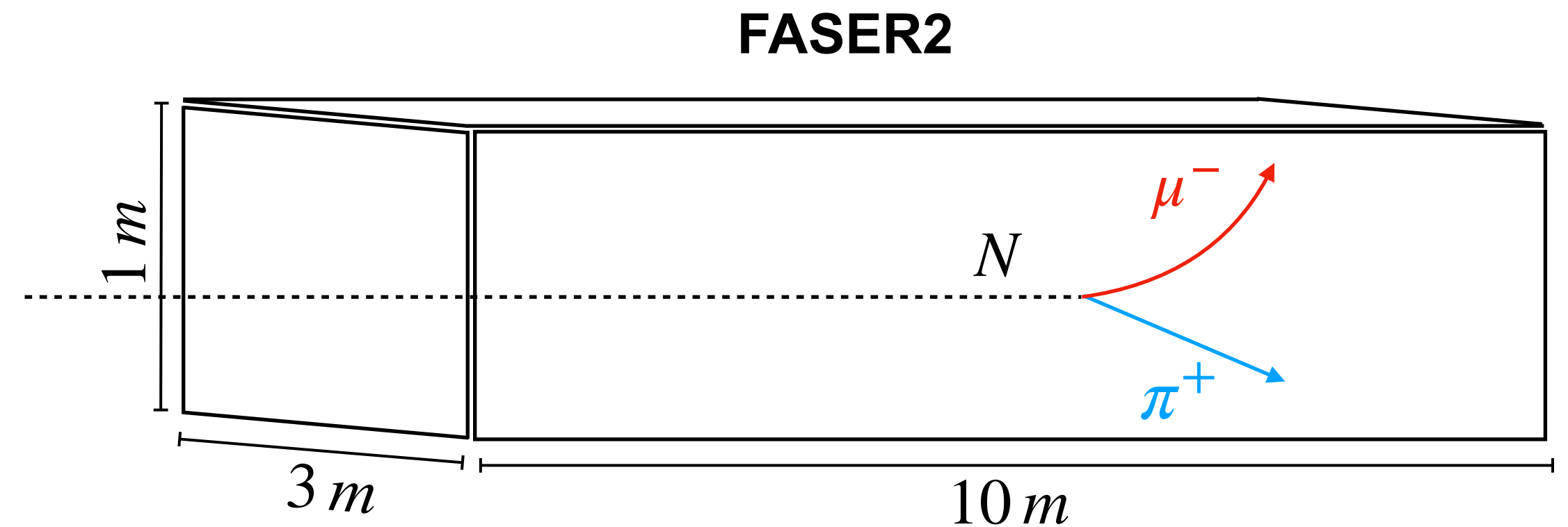
# Another Application: Characterizing HNLs at FASER2

*Collaboration: Jonathan L. Feng, **Alec Hewitt**, **Daniel La Rocco**, and Daniel Whiteson*

[2510.16107 \(2025\)](#)

# Signal Characterization

- In the event an HNL is detected, much work will be done to identify the underlying nature of the observed signal excess.
- In our work, **we assume that a discovery has been made** and answer the following questions:
  - How well can FASER2 estimate the HNL model parameters?
  - Is it possible to discriminate between Dirac and Majorana HNLs?
- Using the FORESEE HNL module, we perform an asymptotic likelihood-based analysis on MC-generated HNL data



# Benchmark Models

- Simplifying Assumptions:
  - $U_e = U_\tau = 0$
  - $N \rightarrow \mu\pi$  only
- Model 1 (High Statistics):
  - 1.84 GeV Majorana HNL
  - $N \sim 8000$
- Model 2 (Low Statistics):
  - 2.0 GeV Majorana HNL
  - $N \sim 80$

|   |   | Model 1   |         | Model 2  |        |              |
|---|---|---|---------|--|--------|--------------|
| HNL Model Parameters                        |   | $m_N = 1.84 \text{ GeV}, U_\mu = 0.0036, \text{Majorana}$ |         | $m_N = 2.00 \text{ GeV}, U_\mu = 0.002, \text{Majorana}$ |        |              |
| $c\tau_N$                                   |   | 2.03 m  |         | 4.33 m   |        |              |
| $\langle E_N \rangle_{\text{FASER2}}$       |   | 820 GeV   |         | 828 GeV  |        |              |
| $\langle E_N \rangle_{\text{FASER2+ATLAS}}$ |   | 458 GeV   |         | 452 GeV  |        |              |
|   |   |   | FASER2  |  | FASER2 | FASER2+ATLAS |
| Production Modes                            | $N_{\text{events}}$<br>at HL-LHC<br>(in $3 \text{ ab}^{-1}$ ) | $D_s \rightarrow \mu N$                                   | 119,000 | $B \rightarrow D^{*0} \mu N$                             | 447    | 56.1         |
|   |   | $B \rightarrow D^{*0} \mu N$                              | 1670    | $B^0 \rightarrow D^* \mu N$                              | 405    | 50.7         |
|   |   | $B^0 \rightarrow D^* \mu N$                               | 1570    | $B \rightarrow D^0 \mu N$                                | 199    | 26.4         |
|   |   | $B_s^0 \rightarrow D_s^* \mu N$                           | 333     | $B^0 \rightarrow D \mu N$                                | 183    | 22.4         |
| Decay Modes                                 | Branching<br>Fraction   | $\mu\rho$   | 0.187   | $\mu\rho$  | 0.162  |              |
|   |   | $\nu\nu\nu$   | 0.129   | $\nu\nu\nu$  | 0.128  |              |
|   |   | $\nu e\mu$  | 0.125   | $\nu e\mu$   | 0.125  |              |
|   |   | $\nu\mu\mu$   | 0.072   | $\nu\mu\mu$  | 0.073  |              |
|   |   | $\mu\pi$  | 0.071   | $\mu\pi$   | 0.060  |              |
|   |   | $\nu\pi^0$  | 0.038   | $\nu\pi^0$   | 0.032  |              |
|   |   | Other   | 0.378   | Other  | 0.419  |              |
| Total FASER2 $N \rightarrow \mu\pi$ Events  |   |   | 8610    |  | 81.8   | 10.6         |

# Kinematic Measurements

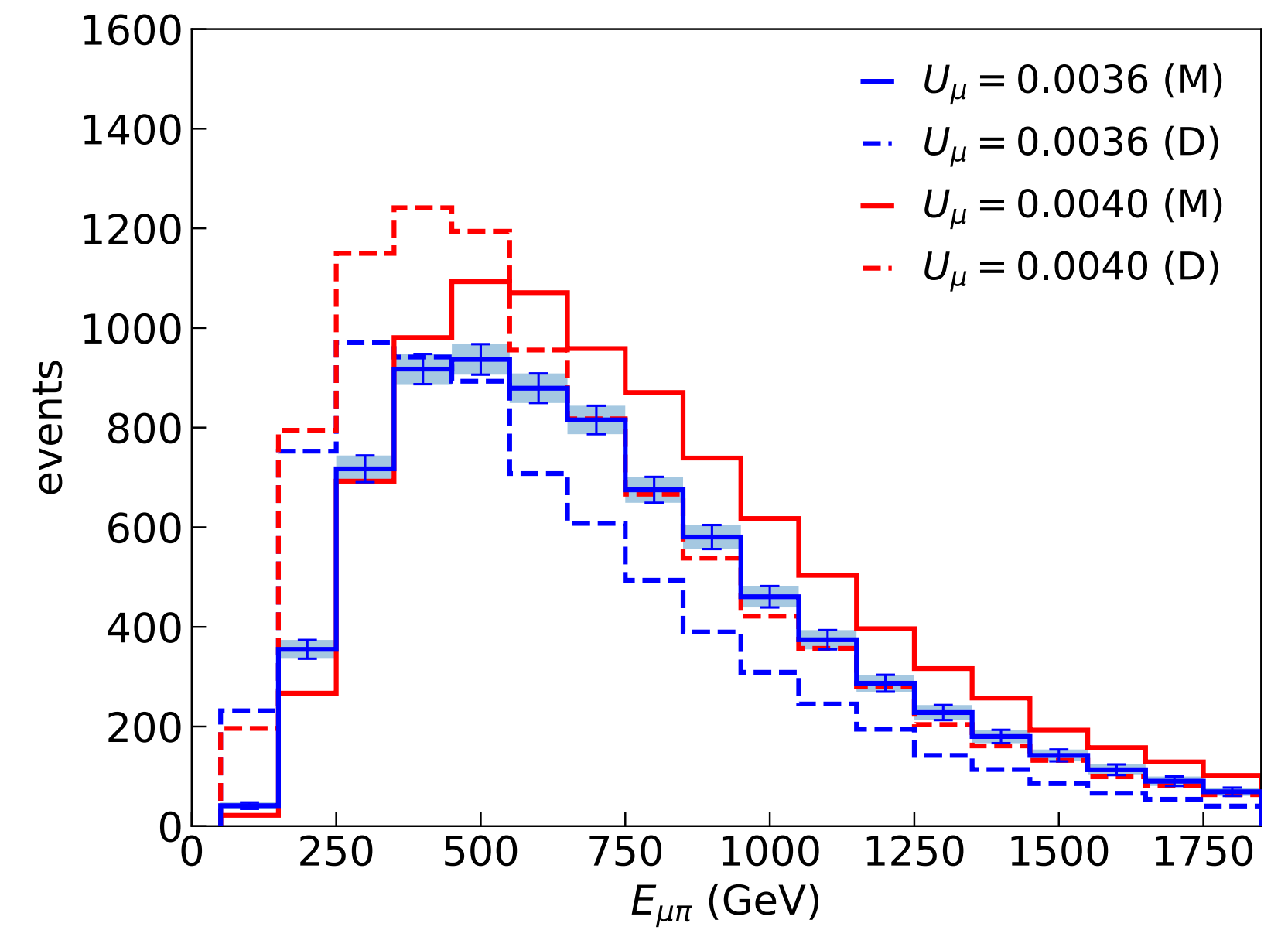
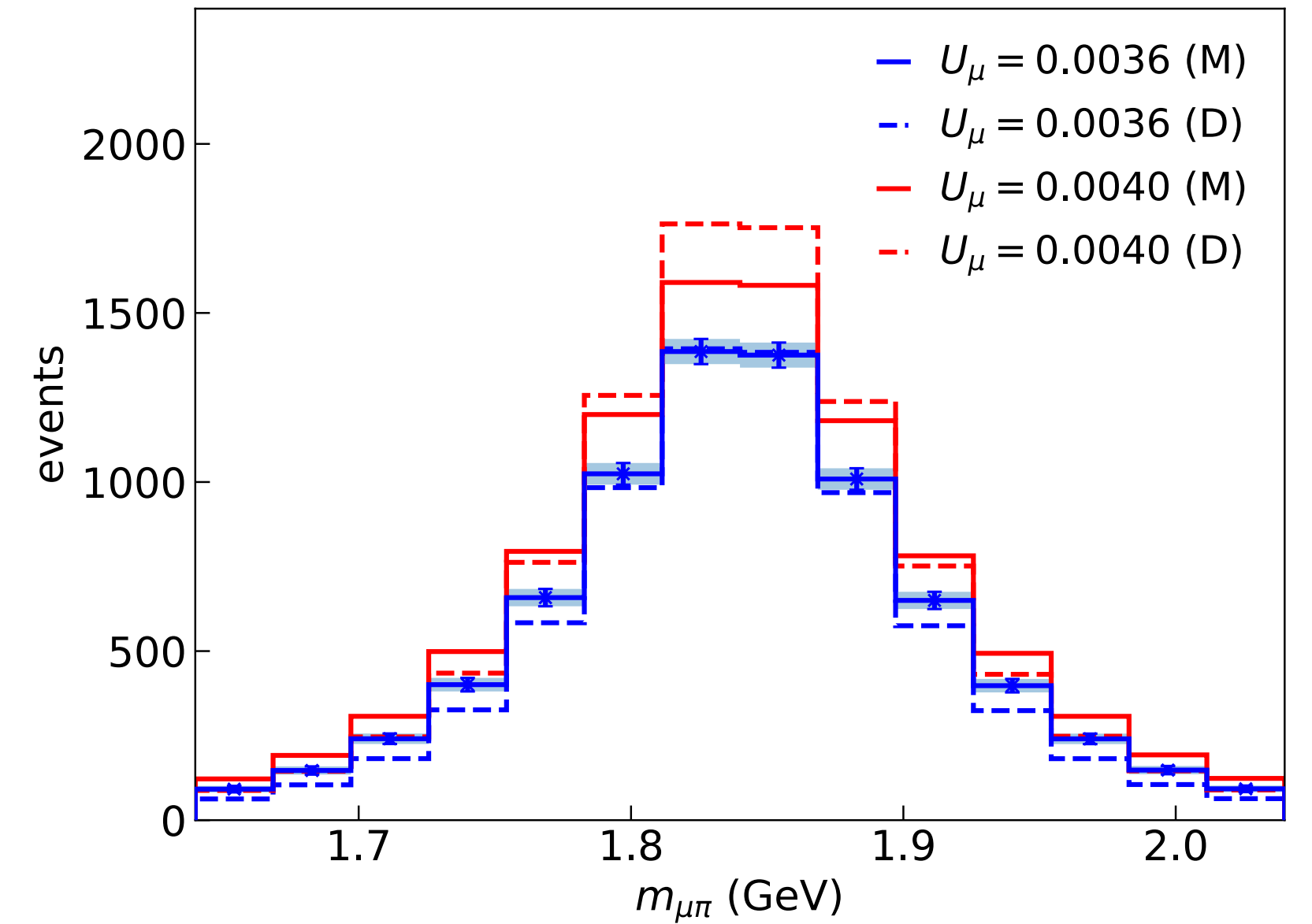
$$m_{\mu\pi}^2 = m_\mu^2 + m_\pi^2 + 2(E_\mu E_\pi - p_\mu p_\pi \cos \theta_{\mu\pi})$$

- Dual-readout hadronic calorimeter
  - Combines scintillation and Cherenkov signals for high precision measurement of the pion energy

$$\frac{\delta E_\pi}{E_\pi} = \frac{35\%}{\sqrt{E_{\pi^\pm}/\text{GeV}}} \oplus 0.5\%$$

- Scintillating Fiber Tracking Stations
  - Measure muon momentum and angular separation

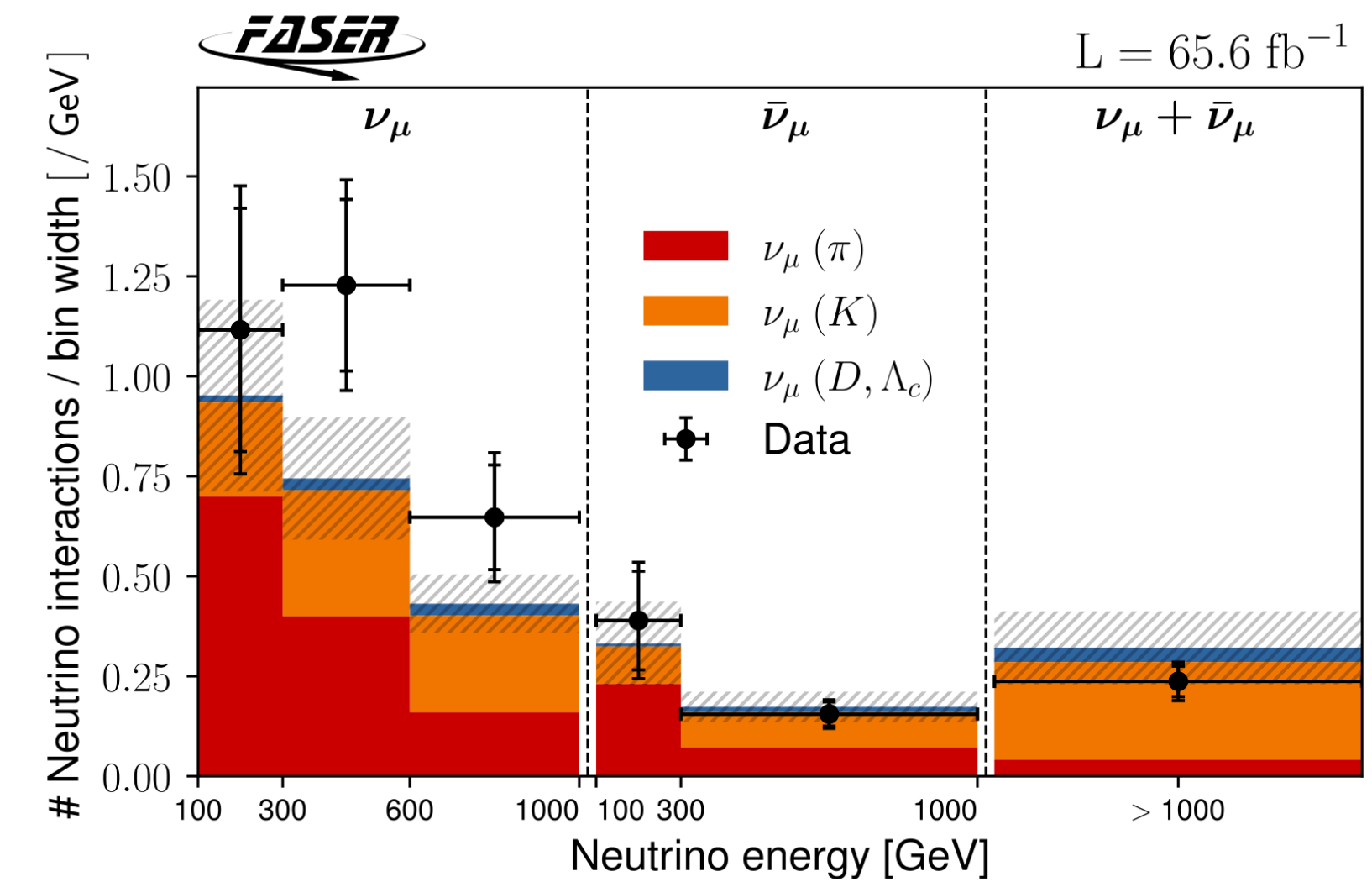
$$\frac{\delta p_\mu}{p_\mu} = 3.3 \times 10^{-5} \left[ \frac{p_\mu}{\text{GeV}} \right], \quad \delta \theta_{\mu\pi} = 250 \mu\text{rad}$$



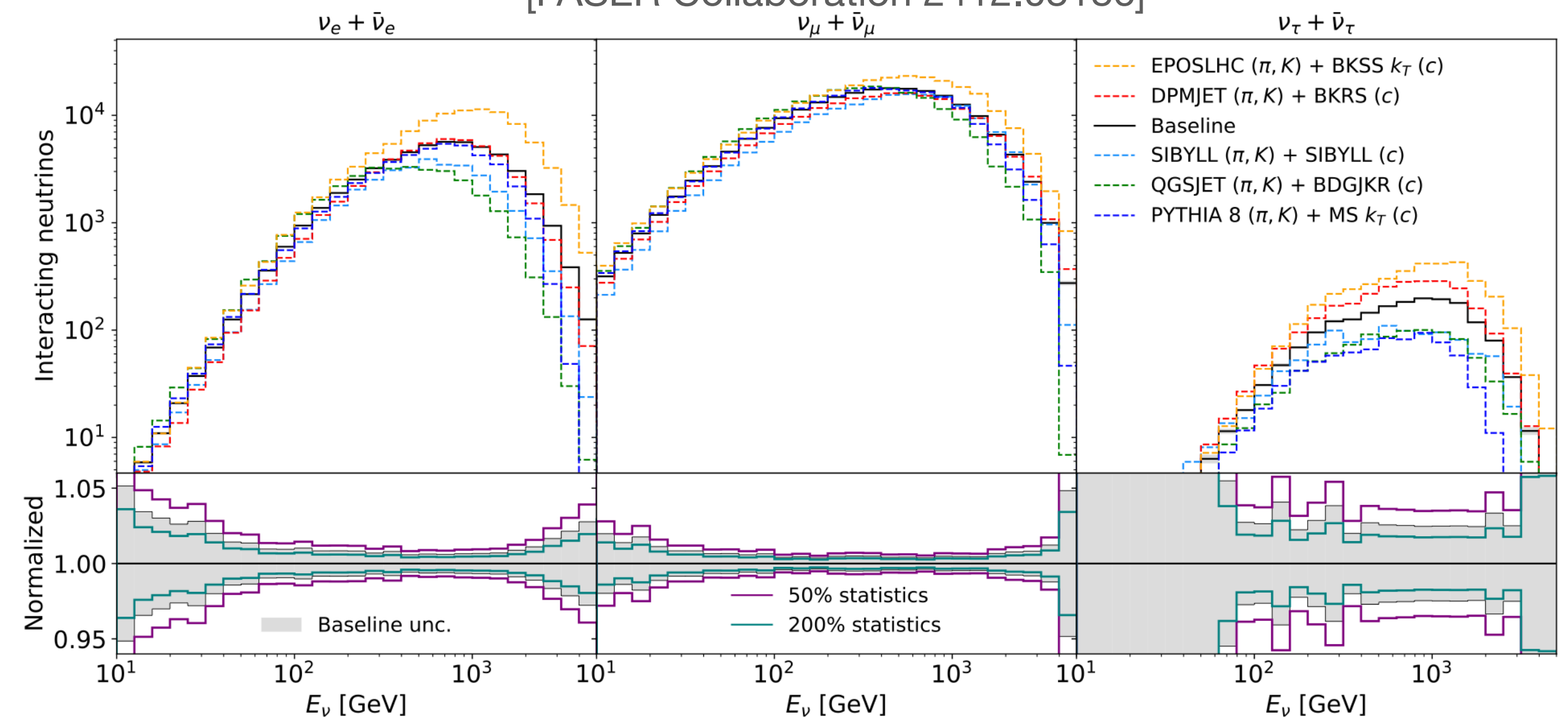


# Theoretical Uncertainty

- The leading theoretical uncertainty in the HNL flux comes from **forward hadron production**
  - Hadron production in the forward direction at the LHC has not been measured historically
  - MC generators are not optimally tuned for the forward direction
- Fortunately, modeling uncertainties will certainly be reduced as FASER $\nu$  continues to measure forward neutrino fluxes
  - “Latest neutrino results from the FASER experiment and their implications for forward hadron production” ([Ohashi et al. 2025](#))



[FASER Collaboration 2412.03186]



[Kling, Makela, and Trojanowski 2309.10417]

# Statistical Methods

## Maximum Likelihood

- We perform an **asymptotic likelihood-based test** to obtain the expected constraints on the HNL model parameters using Wilk's Theorem
- **Nuisance parameters** are incorporated to represent the theoretical uncertainties in the **HNL flux normalization and shape**
- We consider the following scenarios:
  - $\sigma_\eta = 60\%$  and  $\sigma_\gamma = 10\%$  (Current)
  - $\sigma_\eta = 5\%$  and negligible  $\sigma_\gamma$  (Future)

$$L(\vec{d}, m_N; \eta, \vec{\gamma}) = \prod_i f_P(d_i | \eta \gamma_i \mu_i) \underbrace{f_G(1 | \eta, \sigma_\eta)}_{\text{Normalization Uncertainty}} \underbrace{f_G(1 | \gamma, \sigma_\gamma \oplus \sigma_i^{MC})}_{\text{Bin-by-bin Uncertainty (Shape)}}$$

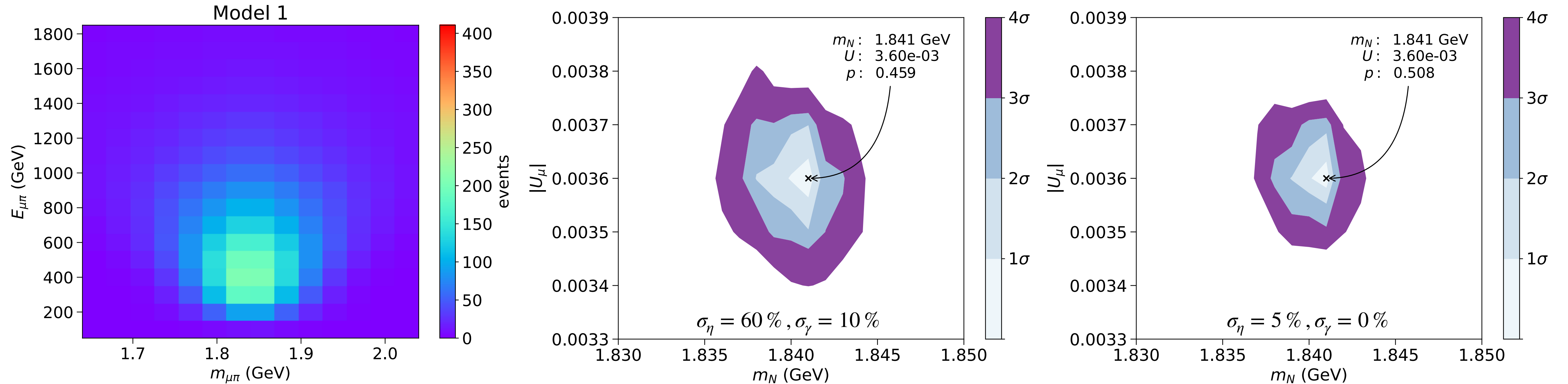
$$\tilde{t}(\vec{d} | m_N, U_\mu) := -2 \ln \frac{L(\vec{d} | m_N, U_\mu; \hat{\eta}, \hat{\vec{\gamma}})}{L(\vec{d} | \hat{m}_N, \hat{U}_\mu; \hat{\eta}, \hat{\vec{\gamma}})}$$

- $d_i$  : Observed bin-count
- $\mu_i(m_N, U_\mu)$  : Mean bin count prediction
- Nuisance Parameters:  $\eta, \gamma_i$
- Theoretical Uncertainties:
  - $\sigma_\eta$  : Normalization (60% , 5%)
  - $\sigma_\gamma$  : Uncorrelated “Shape” (10% , 0%)
  - $\sigma_i^{MC}$  : MC Statistics

# Parameter Estimation

## Model 1 (High Statistics)

$$L(\vec{d}, m_N; \eta, \vec{\gamma}) = \prod_i f_P(d_i | \eta \gamma_i \mu_i) \underbrace{f_G(1 | \eta, \sigma_\eta)}_{\text{Normalization Uncertainty}} \underbrace{f_G(1 | \gamma, \sigma_\gamma \oplus \sigma_i^{MC})}_{\text{Bin-by-bin Uncertainty (Shape)}}$$

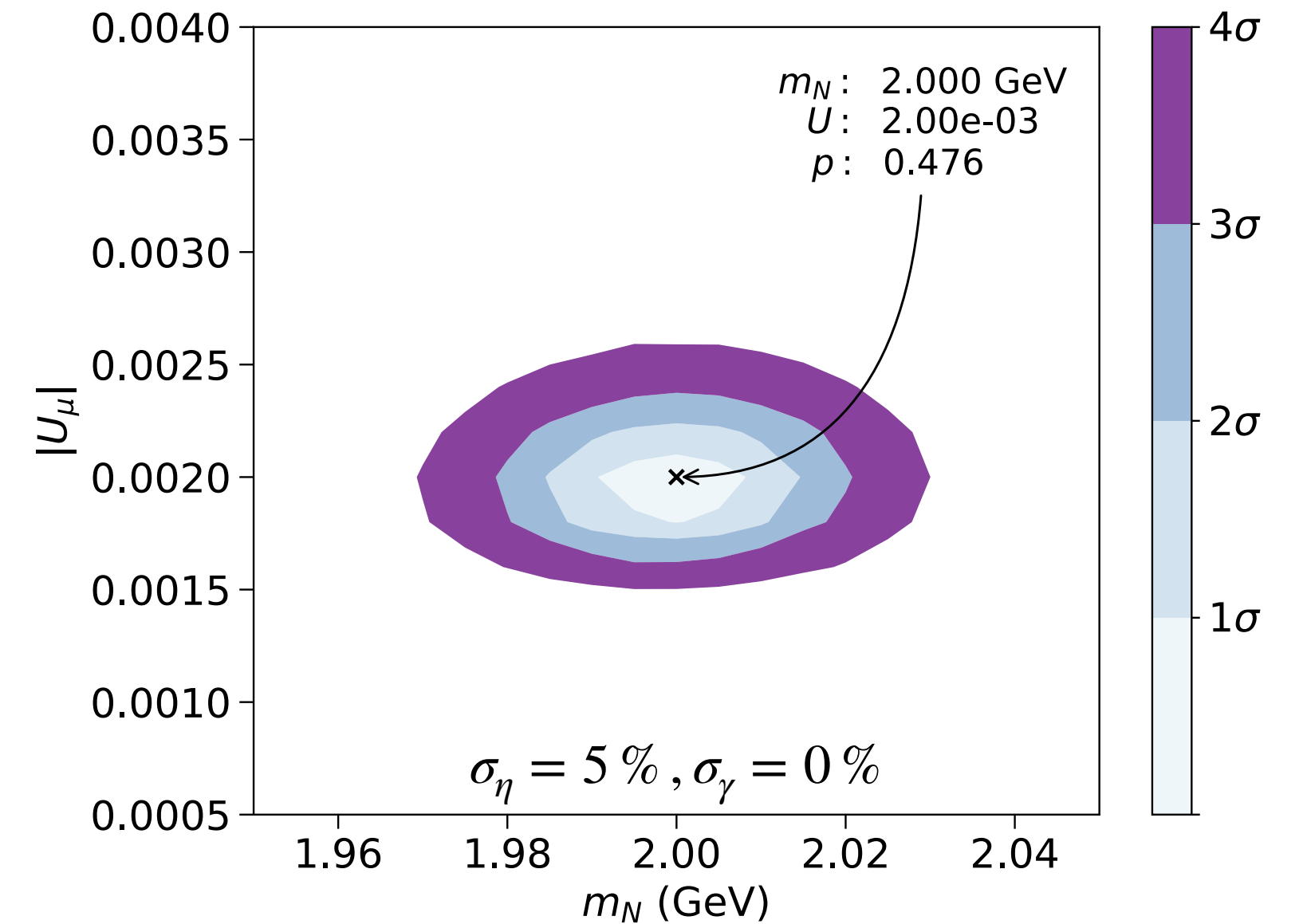
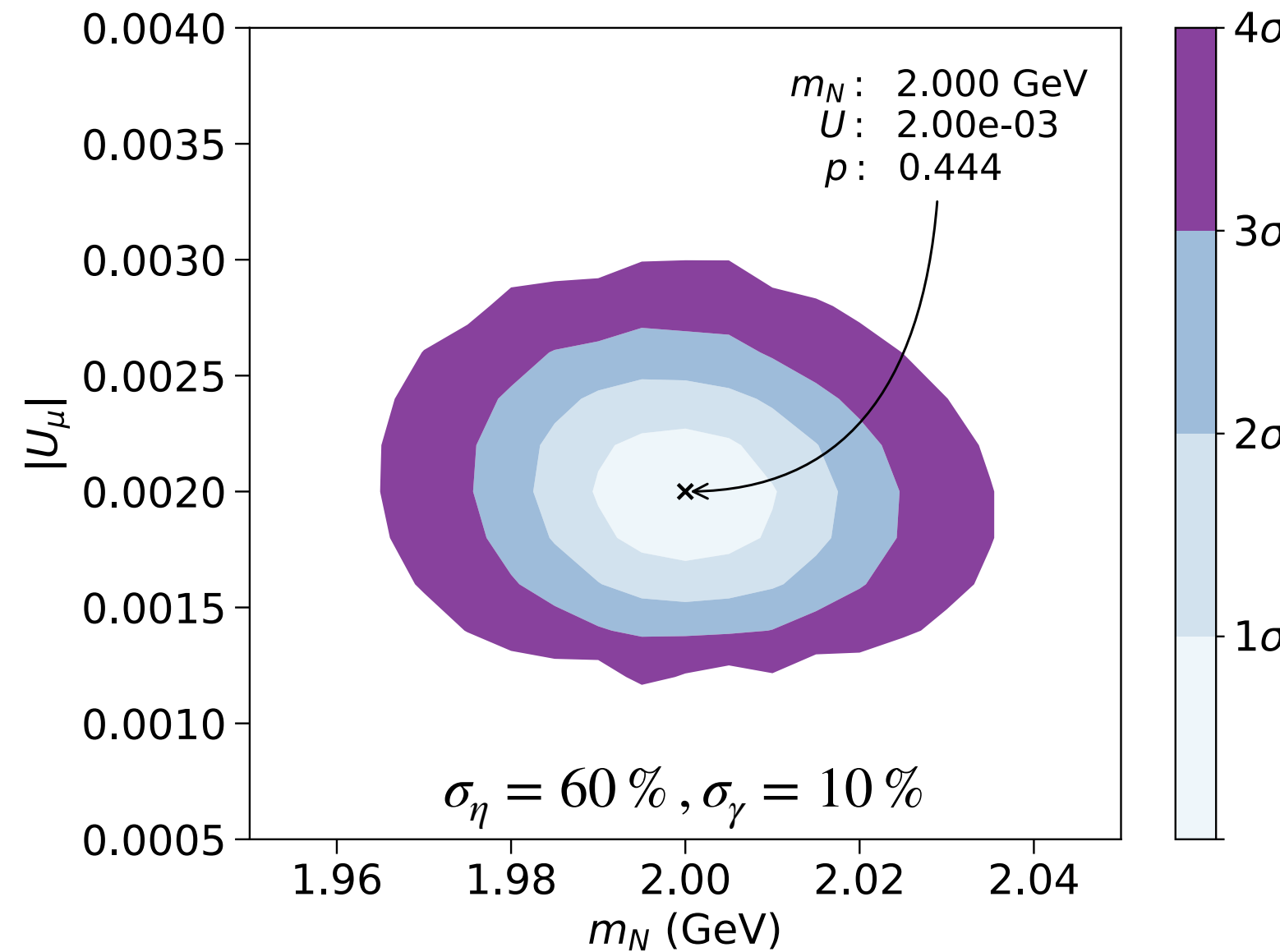
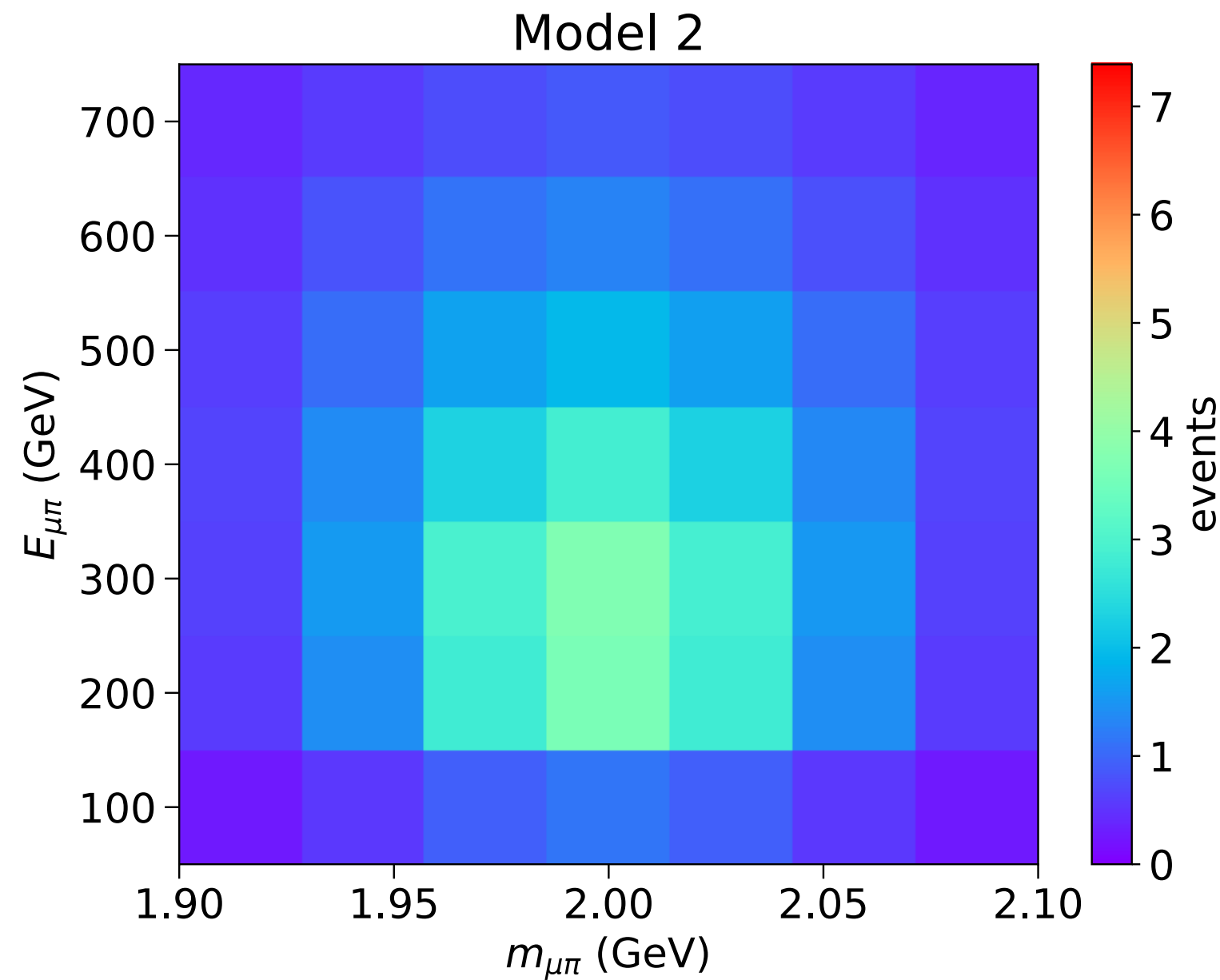


- Assuming current flux uncertainties,  $m_N$  &  $U_\mu$  can be constrained to 0.1 % and 3 % respectively.
- Assuming improved flux uncertainties,  $m_N$  &  $U_\mu$  can be constrained to 0.1 % and 2 % respectively.

# Parameter Estimation

## Model 2 (Low Statistics)

$$L(\vec{d}, m_N; \eta, \vec{\gamma}) = \prod_i f_P(d_i | \eta \gamma_i \mu_i) \underbrace{f_G(1 | \eta, \sigma_\eta)}_{\text{Normalization Uncertainty}} \underbrace{f_G(1 | \gamma, \sigma_\gamma \oplus \sigma_i^{MC})}_{\text{Bin-by-bin Uncertainty (Shape)}}$$



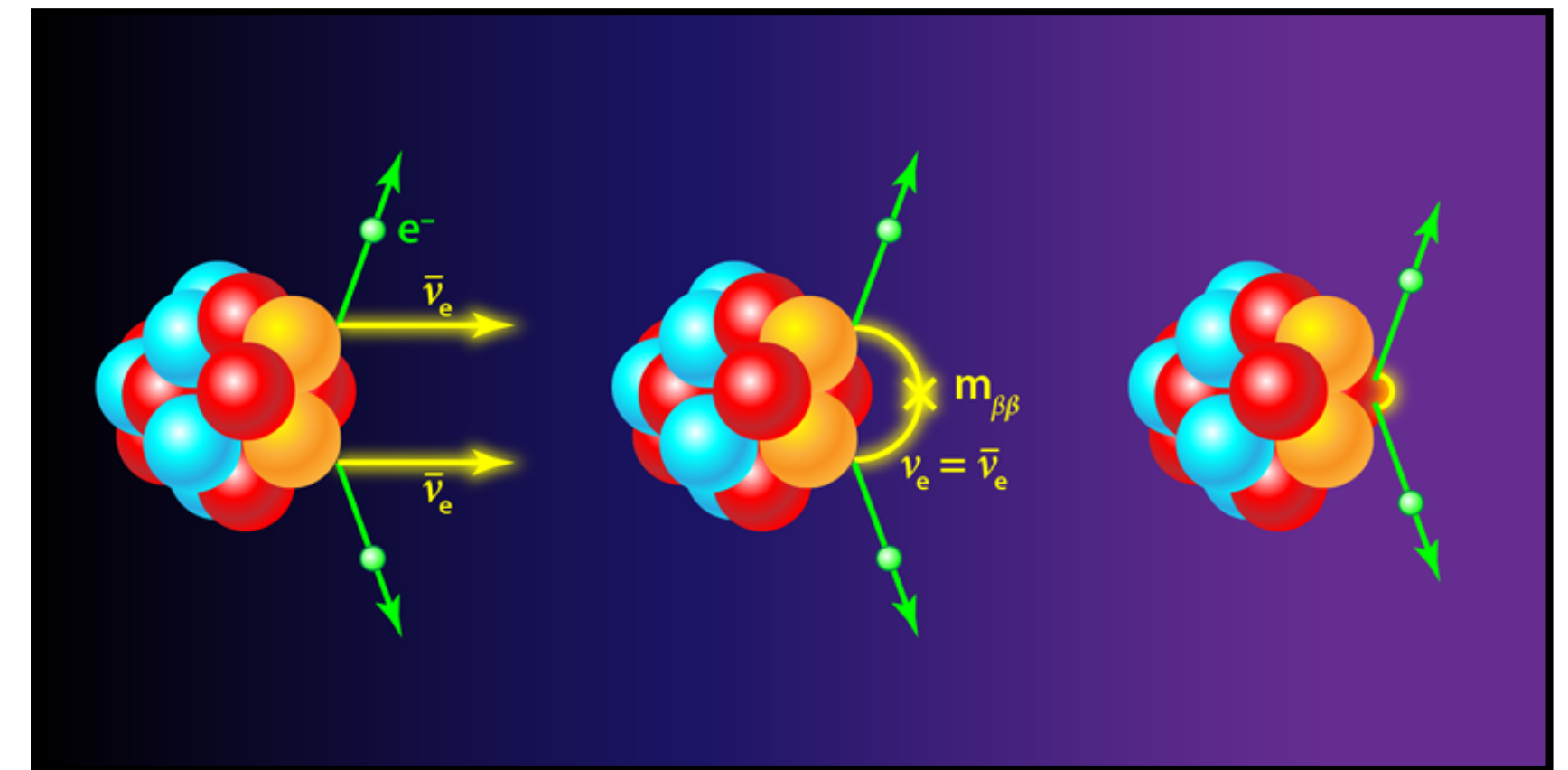
- Assuming current flux uncertainties,  $m_N$  &  $U_\mu$  can be constrained to 1 % and 25 % respectively.
- Assuming improved flux uncertainties,  $m_N$  &  $U_\mu$  can be constrained to 1 % and 15 % respectively.



# Majorana or Dirac?

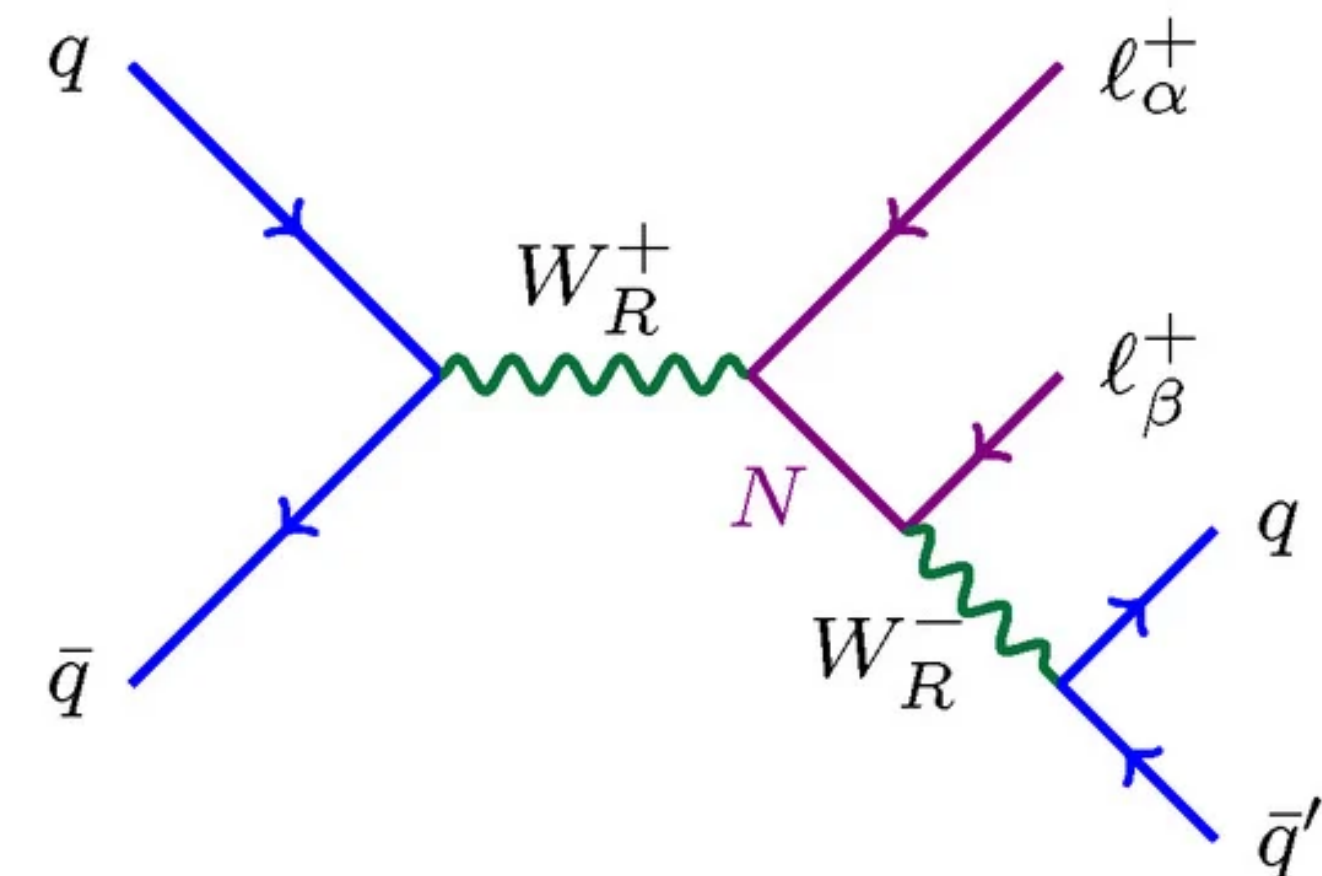
- Some important questions:
  - are neutrinos Dirac or Majorana?
  - is lepton number violation (LNV) allowed in the SM?
    - Implications for cosmology, neutrino oscillations, and dark matter
- Direct tests of LNV have been carried out for decades in lab and collider based experiments:
  - $0\nu\beta\beta$  ([Furry](#) 1939)
  - $pp \rightarrow l^\pm l^\pm jj$  ([Keung and Senjanović](#) 1983)

Neutrinoless double beta decay



[<https://physics.aps.org/articles/v11/30>]

$$pp \rightarrow l^\pm l^\pm jj$$



[<https://www.mdpi.com/2218-1997/8/3/164>]

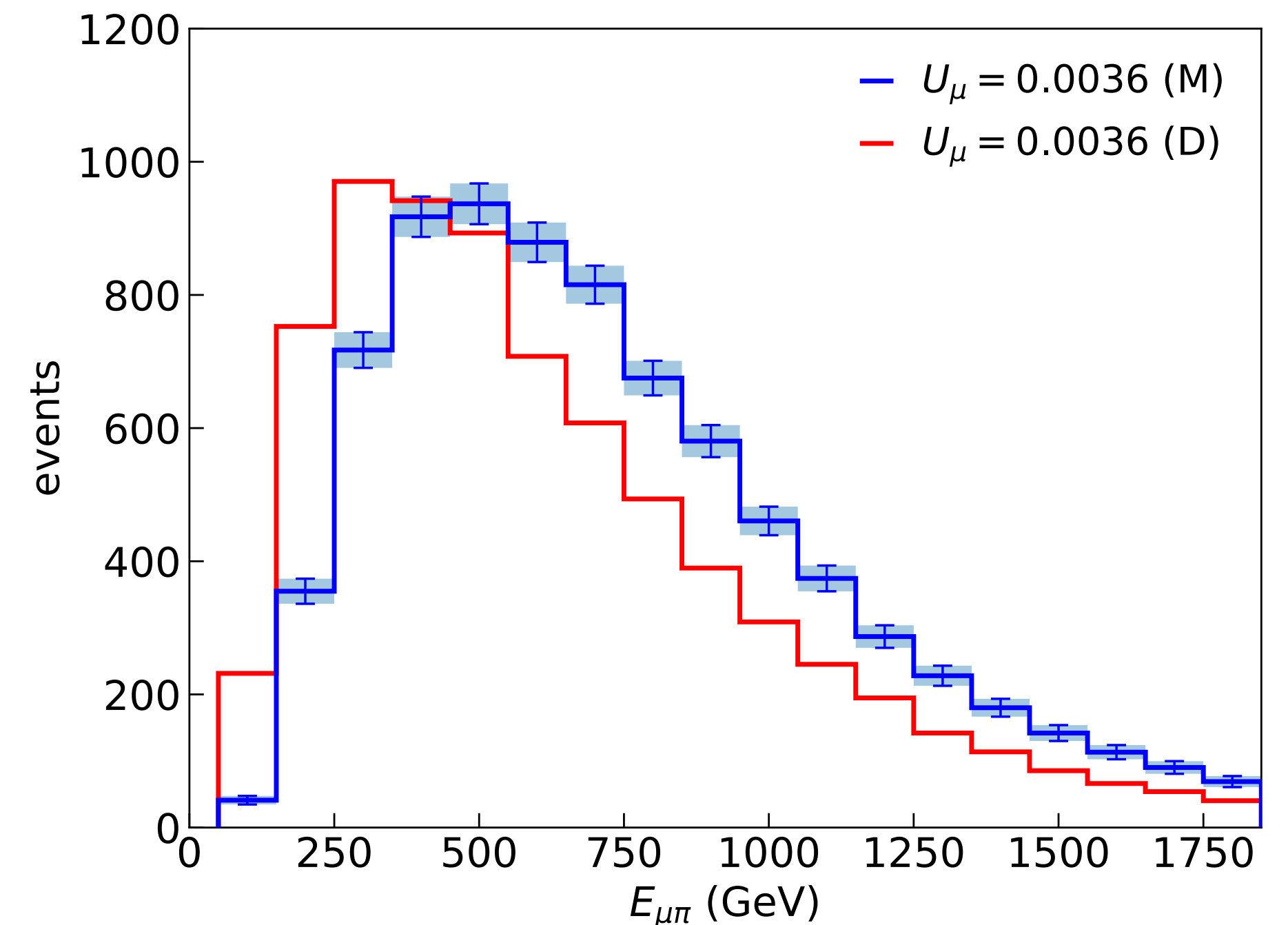
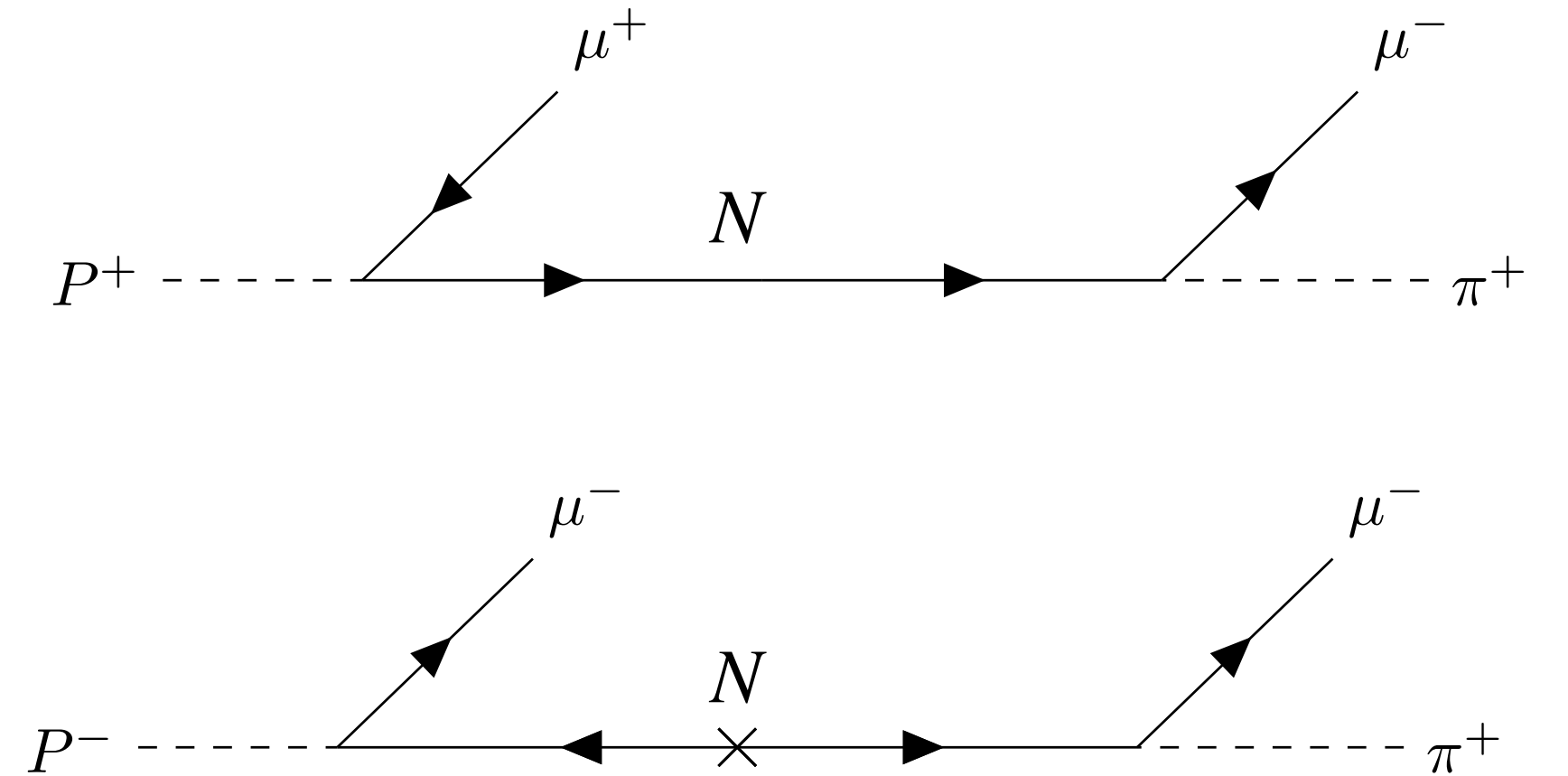
# Majorana vs. Dirac HNLs

- Since SM neutrinos are massless, helicity and chirality eigenstates coincide, causing LNV processes involving SM neutrino to be suppressed by

$$|M|^2 \sim \left( \frac{m_\nu}{E_\nu} \right)^2$$

- However, for on-shell HNL decay, the mass dependence of the amplitude exactly cancels, resulting in **LNC and LNV processes which are equal and unsuppressed**
- Therefore, the lifetimes between Majorana and Dirac HNLs are related by

$$\tau_M = \frac{1}{\Gamma_{LNC} + \Gamma_{LNV}} = \frac{\tau_D}{2}$$



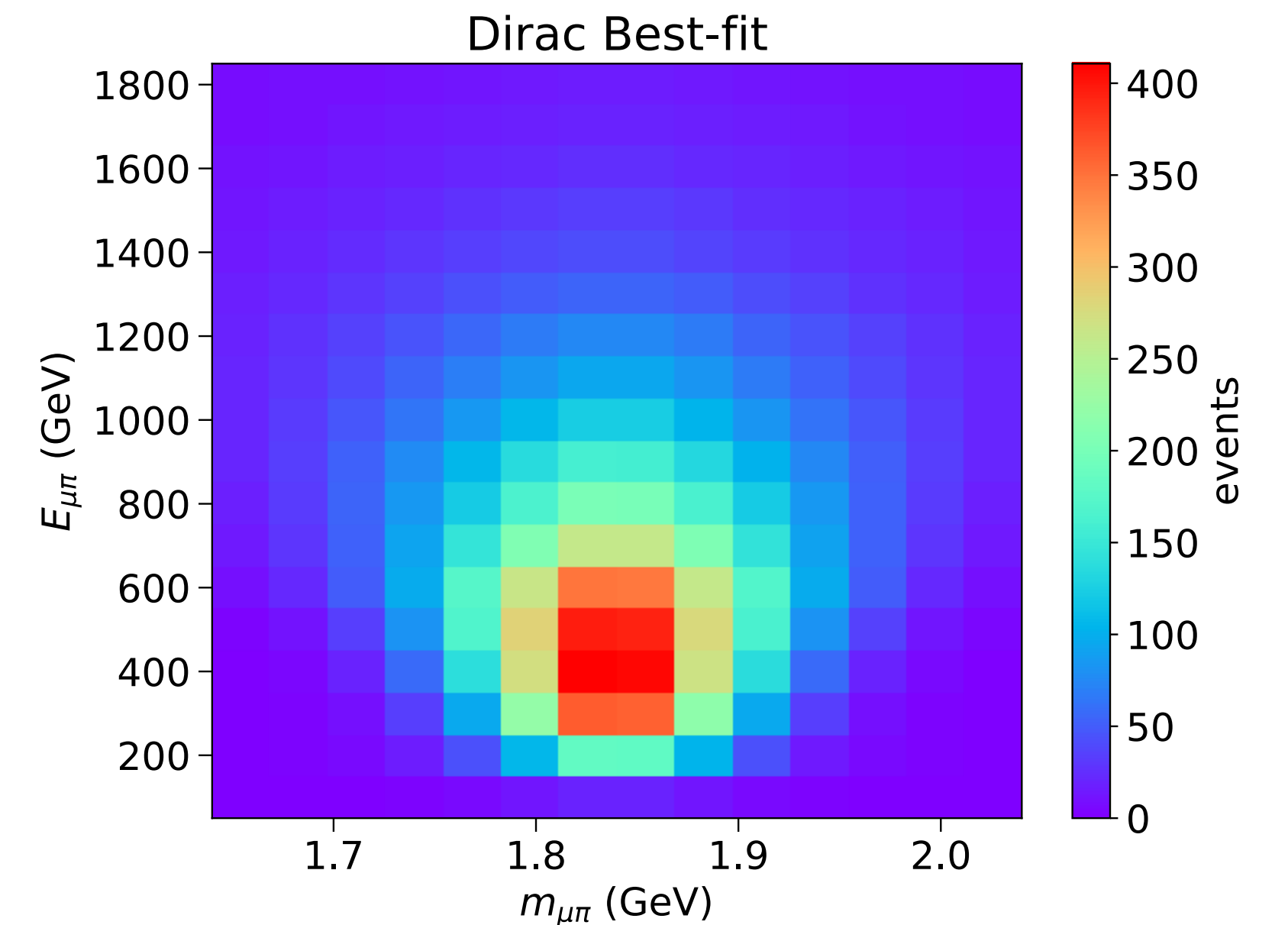
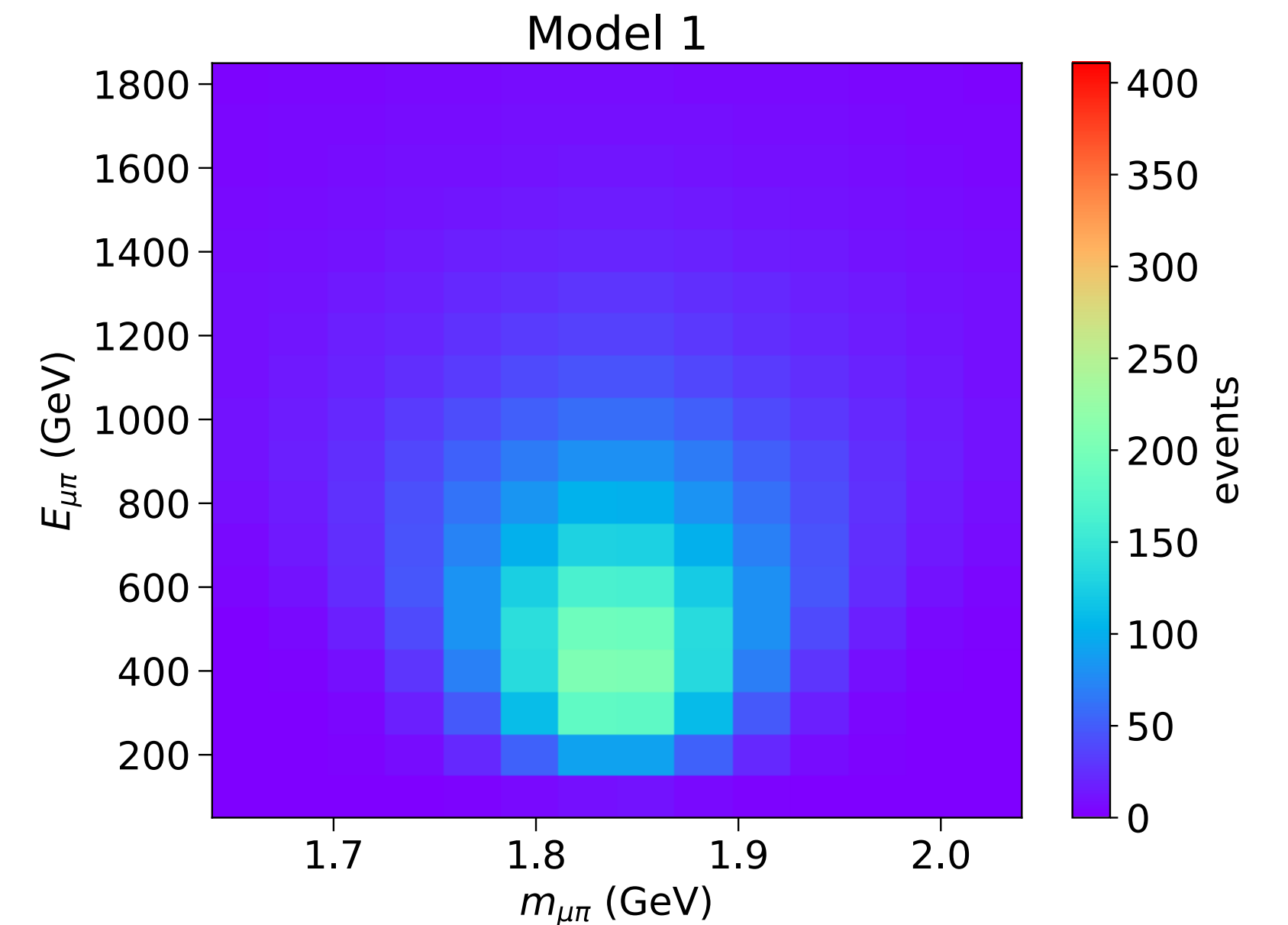
# Majorana vs. Dirac HNLs

- Since SM neutrinos are massless, helicity and chirality eigenstates coincide, causing LNV processes involving SM neutrino to be suppressed by

$$|M|^2 \sim \left( \frac{m_\nu}{E_\nu} \right)^2$$

- However, for on-shell HNL decay, the mass dependence of the amplitude exactly cancels, resulting in **LNC and LNV processes which are equal and unsuppressed**
- Therefore, the lifetimes between Majorana and Dirac HNLs are related by

$$\tau_M = \frac{1}{\Gamma_{LNC} + \Gamma_{LNV}} = \frac{\tau_D}{2}$$



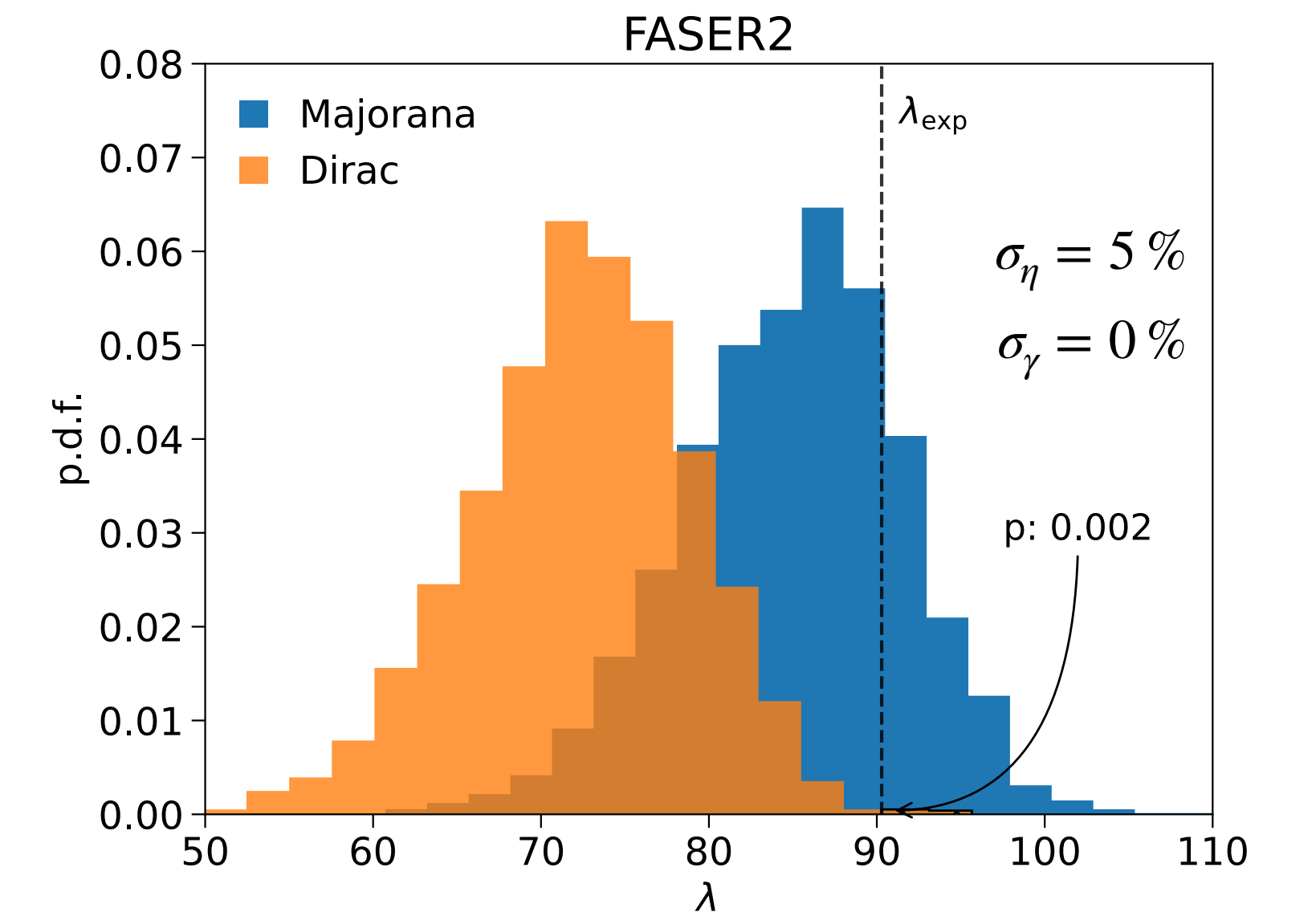
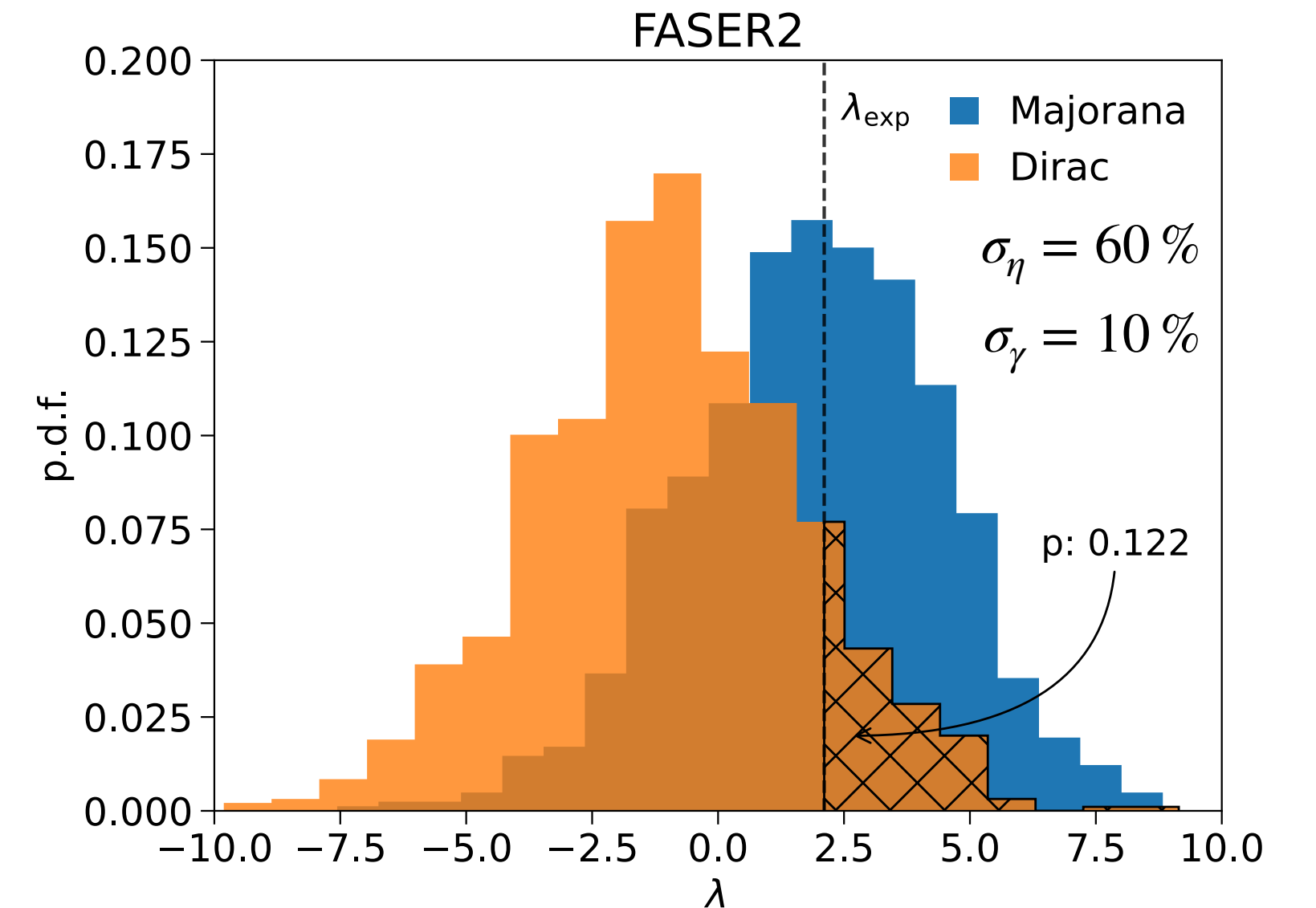
# Discrimination via Kinematics

## Model 1 (High Statistics)

Profiled Likelihood Ratio Test

$$\lambda(\vec{d}) := -2 \ln \frac{L_D(\vec{d} | \hat{m}_N^D, \hat{U}_\mu^D; \hat{\eta}^D, \hat{\gamma}^D)}{L_M(\vec{d} | \hat{m}_N^M, \hat{U}_\mu^M; \hat{\eta}^M, \hat{\gamma}^M)}$$

- Using  $\lambda$ , we compute the probability that a Dirac HNL would fluctuate to produce a signal that looks just as (or more) “Majorana-like” than the expected observation
- Generated via  $\mathcal{O}(10^3)$  pseudo-experiments, where the nuisance parameters for both models have been fixed to their best-fit values.
- Assuming flux uncertainties are improved, we find that FASER2 can expect to reject the Dirac hypothesis with 99.8 % CL ( $2.9\sigma$ )





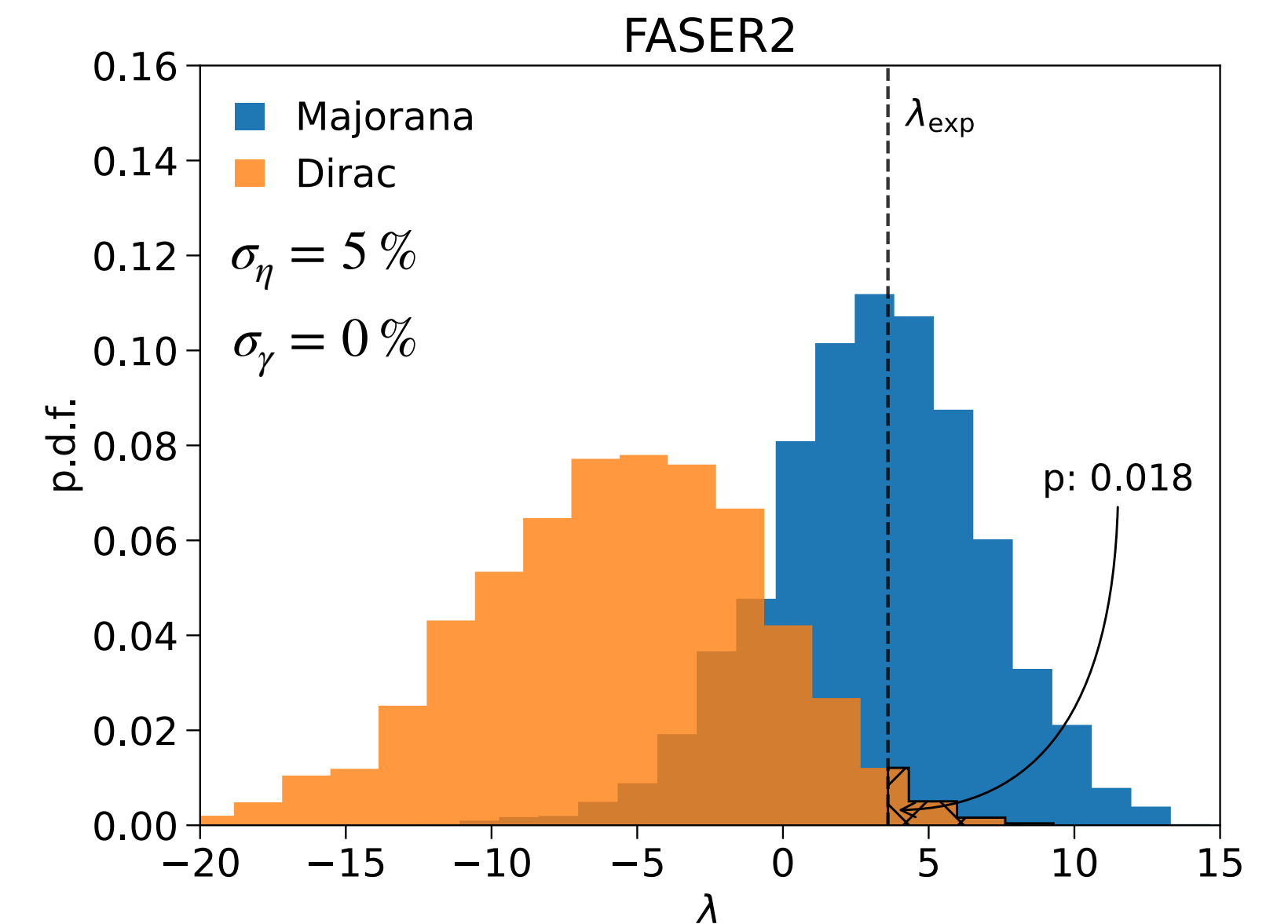
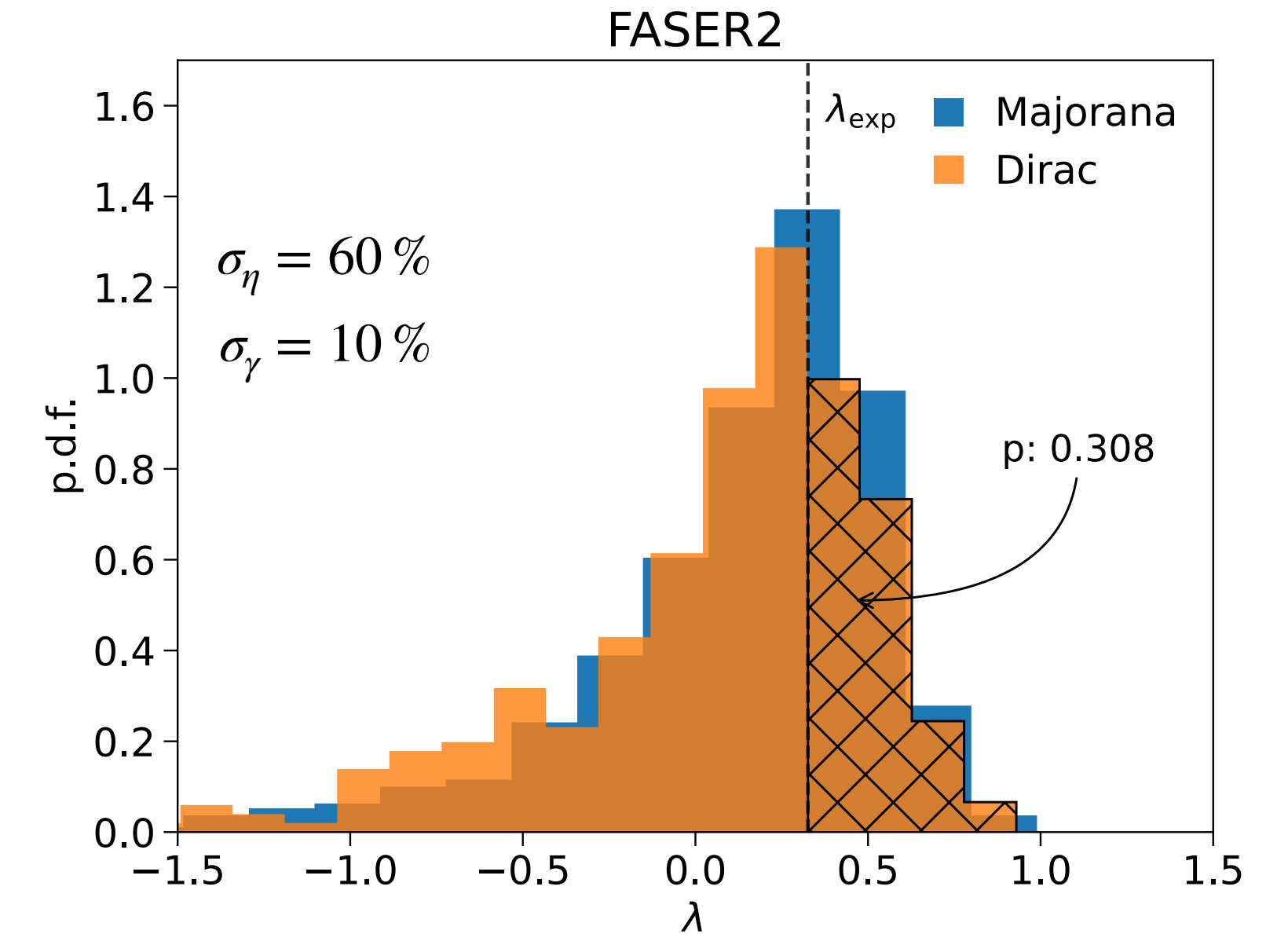
# Discrimination via Kinematics

## Model 2 (Low Statistics)

Profiled Likelihood Ratio Test

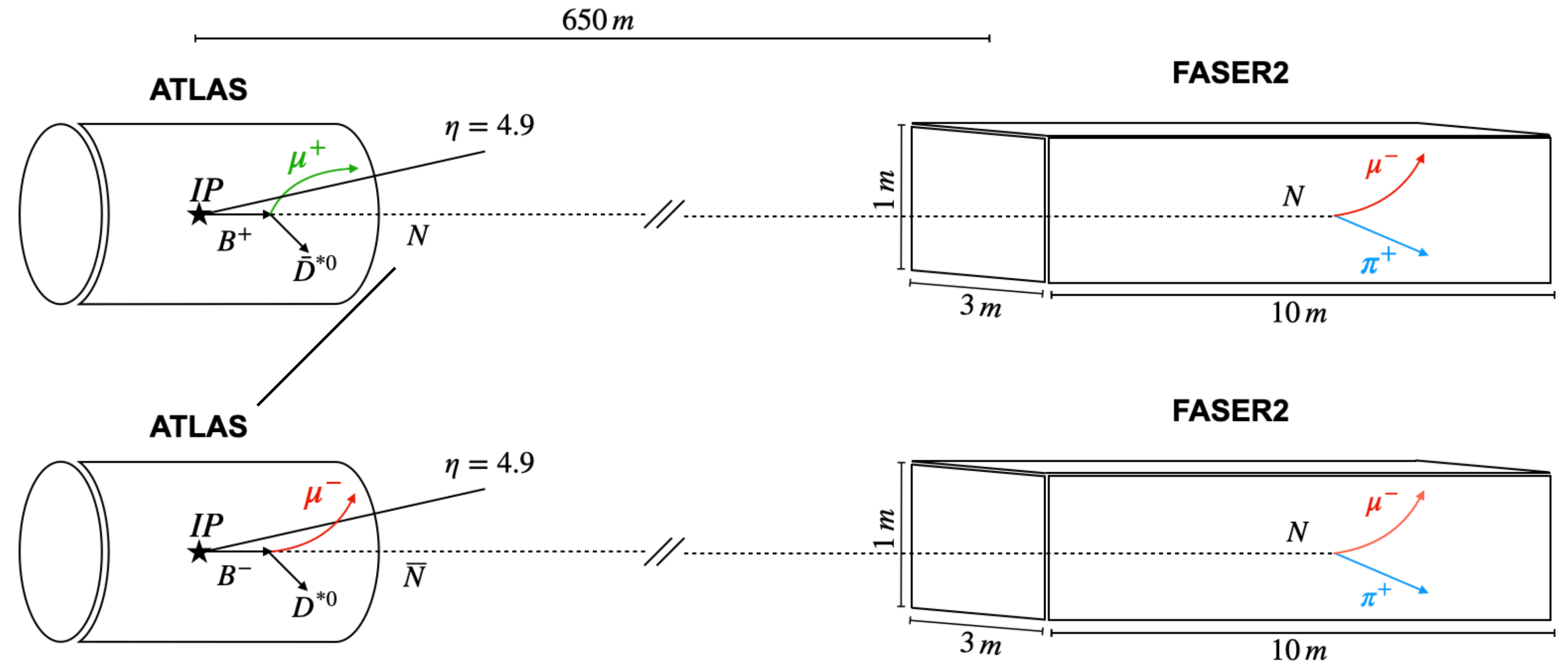
$$\lambda(\vec{d}) := -2 \ln \frac{L_D(\vec{d} | \hat{m}_N^D, \hat{U}_\mu^D; \hat{\eta}^D, \hat{\gamma}^D)}{L_M(\vec{d} | \hat{m}_N^M, \hat{U}_\mu^M; \hat{\eta}^M, \hat{\gamma}^M)}$$

- However, with lower event rates, the procedure is **statistics limited**
- Assuming flux uncertainties are improved, we find that FASER2 can only expect to reject the Dirac hypothesis with 98.2 % CL ( $2.1\sigma$ )
- Therefore, in order to obtain comparable results to the high-statistics scenario, additional information is necessary.



# FASER2 as a Trigger for ATLAS

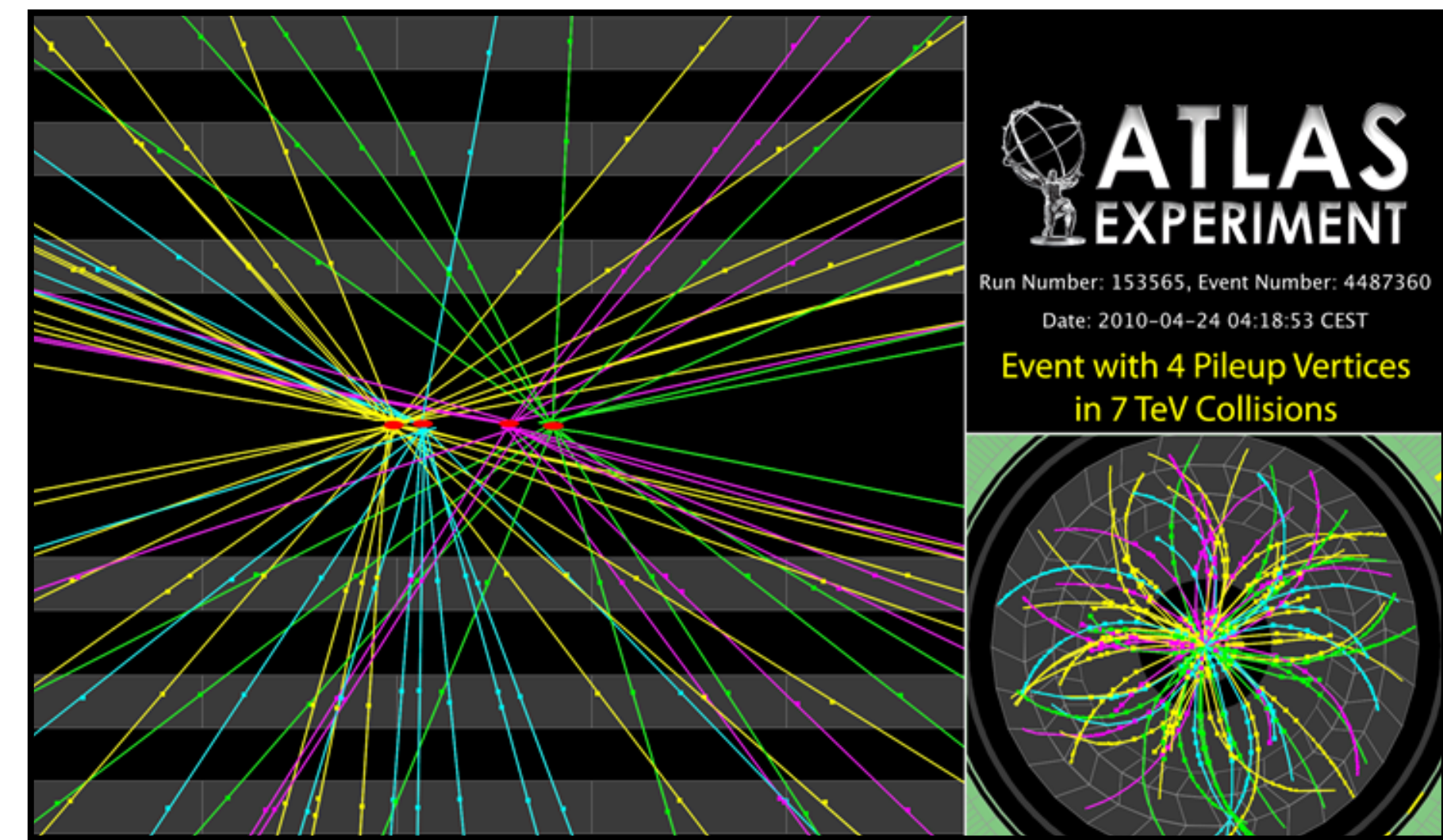
- In our work, we explore the idea of using **FASER2 as a trigger for ATLAS** to measure muons produced in association with HNLs as a probe of LNV.
  - ATLAS L0 Latency:  $6\ \mu\text{s}$
  - Triggering Time:  $2.2\ \mu\text{s} + 2.9\ \mu\text{s}$
- In the absence of background, one could determine LNV on an event-by-event basis. **However this is not in the absence of background!**



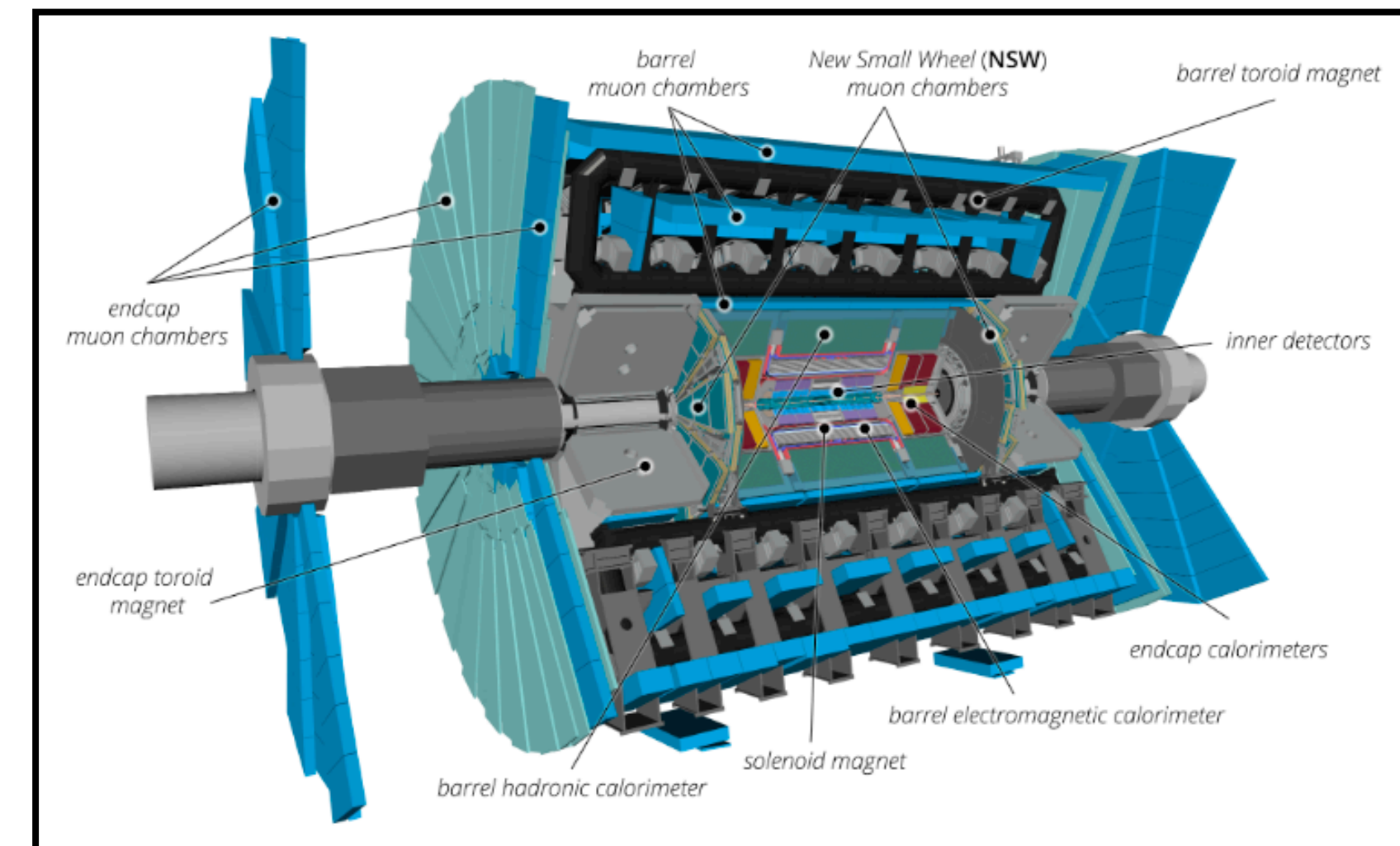


# Pileup Background

- At the HL-LHC, there are  $\sim 10^{11}$  protons per bunch, resulting in  $\langle \mu \rangle = 200$  pile-up events per crossing.
- We use Pythia8 to overlay 200  $pp$  collisions to generate an estimate for the number of background tracks per bunch crossing
- A high- $\eta$  muon tagger is required to reduce background from charged tracks
  - Proposed in ATLAS Phase-II upgrade ([ATLAS Collaboration](#) 2015)



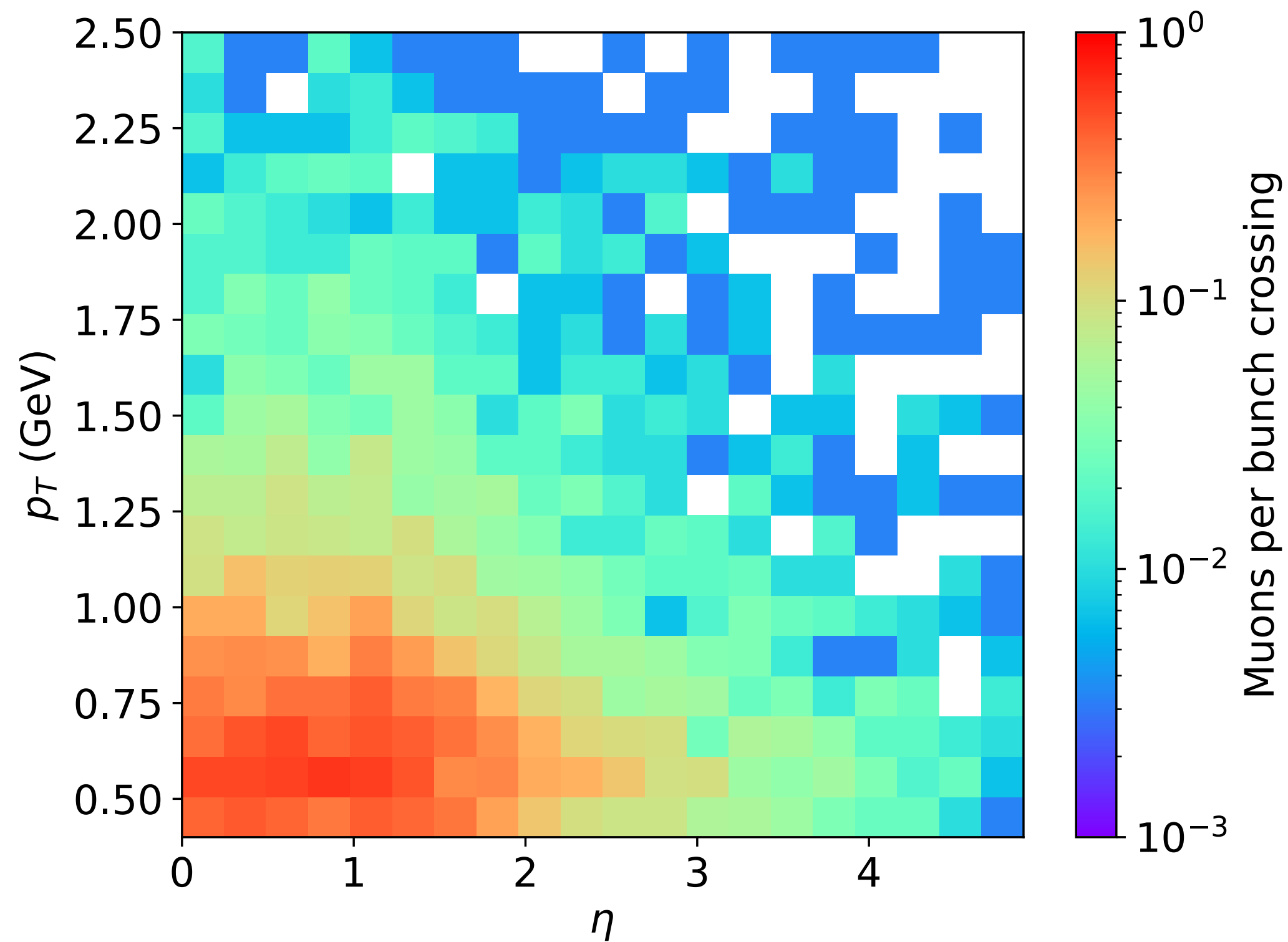
[[https://lhc-closer.es/taking\\_a\\_closer\\_look\\_at\\_lhc/0.pile\\_up/](https://lhc-closer.es/taking_a_closer_look_at_lhc/0.pile_up/)]



[ATLAS Collaboration 2023]

# Pileup Background

- At the HL-LHC, there are  $\sim 10^{11}$  protons per bunch, resulting in  $\langle \mu \rangle = 200$  pile-up events per crossing.
- We use Pythia8 to overlay 200  $pp$  collisions to generate an estimate for the number of background tracks per bunch crossing
- A high- $\eta$  muon tagger is required to reduce background from charged tracks
  - Proposed in ATLAS Phase-II upgrade ([ATLAS Collaboration](#) 2015)
- We find that there is **roughly 1 uncorrelated background muon per bunch crossing**.



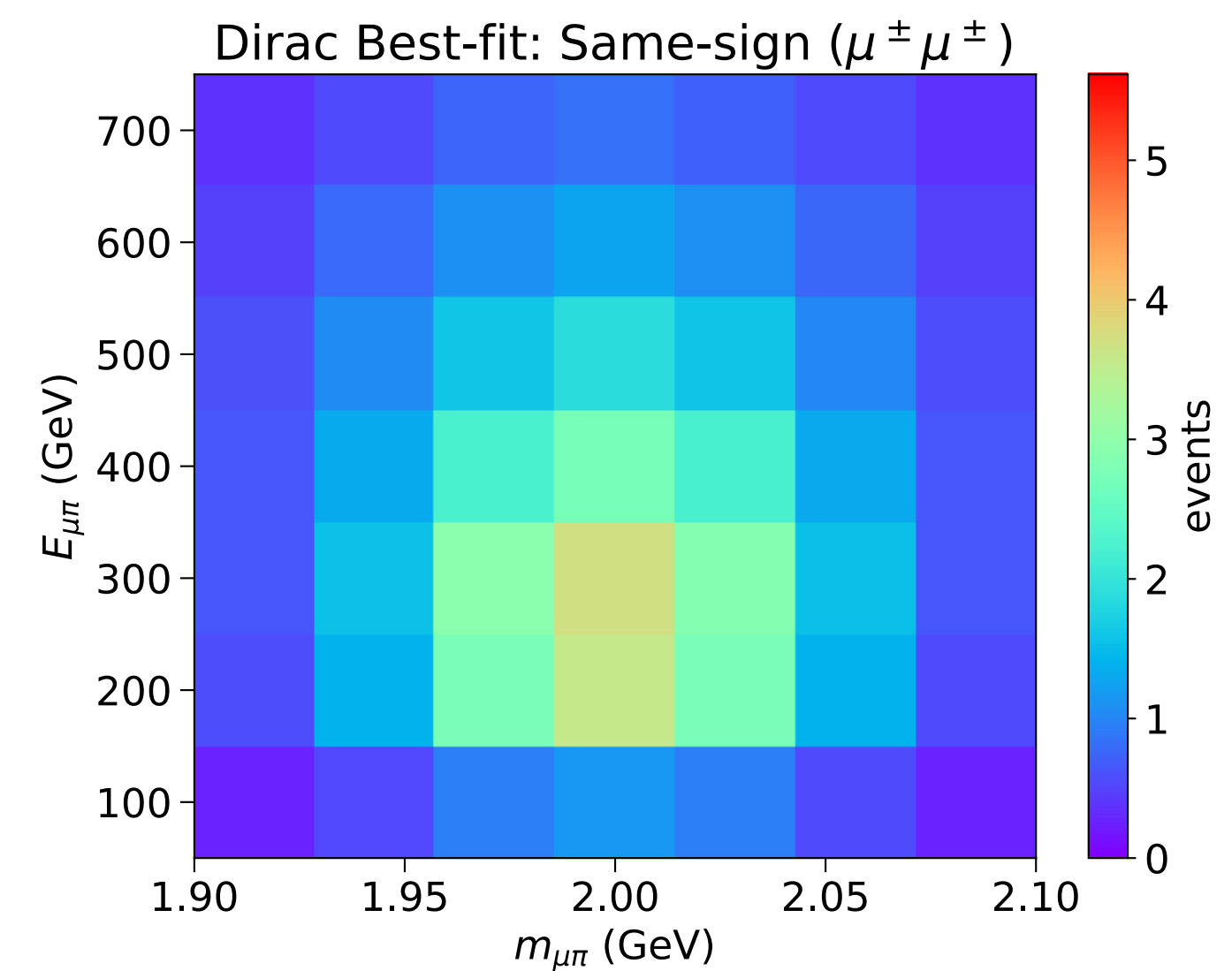
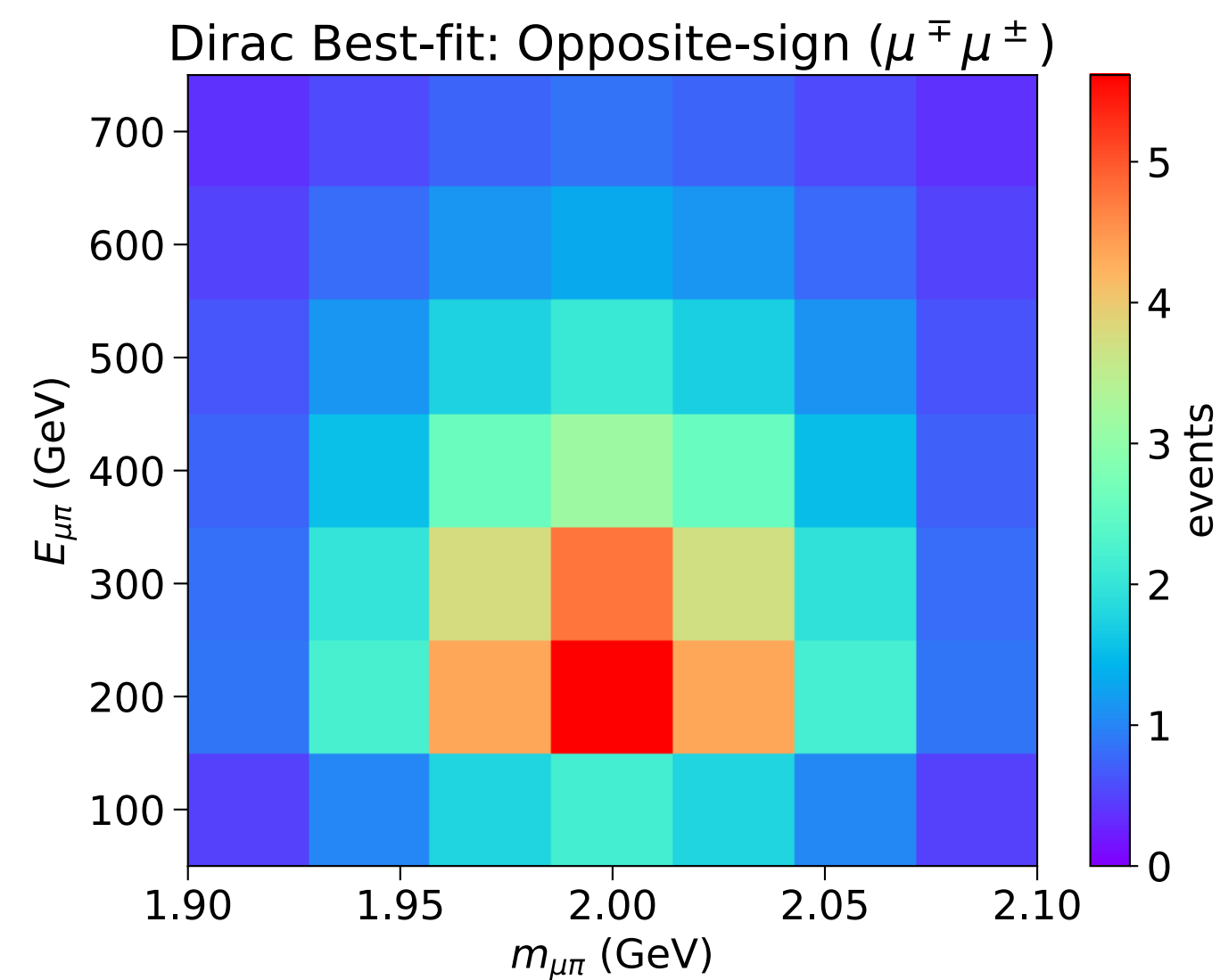
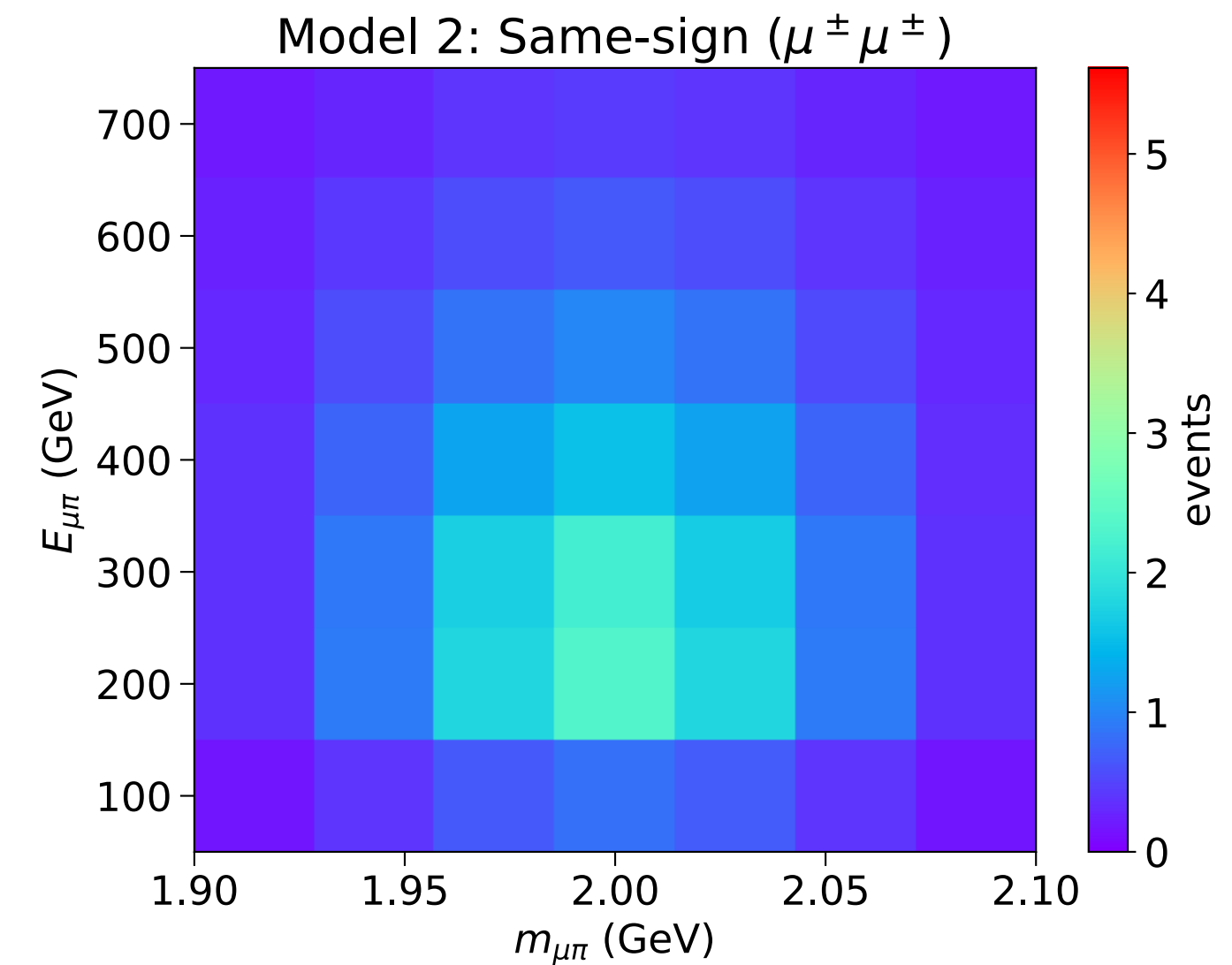
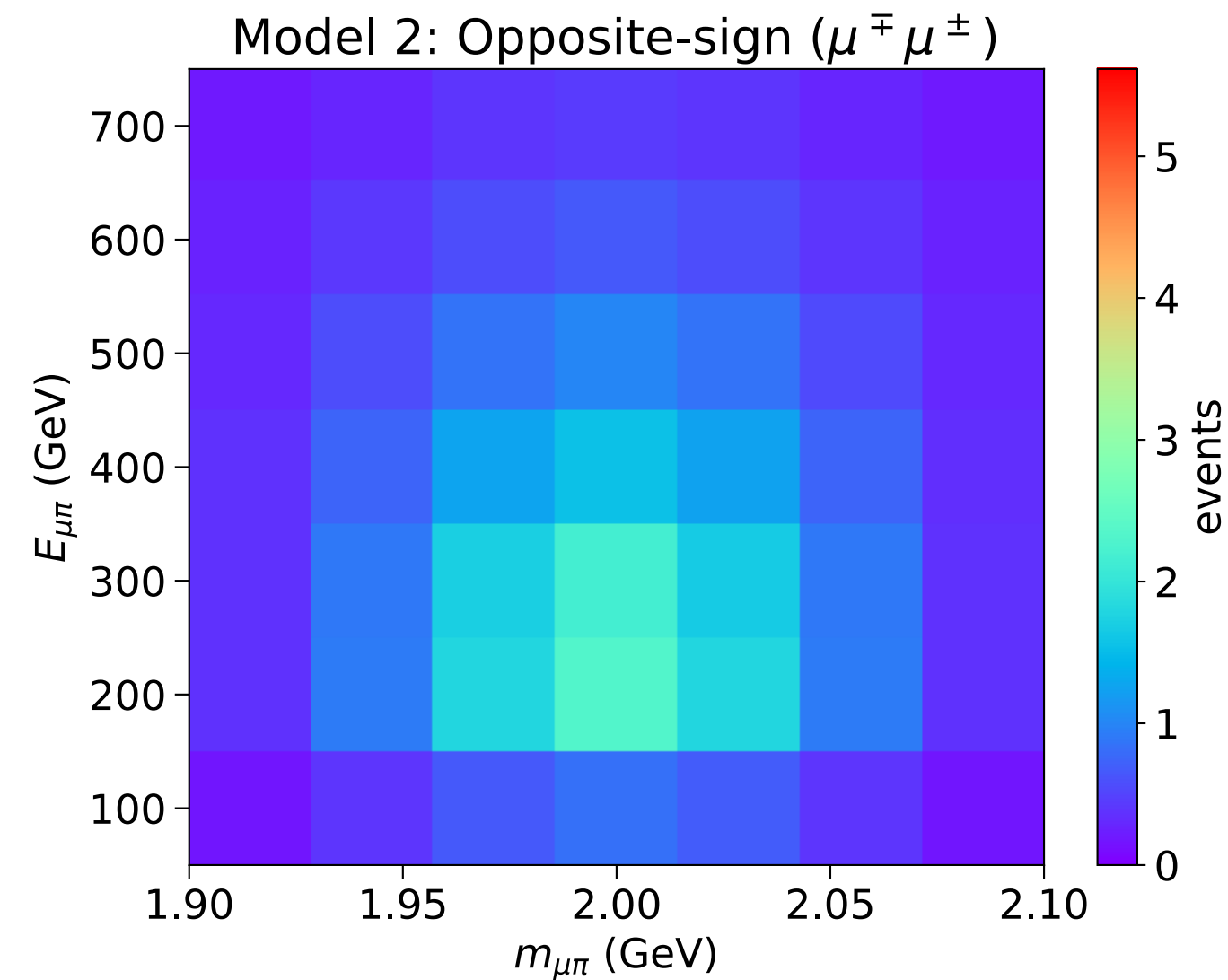
| Parent       | Muons ( $ \eta  < 4.9$ ) | Muons ( $3.5 < \eta < 4.9$ ) |
|--------------|--------------------------|------------------------------|
| $\pi^\pm$    | 31.41                    | 0.43                         |
| $K^\pm$      | 16.09                    | 0.26                         |
| $K_L^0$      | 0.37                     | 0.0033                       |
| Heavy Mesons | 3.34                     | 0.33                         |



# Correlated Signal

$$\begin{aligned}\mu_i^{SS} &= \frac{b}{2} \mu_i^F + \frac{\eta_M}{2} \mu_i^A \\ \mu_i^{OS} &= \frac{b}{2} \mu_i^F + \left(1 - \frac{\eta_M}{2}\right) \mu_i^A\end{aligned}\quad \eta_M = \begin{cases} 1 & \text{Majorana} \\ 0 & \text{Dirac} \end{cases}$$

- We separate each triggered HNL event into the number of muons detected in ATLAS that have either the **same sign (SS)** or **opposite sign (OS)** as the muon detected in FASER2.
- Muons produced in association with **Majorana HNL's** can be found with **OS or SS muons** in FASER2 with equal rates, resulting in an **symmetric distribution**.
- In contrast, **Dirac HNL's** can only be found with **OS muons** in FASER2, resulting in an **asymmetric distribution**.



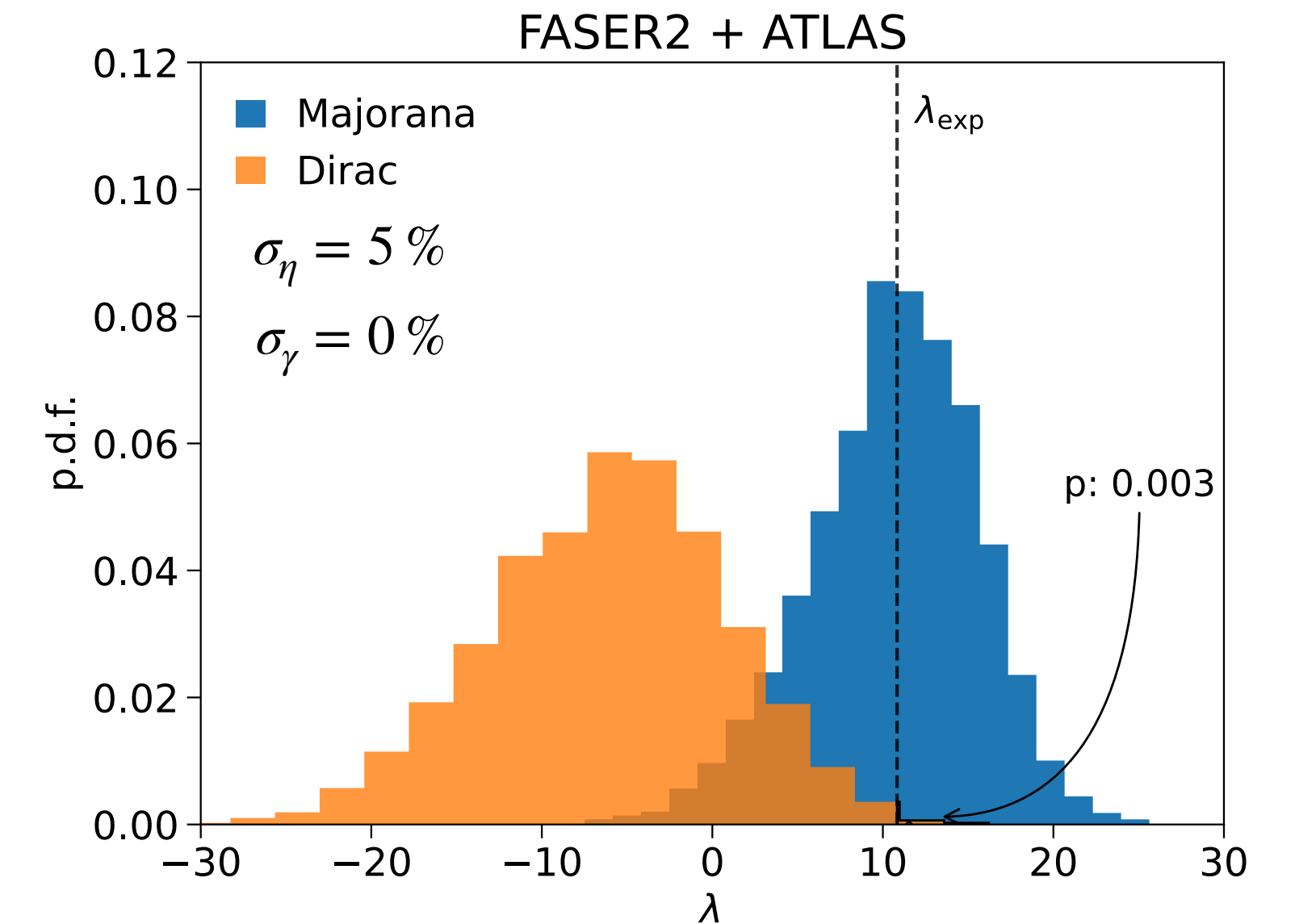
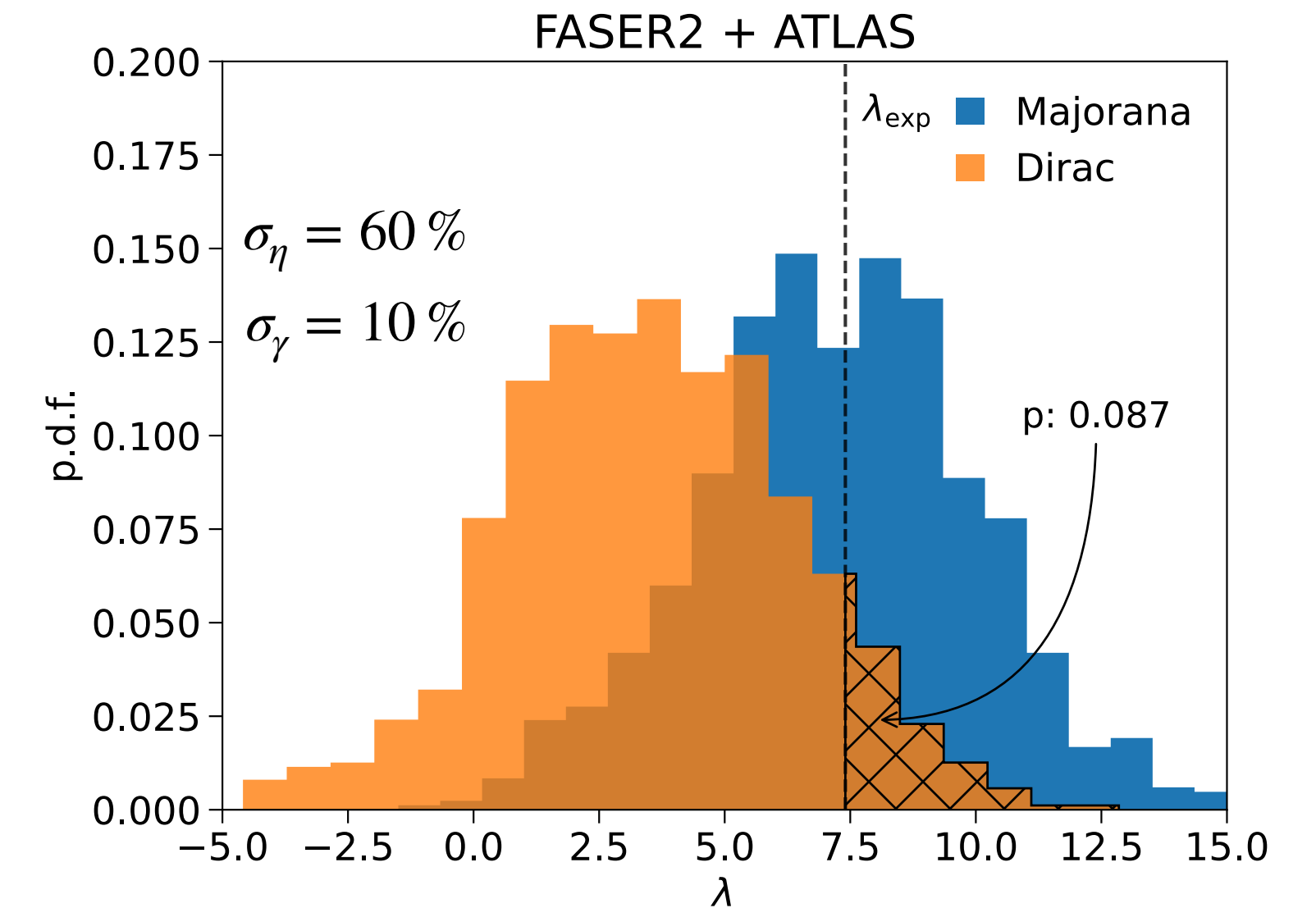
# FASER2 as a Trigger for ATLAS

## Model 2

Profiled Likelihood Ratio Test

$$\lambda(\vec{d}) := -2 \ln \frac{L_D(\vec{d} | \hat{m}_N^D, \hat{U}_\mu^D; \hat{\eta}^D, \hat{\gamma}^D)}{L_M(\vec{d} | \hat{m}_N^M, \hat{U}_\mu^M; \hat{\eta}^M, \hat{\gamma}^M)}$$

- Assuming **improved flux uncertainties**, we find that FASER2 can expect to reject the Dirac hypothesis with 99.7 % CL ( $2.7\sigma$ ), **despite having significantly lower statistics!**
- This illustrates that the main LHC detectors and proposed auxiliary detectors can have a synergistic relationship on an event-by-event basis.



# Conclusion

- Heavy Neutral Leptons are a simple, well-motivated extension to the SM which have a rich phenomenology to be studied at colliders
- We have presented [HNLCalc](#) - a fast, flexible, and comprehensive python package for calculating HNL production and decay rates with arbitrary couplings to active neutrino flavors
- As an application of this package, we have extended the [FORESEE](#) model library to include HNLs, allowing for the study of HNL phenomenology at forward physics experiments
- Using FORESEE, we presented:
  - Discovery prospects for HNLs at FASER/FASER2
  - Capability of FASER2 to measure the mass and coupling of an HNL, in the event of a signal detection
  - Capability of FASER2 to differentiate Majorana and Dirac HNLs using kinematics and FASER2 as a trigger for ATLAS

# Production/Decay Inputs

## Hadron Decay Constants

$$\langle 0 | \bar{q}_1 \gamma^\mu \gamma_5 q_2 | P(k) \rangle = i f_P k^\mu$$

$$\langle 0 | \bar{q}_1 \gamma^\mu q_2 | V(k, \epsilon) \rangle = i f_V M_V \epsilon^\mu$$

| $P$          | $f_P$ (MeV) | $V$           | $f_V$ (MeV) |
|--------------|-------------|---------------|-------------|
| $\pi^0$ [55] | 130.3       | $\rho^0$ [56] | 220         |
| $\pi^+$ [55] | 130.3       | $\rho^+$ [56] | 220         |
| $K^+$ [55]   | 156.4       | $\omega$ [56] | 195         |
| $\eta$ [57]  | 78.4        | $K^{*+}$ [55] | 204         |
| $\eta'$ [57] | -95.7       | $\phi$ [55]   | 229         |
| $D^+$ [58]   | 222.6       |               |             |
| $D_s^+$ [59] | 280.1       |               |             |
| $B^+$ [21]   | 190         |               |             |
| $B_c^+$ [21] | 480         |               |             |

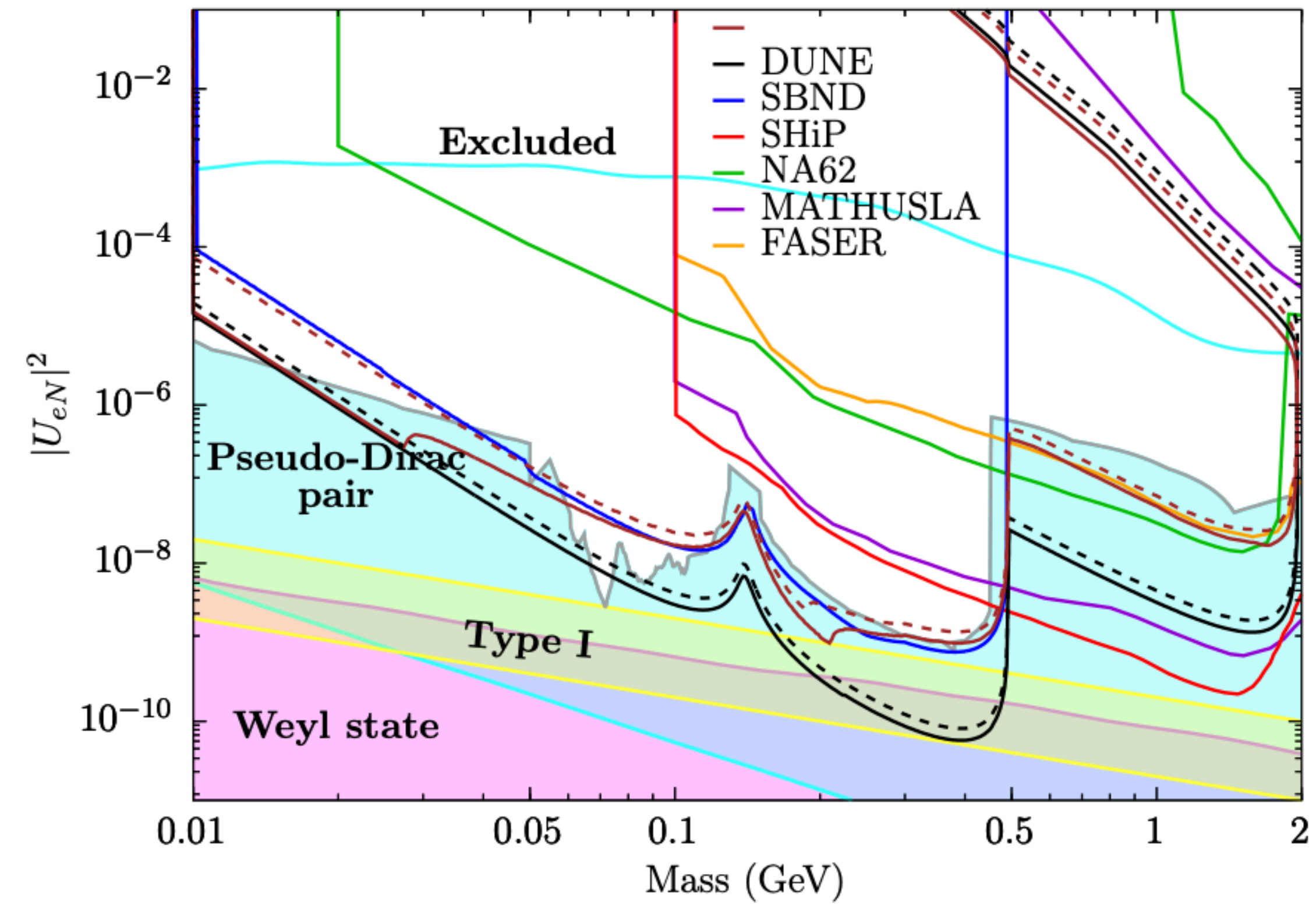
## Hadron Transition Form Factors

$$\langle P_2 | \bar{q}_1 \gamma^\mu q_2 | P_1 \rangle = f_+(q^2)(p_1^\mu + p_2^\mu) + f_-(q^2)q^\mu$$

$$\langle V | \bar{q}_1 \gamma_\mu \gamma^5 q_2 | P \rangle = i \epsilon^{*\nu} \left[ f(q^2) g_{\mu\nu} + a_+(q^2) p_{1\nu} (p_{1\mu} + p_{2\mu}) + a_-(q^2) p_{1\nu} q_\mu \right]$$

|                                     | $A_0$    |            |            | $A_1$    |            |            | $A_2$    |            |            | $V$    |            |            |       |
|-------------------------------------|----------|------------|------------|----------|------------|------------|----------|------------|------------|--------|------------|------------|-------|
| Decay Channel                       | $f_0(0)$ | $\sigma_1$ | $\sigma_2$ | $f_0(0)$ | $\sigma_1$ | $\sigma_2$ | $f_0(0)$ | $\sigma_1$ | $\sigma_2$ | $f(0)$ | $\sigma_1$ | $\sigma_2$ | $c_V$ |
| $D^0 \rightarrow \rho^-$ [64]       | 0.66     | 0.36       | 0          | 0.59     | 0.50       | 0          | 0.49     | 0.89       | 0          | 0.90   | 0.46       | 0          | 1     |
| $D^0 \rightarrow K^{*-}$ [64]       | 0.76     | 0.17       | 0          | 0.66     | 0.3        | 0          | 0.49     | 0.67       | 0          | 1.03   | 0.27       | 0          | 1     |
| $D^+ \rightarrow \rho^0$ [64]       | 0.66     | 0.36       | 0          | 0.59     | 0.50       | 0          | 0.49     | 0.89       | 0          | 0.90   | 0.46       | 0          | 1/2   |
| $D^+ \rightarrow \omega$ [64]       | 0.66     | 0.36       | 0          | 0.59     | 0.50       | 0          | 0.49     | 0.89       | 0          | 0.90   | 0.46       | 0          | 1/2   |
| $D^+ \rightarrow \bar{K}^{*0}$ [64] | 0.76     | 0.17       | 0          | 0.66     | 0.3        | 0          | 0.49     | 0.67       | 0          | 1.03   | 0.27       | 0          | 1     |
| $D_s^+ \rightarrow K^{*0}$ [64]     | 0.67     | 0.2        | 0          | 0.57     | 0.29       | 0.42       | 0.42     | 0.58       | 0          | 1.04   | 0.24       | 0          | 1     |
| $D_s^+ \rightarrow \phi$ [64]       | 0.73     | 0.10       | 0          | 0.64     | 0.29       | 0          | 0.47     | 0.63       | 0          | 1.10   | 0.26       | 0          | 1     |
| $B^+ \rightarrow \rho^0$ [64]       | 0.30     | 0.54       | 0          | 0.26     | 0.73       | 0.1        | 0.29     | 1.4        | 0.5        | 0.31   | 0.59       | 0          | 1/2   |
| $B^+ \rightarrow \omega$ [64]       | 0.30     | 0.54       | 0          | 0.26     | 0.54       | 0.1        | 0.24     | 1.40       | 0.50       | 0.31   | 0.59       | 0          | 1/2   |
| $B^+ \rightarrow \bar{D}^{*0}$ [64] | 0.69     | 0.58       | 0          | 0.66     | 0.78       | 0          | 0.62     | 1.04       | 0          | 0.76   | 0.57       | 0          | 1     |
| $B^0 \rightarrow \rho^-$ [64]       | 0.30     | 0.54       | 0          | 0.26     | 0.54       | 0.1        | 0.24     | 1.40       | 0.50       | 0.31   | 0.59       | 0          | 1     |
| $B^0 \rightarrow D^{*-}$ [64]       | 0.69     | 0.58       | 0          | 0.66     | 0.78       | 0          | 0.62     | 1.04       | 0          | 0.76   | 0.57       | 0          | 1     |
| $B_s^0 \rightarrow K^{*-}$ [64]     | 0.37     | 0.60       | 0.16       | 0.29     | 0.86       | 0.6        | 0.26     | 1.32       | 0.54       | 0.38   | 0.66       | 0.30       | 1     |
| $B_s^0 \rightarrow D_s^{*-}$ [71]   | 0.67     | 0.35       | 0          | 0.70     | 0.463      | 0          | 0.75     | 1.04       | 0          | 0.95   | 0.372      | 0          | 1     |
| $B_c^+ \rightarrow D^{*0}$ [69]     | 0.56     | 0          | 0          | 0.64     | 0          | 0          | -1.17    | 0          | 0          | 0.98   | 0          | 0          | 1     |





[Ballet et al. 1905.00284]